INTERNATIONAL ENERGY AGENCY
Solar Heating & Cooling Programme

Transparent Insulation Material Modeling

A report of Task 12: Building Energy Analysis and Design Tools for Solar Applications
Subtask A: Model Development
Subtask A.1: High Performance Glazings

October 1993

Transparent Insulation Material Modeling

Task 12:	**Building Energy Analysis and Design Tools for Solar Applications**
Subtask A:	**Model Development**
Subgroup A.1:	**High–Performance Glazing**

Hans Erhorn
Fraunhofer Institut für Bauphysik
Nobelstr. 12
D – 70569 Stuttgart
Germany

Rolf Stricker
B.E.S.T. – Ingenieurbüro für
Bauphysik und Energiespartechnik
Katzenbachstr. 44
D – 70563 Stuttgart
Germany

October 25, 1993

PREFACE

INTRODUCTION TO THE INTERNATIONAL ENERGY AGENCY

BACKGROUND

The International Energy Agency was founded in November 1974 as a cooperation among industrialized nations to address energy policy issues. It is an autonomous body within the framework of the Organization for Economic Cooperation and Development (OECD). Twenty-one countries are presently members, with the Commission of the European Communities also participating in the work of the IEA under a special agreement.

One element of the IEA's program involves cooperation in the research and development of alternative energy resources in order to reduce excessive dependence on oil. A number of new and improved energy technologies which have the potential of making significant contribution to global energy needs were identified for collaborative efforts. The IEA Committee on Energy Research and Development (CRD), comprising representatives from each member country, supported by a small Secretariat staff, is the focus of IEA RD&D activities. Four Working Parties (in Conservation, Fossil Fuels, Renewable Energy, and Fusion) are charged with identifying new areas for cooperation and advising the CRD on policy matters in their respective technology areas.

SOLAR HEATING AND COOLING PROGRAM

Solar Heating and Cooling was one of the technologies selected for joint activities. During 1976–1977, specific projects were identified in key areas of this field and a formal Implementing Agreement drawn up. The Agreement covers the obligations and rights of the Participants and outlines the scope of each project or "task" in annexes to the document. There are now eighteen signatories to the Agreement:

Australia	Federal Republic of Germany	Norway
Austria	Greece	Spain

Belgium	Italy	Sweden
Canada	Japan	Switzerland
Denmark	Netherlands	United Kingdom
Commission of the European Communities	New Zealand	United States

The overall program is managed by an Executive Committee, while the management of the individual tasks is the responsibility of Operating Agents. The tasks of the IEA Solar Heating and Cooling Program, their respective Operating Agents, and current status (ongoing or completed) are as follows:

Task 1 Investigation of the Performance of Solar Heating and Cooling Systems–Technical University of Denmark (Completed).

Task 2 Coordination of Research and Development of Solar Heating and Cooling–Solar Research Laboratory–GIRN, Japan (Completed).

Task 3 Performance Testing of Solar Collectors–University College, Cardiff,U.K. (Completed)

Task 4 Development of an Isolation Handbook and Instrument Package–U.S. Department of Energy (Completed)

Task 5 Use of Existing Meterological Information for Solar Energy Application–Swedish Meterological and Hydrological Institute (Completed).

Task 6 Performance of Solar Heating, Cooling, and Hot Water Systems using Evacuated Collectors–U.S. Department of Energy (Completed).

Task 7 Central Solar Heating Plants with Seasonal Storage–Swedish Council for Building Research (Completed).

Task 8 Passive and Hybrid Solar Low Energy Building–U.S. Department of Energy (Completed).

Task 9	Solar Radiation and Pyranometry Studies, KFA, Jülich, Federal Republic of Germany (Completed).
Task 10	Solar Materials R&D–AIST, Ministry of International Trade and Industry, Japan (Completed).
Task 11	Passive and Hybrid Solar Commercial Building–Swiss Federal Office of Energy (Completed).
Task 12	Building Energy Analysis and Design Tools for Solar Applications–U.S. Department of Energy (Ongoing).
Task 13	Advanced Solar Low Energy Buildings–Norwegian Insititute of Technology (Ongoing).
Task 14	Advanced Active Solar Energy Systems–Canadian Department of Energy Mines and Resources (Ongoing).
Task 15	Advanced Central Solar Heating Plants with Seasonal Storage (In Planning Stage).
Task 16	Photovoltaics in Buildings–KFA, Jülich, Germany (Ongoing).
Task 17	Measuring and Modelling Spectral Radiation Affecting Solar Systems and Buildings – KFA, Jülich, Germany (Ongoing).
Task 18	Advanced Glazing Materials–U.K. Department of Energy (Ongoing).
Task 19	Solar Air Systems in Buildings – Swiss Federal Office of Energy (Ongoing)
Task 20	Solar Energy in Building Renovation – Swedish Council for Building Research (Ongoing)

TASK 12: BUILDING ENERGY ANALYSIS AND DESIGN TOOLS FOR SOLAR APPLICATIONS

The scope of Task 12 includes: (I) selection and development of appropriate algorithms for modeling of solar energy related materials, components and systems within the building in which these solar elements are integrated; (2) selection of analysis and design tools and evaluation of the algorithms as to their ability to model the dynamic performance of the solar elements in respect to accuracy and ease of use, and (3) improvement of the usability of the analysis and design tools, through preparation of common formats and procedures, and by standardization of specifications for input/output, default values and other user–related factors.

The subtasks of this project are:

A: Model Development
B: Model Evaluation
C: Model Use

The participants in this Task are: Denmark, Finland, Federal Republic of Germany, Norway, Spain, Sweden, Switzerland, and the United States. The United States serves as Operating Agent for this Task. Michael Holtz of Architectural Energy Corporation serves the Operating Agent on behalf of the U.S. Department of Energy.

This report documents work carried out under Subtask A.I of this Task entitled High Performance Glazing.

EXECUTIVE SUMMARY

This document presents the work conducted as part of Subtask A, Model Development, Subgroup A1, High–Performance Glazing, of Task 12 of the IEA Solar Heating and Cooling Program. The participants believe that transparent insulation technology holds considerable promise, and that algorithms to accurately model their dynamic behaviour are needed.

The purpose of this subtask was to develop algorithms that could be incorporated into an annual building energy simulation tool for predicting the thermal and optical performance of transparent insulation systems. Building applications and construction details are included, followed by a description of methods for modeling such systems in buildings. Examples of the algorithms are included. They correct some of the shortcomings in the existing techniques, and could be adapted for use in similar programs, such as providing more detailed calculations needed for evaluating the short–term (hourly and daily) impact of transparent insulation systems on the energy and daylighting performance of a building.

The algorithms presented in this report are intended to compute the interaction of transparent insulation systems and the temperature behavior of the entire building. These algorithms can be incorporated into any building energy analysis simulation tool that computes building energy balances on the basis of hourly weather data sets. A prerequisite for adaptation is, however, that the superposition of direct solar gains (window) of a transparent system and indirect solar gains (due to phase delay) can be taken into account in the respective building energy analysis simulation tool.

The compilation of these algorithms is preceded by an overview of building applications and constructions of TIM systems which will give an impression of the overall range of applications. The results presented in this study, particularly those concerning the cost–benefit relations suggest very clearly, that it is not so much an increase in the system's energetic efficiency, but rather a drastic cost reduction in case of the required shading devices, in particular, that is of primary importance to make a TIM system economically interesting. Here, the application of fixed lamellar systems is a good approach, although energy efficiency will be slightly reduced, while total costs of a TIM system may be cut by 50 % in this way.

Transparent Insulation Material Modeling

Contents

1. INTRODUCTION

1.1 Background

Transparent insulation materials (TIM) are among the most promising materials for reducing energy consumption in residential buildings. These materials can be used in, for instance, windows or as outside insulation of walls. Both options combine high solar gains and high heat resistance. The concept of a TIM wall covering has an advantage over direct solar gain through windows in that the heat collected is buffered by the wall and only several hours later passes into the house (phase shift in solar gain).

The thermal behaviour of TIMs can be transferred into a calculation model at various levels of accuracy. For detailed calculations, which are primarily directed at simulating the behaviour of the material itself, specific computer programs are used and developed by research institutes. For simulation of temperatures and heating loads within a total model of (part of) a building, less accuracy will often suffice as regards the algorithms simulating the material.

More detailed computer models for (multi–zone) energy simulation of a building make use of the following physical model for transparent elements: based on optical formulae (Fresnel and others), an hourly transmission coefficient for direct and diffuse radiation is calculated for each transparent element (optionally after making a shading calculation). Also, the per layer amount of absorbed solar energy is calculated and divided into an in–flowing source term and an out–flowing portion according to a resistance model.

1.2 Purpose of This Report

The purpose of this report is to review and improve upon existing algorithms for modeling transparent insulation materials, within simulation programs which model the thermal performance of buildings.

The importance of modeling transparent insulation materials in building energy simulation programs lies in the need to predict the energy savings potential of this

technology and to formulate performance guidelines to aid research in their development. This requires an hourly simulation model that adequately accounts for thermal, solar optical and daylighting impacts of the transparent insulation systems. The guidelines need to address questions concerning temperature behavior of the transparent insulation material, the angular dependence of the optical properties, and how each of these relate to building design issues such as size and orientation and lighting requirements. Furthermore, the successful development of control strategies for transparent insulation systems requires models that imitate the dynamic behavior of the window.

1.3 Structure of the Report

Sections II – VI review current applications, system construction techniques, range of materials and physical properties of transparent insulation materials.

Section VII presents monitoring results of physical properties which will be incorporated within the modeling algorithms and system thermal behaviour as a basis for evaluation of simulation results.

Sections VIII – XI look at proposed algorithms for modeling transparent insulation materials and systems in terms of system performance and building energy performance. Simulation results are described and cost–benefit ratios are discussed leading to a set of conclusions.

Appendices A – E include source code listings of the algorithms described in Section VIII, which can be incorporated as functions or subroutines within building energy simulation programs (e.g. SERIRES/SUNCODE, DOE–2, TRNSYS) on the basis of hourly energy balances.

1.4 Intended Audience

The primary audience for the transparent material insulation material modeling algorithms are researchers, engineers, and manufacturers. The intention of this work is to provide tools for more accurate assessment of the potential of transparent insulation technologies, and to further the development of the technology.

1.5 Acknowledgments

This report was instigated through cooperation between the IEA participating researchers and the government agencies which sponsored the work in their respective countries. The participants who provided comments and criticism on earlier drafts are thanked for their effort, without which this report could not have been completed.

1.6 List of Experts From Participating Countries within Subtask A

Mr. Kjeld Johnsen
Danish Building Research Institute
P.O.Box 119
DK–2970 Hoersholm
Denmark

Mr. Kurt Kallblad
Department of Building Science
University of Lund
Box 118
S–2200 Lund
Sweden

Ms. Susan Reilly
Mr. Stephen Selkowitz
Mr. Fred Winkelmann
Lawrence Berkeley Laboratory
1 Cyclotron Road
Berkeley, Carlifornia 94720
United States of America

Mr. Helge Hartwig
Ernst Schweizer AG
Metallbau
Ch–8908 Hedingen
Switzerland

Mr. Atle Nordgard
Solar Energy Applications Laboratory
University of Wisconsin
1500 Johnson Drive
Madison, WI 53706
United States of America

2. SOLAR CONCEPT

The principal function of a wall provided with conventional opaque insulation and of a mass wall with transparent insulation is shown in figure 1 in a conceptual diagram. At the wall covered with opaque insulation, solar radiation is absorbed by the outside layer. The influence on transmission heat losses is small, because the insulation layer is covered with plaster or other protective material. On the contrary, with transparent insulation, solar radiation will be partially transmitted through the insulating layer to be absorbed at the exterior surface of the wall behind the insulating layer. Due to the transparent insulation, a high percentage of the absorbed energy is conducted into the wall. Depending on the amount of solar radiation, the wall will heat up and a temporary heat transfer inversion from the outside to the inside can be achieved.

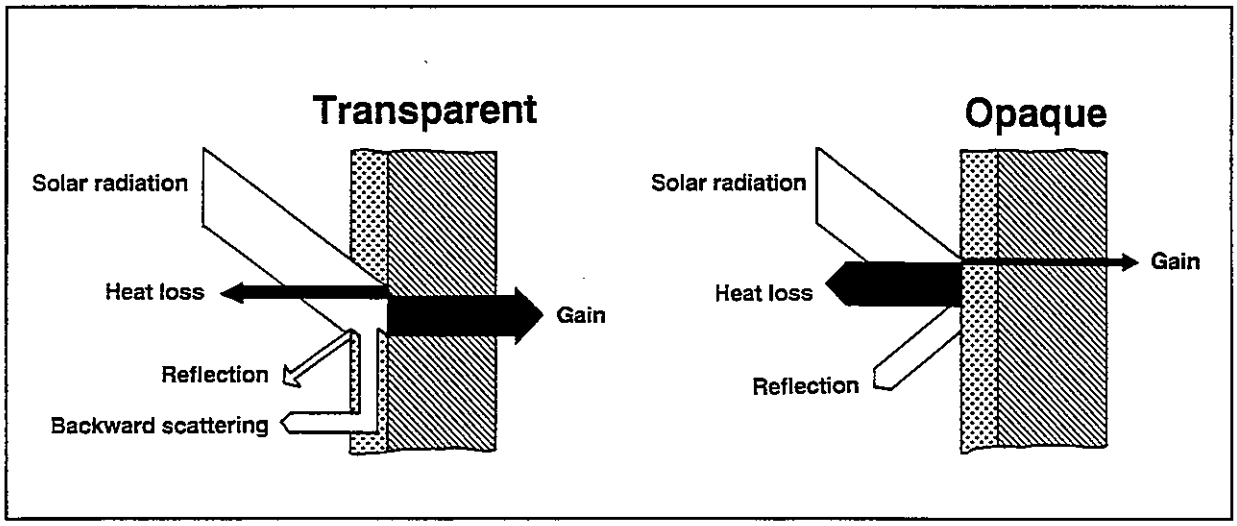

Fig. 1: Principal function of an opaque and a transparent insulated mass wall.

During periods of weak or no radiation at all, heat losses are minimised by the insulating effect of the material layer. During periods of solar radiation, the external wall becomes a radiation absorber, a heat store and a temporary surface heater for the adjoining space.

3. AREAS OF APPLICATION

Transparent thermal insulation materials can be applied to transparent facade areas (windows, glazings) as well as to mass walls. If transparent thermal insulation is applied to exterior walls, the insulating effects are enhanced by some additional heat gains from solar radiation. The system is especially appropriate for moderate and cold climates with strong solar radiation.

After first applications in housing, transparent thermal insulation is now being employed for commercial buildings.

Among the many possibilities of applying transparent thermal insulation materials, two commercial building applications will now be discussed: a supermarket and a recreation building.

COMMERCIAL BUILDINGS

With the present state–of–the–art, and due to cost–effectiveness considerations, it is recommended that transparent thermal insulation systems be applied in two cases:

(1) If additional solar shading devices are unnecessary;

(2) If large frame elements of uniform size can be applied (firstly to reduce the portion of wall surface covered by frames, which do not represent an energy gain area and have a lower insulating effect, and secondly to lower construction costs through mass production).

Commercial buildings which often have large windowless facade areas, frequently meet those conditions. Due to their visual aspect, many industrial buildings are often given the label "shoebox–architecture". In the industrial sector, energy considerations play only a small role, since the price of energy is included in the price of the products. Under such conditions it is not a miracle that a waste of energy takes place in many commercial buildings. If, for reasons of image, steps are taken to improve the visual aspect of facades, transparent thermal insulation should also be considered. Careful detailing and consideration of boundary conditions for use are however required.

A SUPERMARKET

Supermarkets are buildings that do not stand out for their architectural beauty. The following case study shall demonstrate how this type of building can be given an attractive look through cost-effective retrofitting measures. Thus, shopping becomes an event merely by taking a look at the building itself.

The annual electricity consumption is 500,000 kWh (30 % accounting for illumination, 24 % for cooling foods, and 22 % for ventilation). An overview of the annual energy consumption of this supermarket is given in the following table.

Annual Energy Consumption		**Specific Consumption Per Unit Area**
Fuel	600,000 kWh	44 kWh/m^2
Electricity	500,000 kWh	37 kWh/m^2
– Illumination	30 %	11 kWh/m^2
– Cooling	24 %	9 "
– Ventilation	22 %	8 "
– Others	24 %	9 "

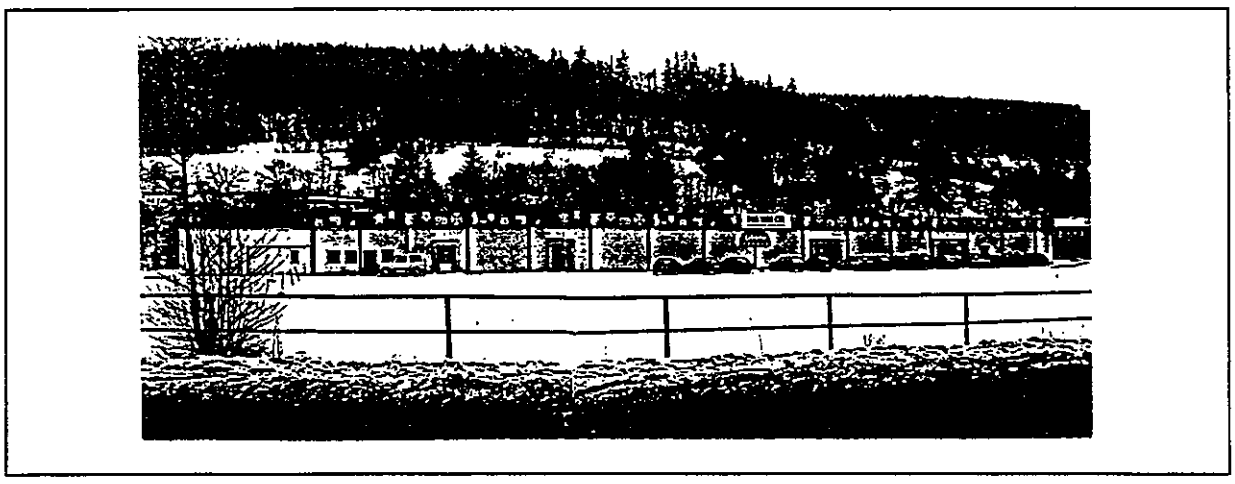

Fig. 2: Typical supermarket facade architecture.

The building is constructed of a reinforced concrete post and beam structural system with a distance of 3 m between beams. Spaces are filled with 175 mm core brick masonry. The roof, made of 120 mm reinforced concrete slabs, is provided with a 30 mm external insulation layer with gravel filling. Measures aimed at improving

thermal insulation have to start with the roof, which has the largest external surface. By increasing the thickness of the insulation layer to 200 mm, the annual heating energy consumption can be reduced by 20 % (see figure 3). Full-face opaque insulation of the 950 m² of the exterior wall surface with a 100 mm insulating layer would result in an additional reduction of the current demand to 60 % (CIS, conventional insulation system). However, if part (340 m²) of external wall surface was equipped with transparent thermal insulation, the annual heating energy consumption could be reduced to 45 %. The high air change rates during opening hours in the range of 1.5 and 3 h^{-1} (s. column 'Ventilation'), which can be controlled manually depending on the number of clients, are a good reason for selecting transparent thermal insulation with a ventilated insulating layer. The preheated supply air between air space and insulation layer is driven by a solar-controlled fan. According to numerical calculations, the annual heating energy consumption could thus be reduced to 20 % approx. of the current demand. At this point, the building heat requirements could sufficiently be covered by heat gains from light (s. column 'Lighting') and waste heat from the cooling system.

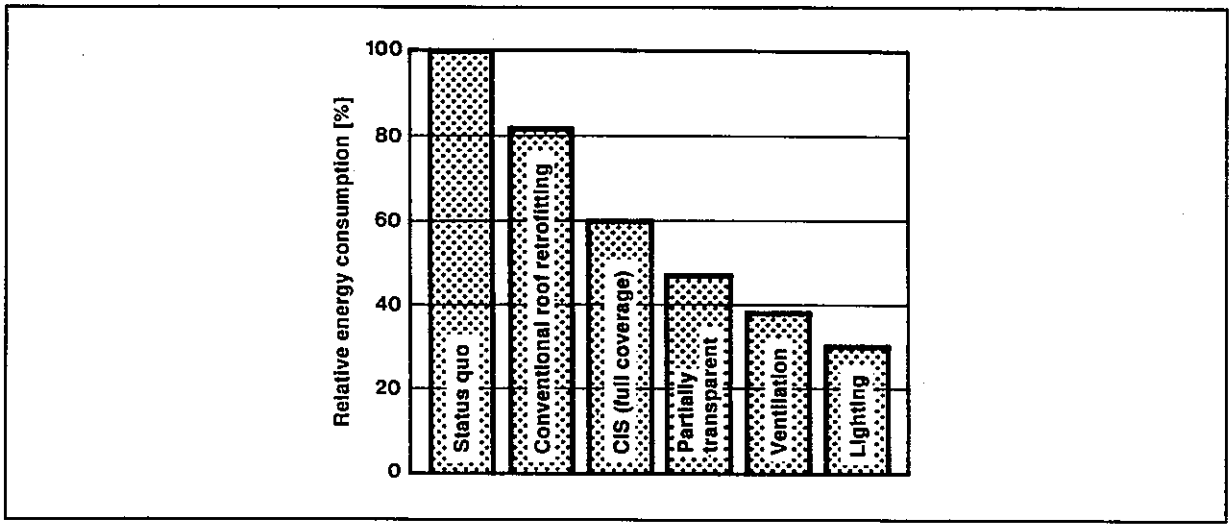

Fig. 3: Effects of different retrofitting measures on the supermarket.

If the roof is provided with improved thermal insulation, the absolute maximum indoor temperature will be lower than the status quo, even if transparent thermal insulation is applied (cf. figure 4). In this supermarket, it is easy to save large quantities of energy. Compared to housing, the same amount of energy can only be saved with a large number of apartments (with more effort in terms of material and costs).

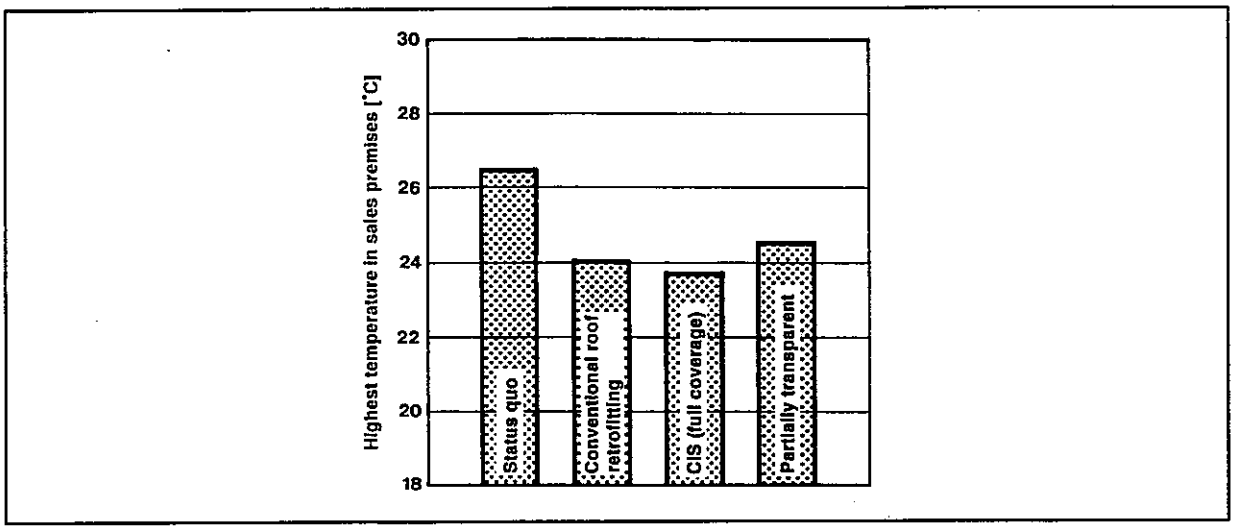

Fig. 4: Absolute maximum of air temperatures within sales area of supermarket for different retrofitting measures.

RECREATION BUILDING

A recreation building of an industrial company with about 100 employees further demonstrates the advantages of transparent thermal insulation. The building has a floor area of 24 m by 12 m and a north–south axis. In the two–storey building, half of the ground floor is taken up by sanitary and technical installations, the other half by social rooms. The ventilation system is installed on the top floor. A section of the building is presented in figure 5.

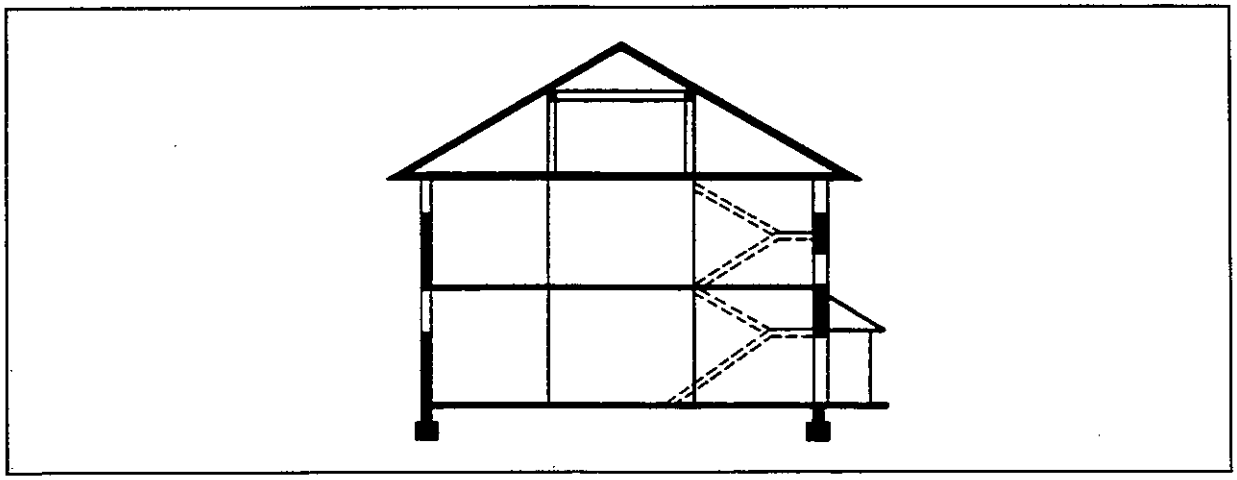

Fig. 5: Sectional view of the two–storey social building of an industrial company.

According to the conventional design, a 60 mm thermal insulation system is to be mounted externally. The total building surface to be insulated is 304 m^2. The window area is 60 m^2. Those are ideal conditions for transparent thermal insulation. The walls of the building are made of concrete, with a thickness of 200 mm for external walls, and of 120 mm for internal walls.

With transparent thermal insulation at the building's south facade the annual heating energy consumption can be reduced to approximately 30 % (additional opaque insulation = 40 %, s. figure 6). The heating and ventilation systems can be reduced to 60 % of their current size. Solar shading devices are not required, if damage to wall construction and insulation system is precluded through careful dimensioning. During shift change, large internal gains occur through illumination, people and hot water consumption. Due to the very high air change rates, these heat gains are almost completely extracted (s. column Ventilation heat = 94 % of reference case heat consumption, U = 0.6 W/m^2K).

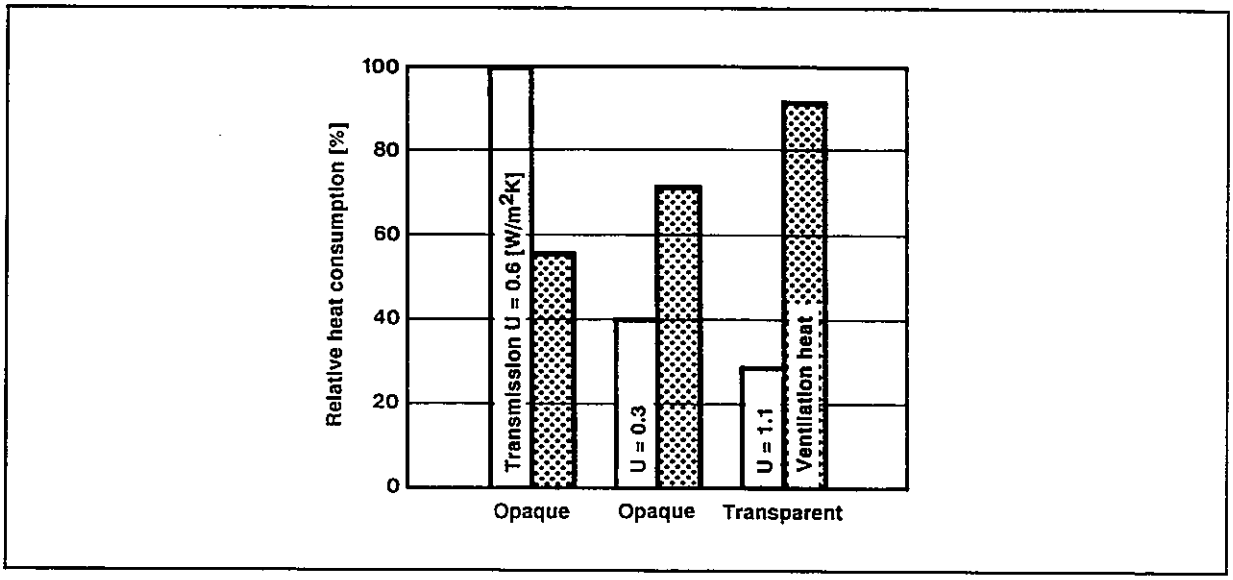

Fig. 6: Annual heat consumption of the social building (relative figures as compared to conventional construction) for additional opaque or transparent insulation.

Therefore in this case, by applying transparent thermal insulation, an additional heating equipment seems to be not necessary : the amount of heating energy required can largely be obtained from waste heat recovery .

4. RANGE OF TI-MATERIALS

TI-Materials can be classified according to their geometric structure [1-3].

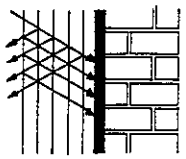

parallel structures

* multi-glazings
* plastic foils
* low-e reflecting layers

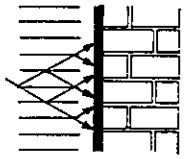

perpendicular structures

* honeycomb
* capillaries
* slit

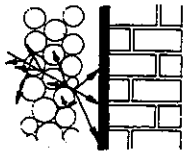

hollow core structures

* grid plates
* foam
* glass bubbles
* fibers
* granulated aerogel

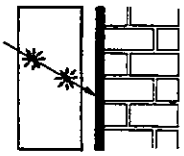

quasi-homogeneous material

* glass felt
* glass wool
* aerogel plates

Fig. 7: Geometric classification of TI-Materials.

A schematic presentation of different types of transparent thermal insulation materials between window panes is given in figure 8. Convection reducing material structures like honeycombs, capillaries, foams, fibers, microspheres or granulates,

partly scatter transmitted light. The transmittance is more or less reduced by material thickness. But light scattering prevents looking through these (translucent) types of materials. As shown by experience in material optimisation, it is possible to produce more or less translucent layers without a deterioration of their thermal properties. Besides, there are also microporous, quasi–homogeneous thermal insulation materials available which have a clear transparence.

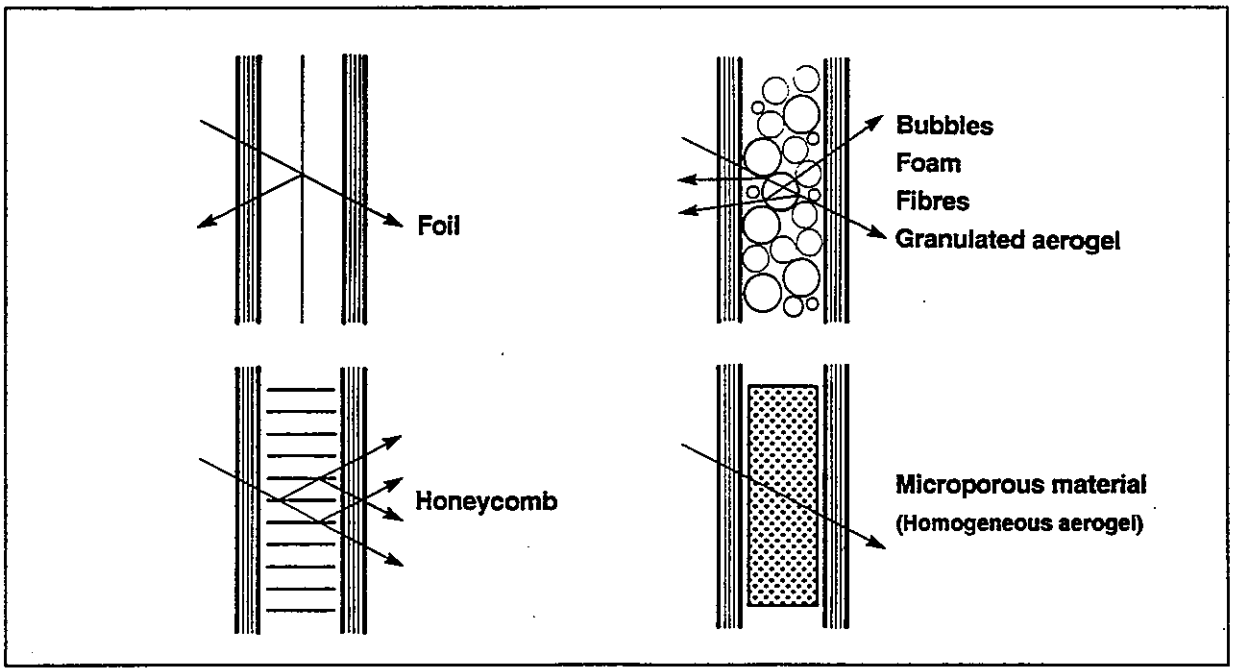

Fig. 8: Different types of transparent insulation materials inserted between two glass panes. Arrows indicate the propagation of light rays within the transparent insulation layer.

CURRENTLY AVAILABLE TRANSPARENT INSULATION MATERIALS

Organic plastic materials such as polycarbonate (PC) honeycombs, capillary structures or acrylic foam, and inorganic glass fiber materials or aerogel, are appropriate materials to be used in transparent insulation systems. To furnish those products with sufficient mechanical properties and to ensure good weather and fire protection, they are used behind single glass or sandwiched within double glazings. Figure 9 shows photographs of various material samples: capillaries, PC–honeycombs, glass fibers, polymethylmetacrylate (PMMA) foams, granulated and homogeneous aerogel.

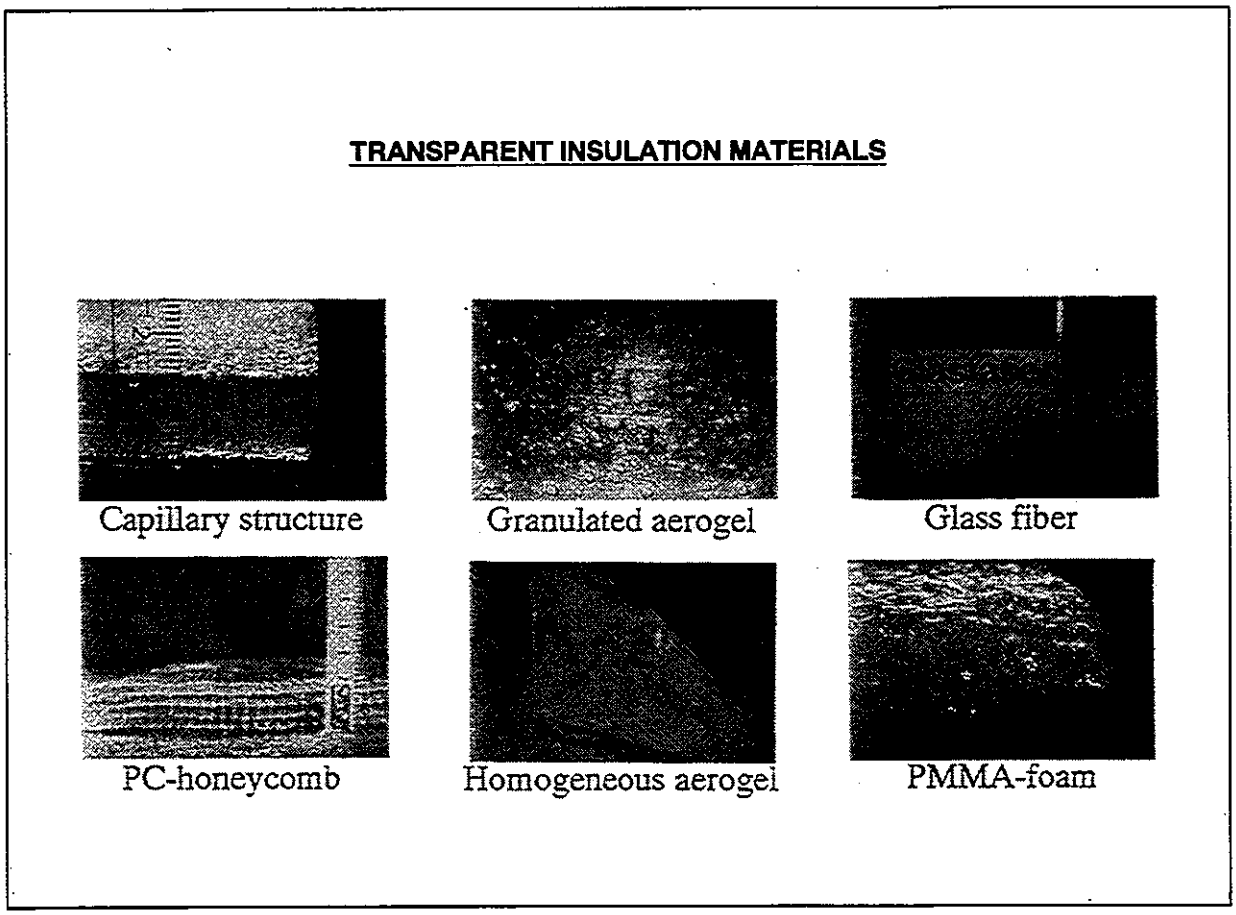

Fig. 9: Photographs of various transparent insulating materials.

5. PHYSICAL PROPERTIES OF TI-MATERIALS

Air convection within materials is reduced by structures like honeycombs, capillaries, foams, fibers, microspheres or granulates, and partly transmitted light is scattered. The transmittance is more or less reduced by material thickness, depending on material structure.

Figure 10 indicates the impact of the layer thickness on the diffuse solar transmittance, as well as the dependence of U-values on diffuse solar transmittance. In the case of materials enhancing scattering effects, for instance PMMA-foams or granulated aerogel, the diffuse transmittance amounts to 0.3, for granulated aerogels between 2 mm panes it amounts to 0.45, for capillary materials it amounts to more than 0.6, and for honeycombs to nearly 0.8, all at the same U-value. The diffuse solar transmittance approximately equals the total energy transmission for most of the transparent insulation materials, since their absorption is very low.

The thermal conductivity of the different transparent insulation materials shows a strong dependence on temperature [4]. For instance the heat conductance Λ of PC–honeycomb (d = 100 mm) at a temperature of 15°C is 1.2 W/m²K; at 80 °C it is 1.8 W/m²K. The values in between can be obtained by linear interpolation. Table 1 gives an overview of the mean values that could be used for calculations. Very low values of 0.02 W/(mK) are obtained for aerogel, and relatively high values of 0.09 W/(mK) for honeycomb materials; detailed information is given in refs [5–10].

Table 1: **Thermal conductivity of transparent insulation materials (mean values for about 20 °C average temperature).**

Material	Density [kg/m³]	Thermal conductivity [W/mK]
Capillaries	40	0.07
PC-honeycomb	32	0.09
Glass fiber	18	0.04
PMMA-foam	15	0.06
Granulated aerogel	110	0.02
Homogeneous aerogel	180	0.02

The temperature limit of polymethylmetacrylate (PMMA) materials is approximately 80 °C and that of PC honeycombs about 125 °C. The densities of the different plastic materials and of glass fibers range from 10 to 40 kg/m^3, and that of aerogel from 100 to 200 kg/m^3. Only glass fibers and aerogel are incombustible.

Aerogels (SO_2–gels) are made by hydrolysing and polymerising silicon alcoholates (alcogels) in alcoholic solutions [11,12]. The drying of these gels is performed in an autoclave at supercritical conditions. When alcohol is removed, alcogel becomes aerogel with an extremely porous microstructure. This structure gives the material its characteristic optical and thermal behaviour. For practical use it must be sandwiched within glass panes.

The impact of the layer thickness on the diffuse solar transmittance is indicated in Figure 10. With capillary diameters of 1 to 1.5 mm and layers of 25 to 60 mm for capillary materials, transmittance decreases to about 65 % (see also [13–19]).

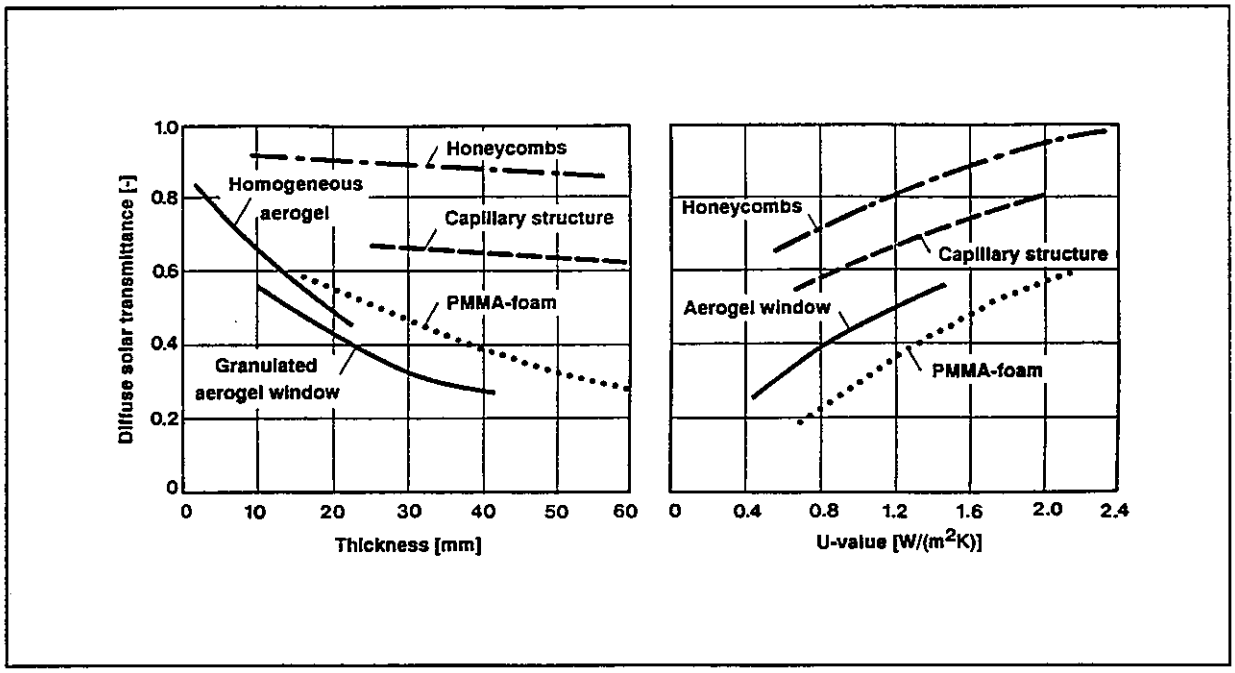

Fig. 10: Influence of layer thickness on the diffuse solar transmittance (diagram on left) and U-value for different transparent insulation materials (granulated aerogel is inserted between 2 mm glass panes).

6. TIM-CONSTRUCTION AND SYSTEMS

INSTALLATION TECHNIQUES FOR TRANSPARENT THERMAL INSULATION MATERIALS

There are 2 ways of applying transparent thermal insulation with frame systems:

(1) A frame system is mounted to the wall; glazings and transparent thermal insulation are subsequently inserted into the frame system (see example figure 11).

(2) Framed units are prefabricated and mounted to the wall (see figure 12).

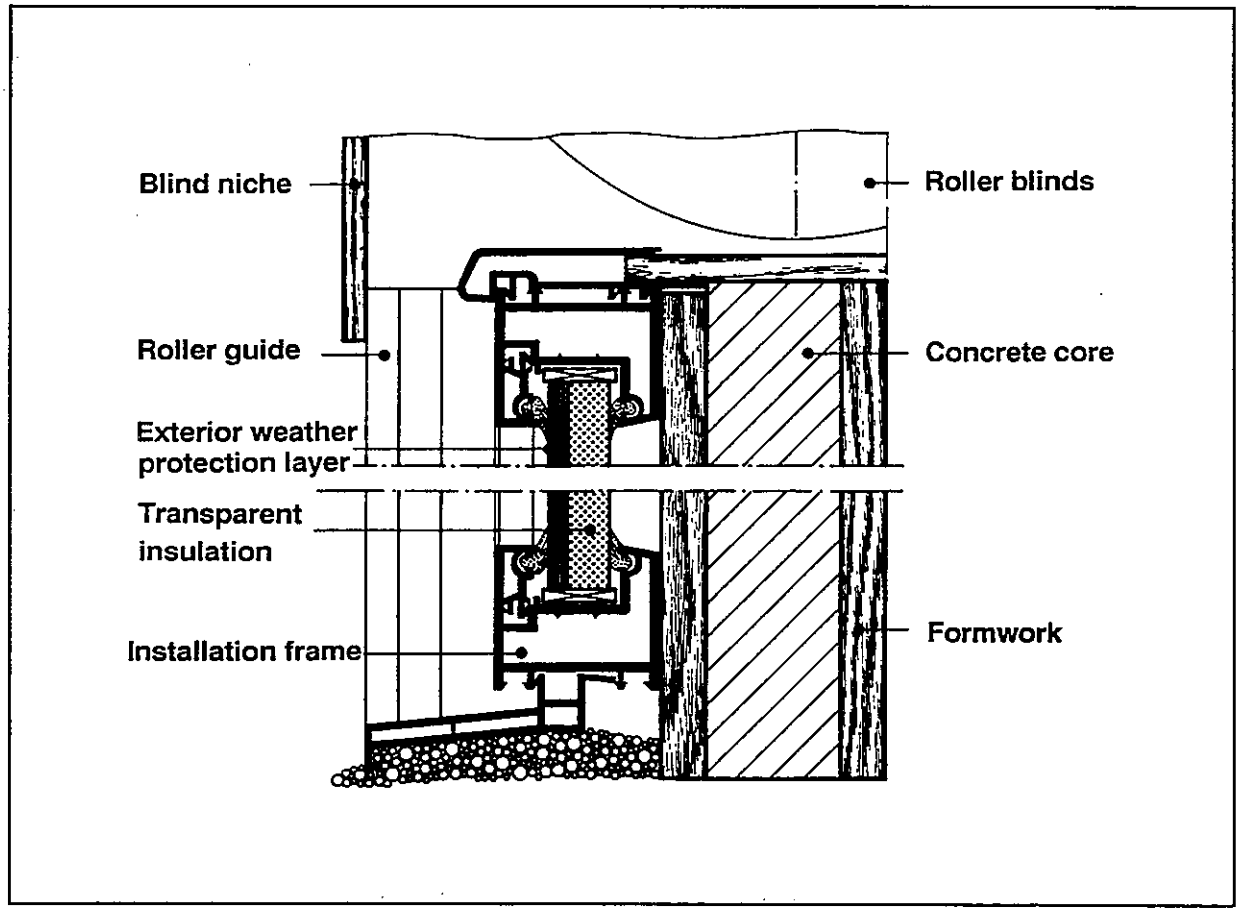

Fig. 11: Frame system mounted to the wall with transparent insulation and external solar protection equipment. (Example under practical investigation since 1986).

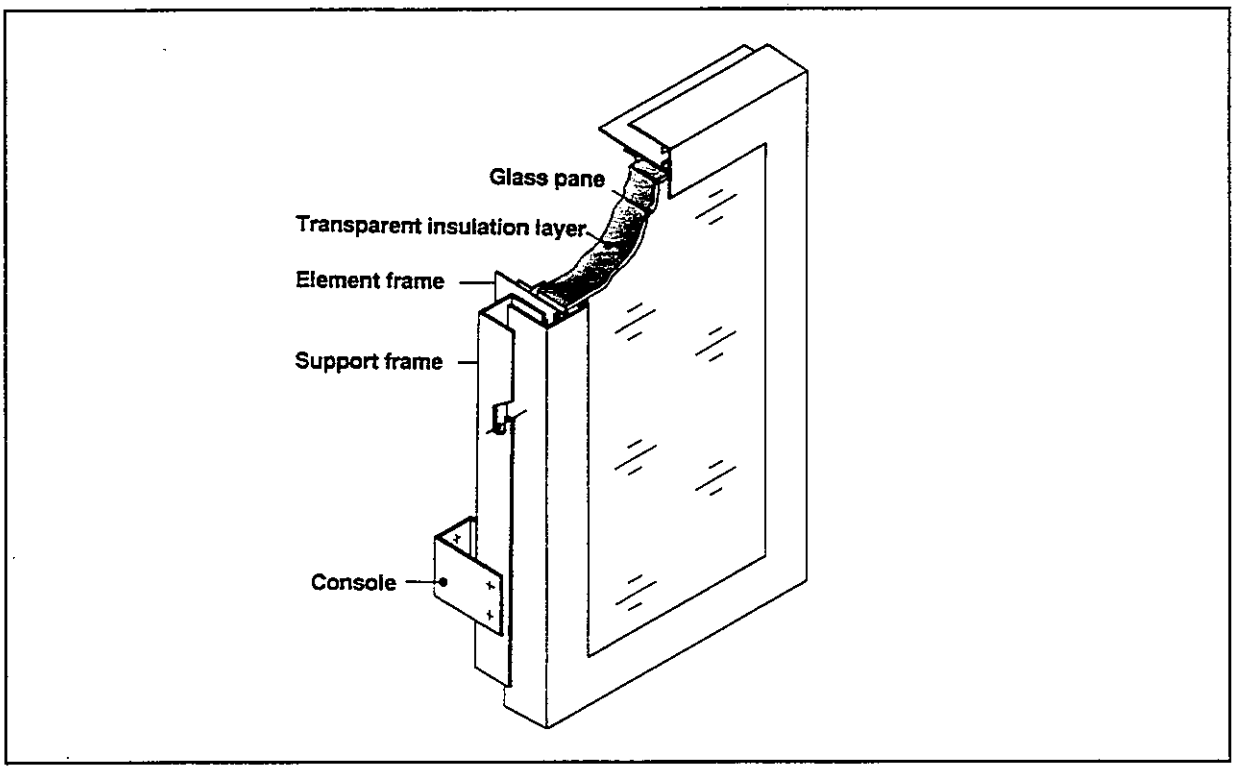

Fig. 12: Prefabricated frame system for transparent thermal insulation (developed in 1985)

A frameless, transparent thermal insulation system is currently being developed. With this system, the insulation layer is directly bonded to the wall. As for traditional insulation systems, a finishing material – in this case a transparent one – is applied for weather protection.

CONTROLLED SYSTEMS

The application of controlled systems is without risk, since overheating of constructions and interior spaces is prevented by solar shading devices. Figure 13 shows a typical, controlled transparent insulating system with roller blinds.

SOLAR SHADING DEVICES

Roller blinds, venetian blinds and awnings can be used as active solar shading devices. Depending on the system, they can be externally mounted; if necessary behind an additional pane that serves as a weather protection, or in front of the weather protection layer. A schematic representation of various sun shading installations is given in figure 14.

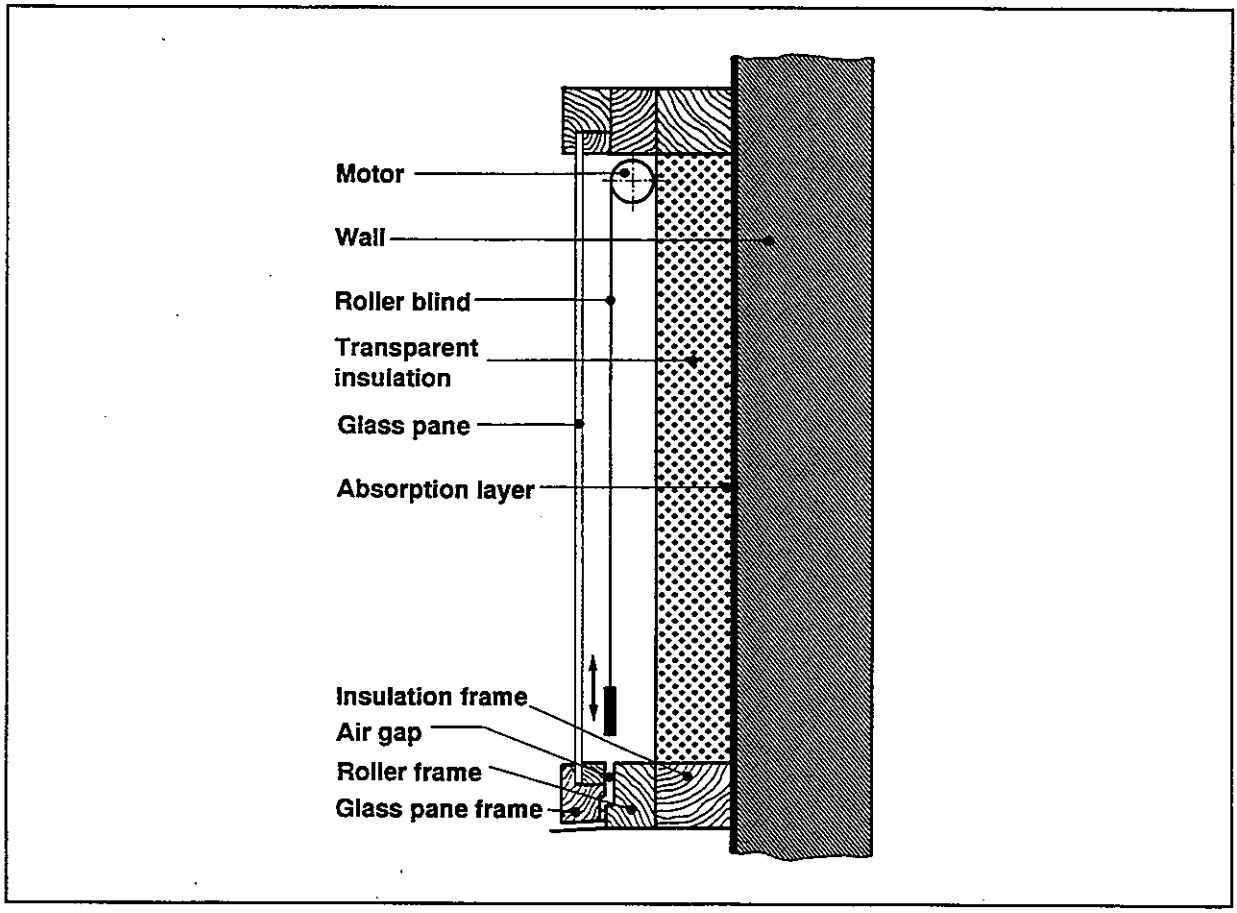

Fig. 13: Controlled transparent insulation system with roller blinds (schematic representation).

Externally mounted shading devices need frequent repairing because of their exposure to the weather. Protected roller blinds or venetian blinds mounted behind glass panes are exposed to higher temperatures than external ones. Their working satisfactorily can only be ensured by selecting the appropriate materials and by careful manufacture and installation.

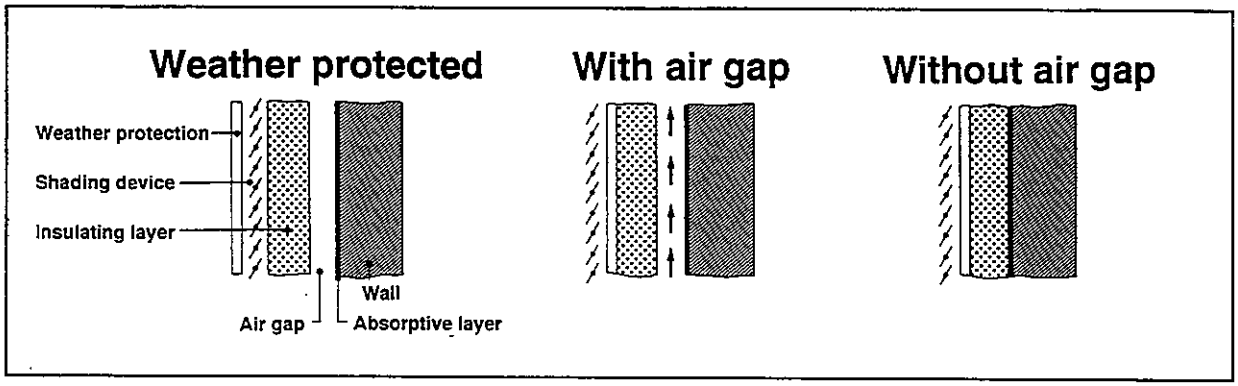

Fig. 14: Schematic representation of various sun shading installations.

SWITCHABLE GLAZINGS

Solar shading can also be managed with optically switchable glazings. To exclude undesired solar energy, there are three basic types of switchable glazings where the control depends on the glazing itself: chromogenic, physio–optic and electro–deposition systems. Chromogenic energy control sheet materials, also called "optical shutters", change the absorption or reflection of the glazing in response to heat, electricity or light. Windows darken or lighten to vary the amount of solar radiation and heat entering the building. The material is classified as thermochromic, if it responds to heat by changing colour, thermotropic, if it responds to heat or temperature by a change of transmission, electrochromic, if the change of colour is the reaction to an applied electric field or current, and photochromic, if it responds to light only.

Electrochromic systems and entirely passive thermotropic shading systems are currently being developed. The characteristics of these switchable glazings are illustrated in figure 15. With electrochromic switchable glazings the glass is coated with a flexible polymer film encapsulating tiny spheres of liquid crystals. The liquid crystals scatter incoming light when the spherical walls of the cells are nonaligned. Light passes uninterrupted through a panel, when a rheostat–controlled electric field aligns crystals within cells.

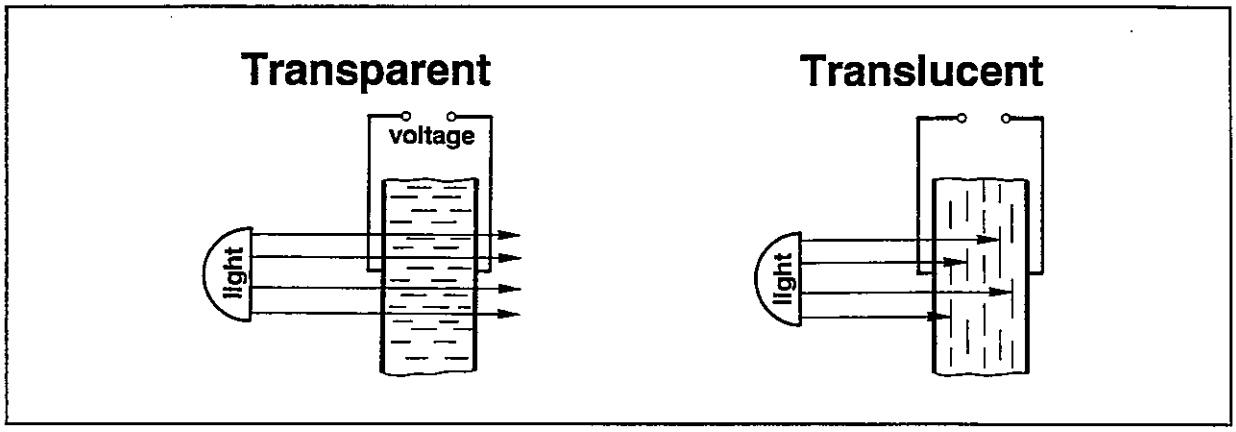

Fig. 15: Characteristics of an electrochromic switchable glazing.

The most cost–effective technology seems to be the thermotropic "TALD" gel [20]. In a ground state at low temperature this material has a clear transparence. With

increasing temperature, clouding occurs due to dissolved water molecules and increasing molecular chains within the gel. The clouding point can be regulated within a wide temperature range. A concept drawing of a glazing element with thermotropic sun protection system is shown in figure 16.

TEMPORARY INSULATION SYSTEMS

To avoid overheating, transparent thermal insulation can also be constructed as moveable systems, which may temporarily be removed or put away from the wall.

OTHER SOLAR SHADING DEVICES

In some cases, cantilevered building components or naturally growing vegetation are sufficient as shading devices.

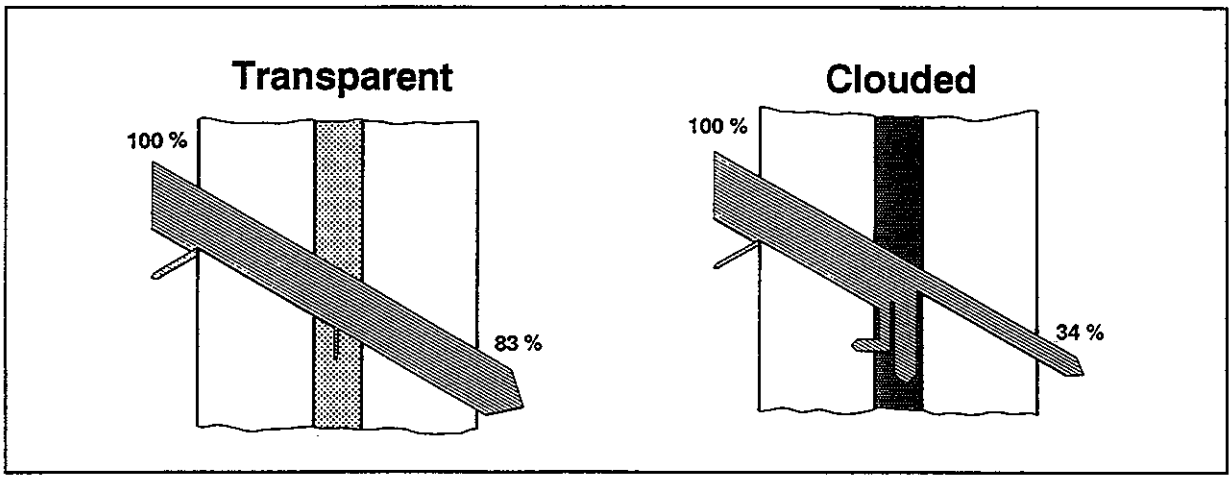

Fig. 16: Concept of a glazing element with thermotropic sun protection system.

UNCONTROLLED SYSTEMS

One of the most promising solutions for solar shading is represented by Lamella grids. The effect is based on angle-dependent light transmittance: for the low position of the winter sun it has the highest light transmittance, for the high summer sun position, the reflection of the lamella grid has its maximum.

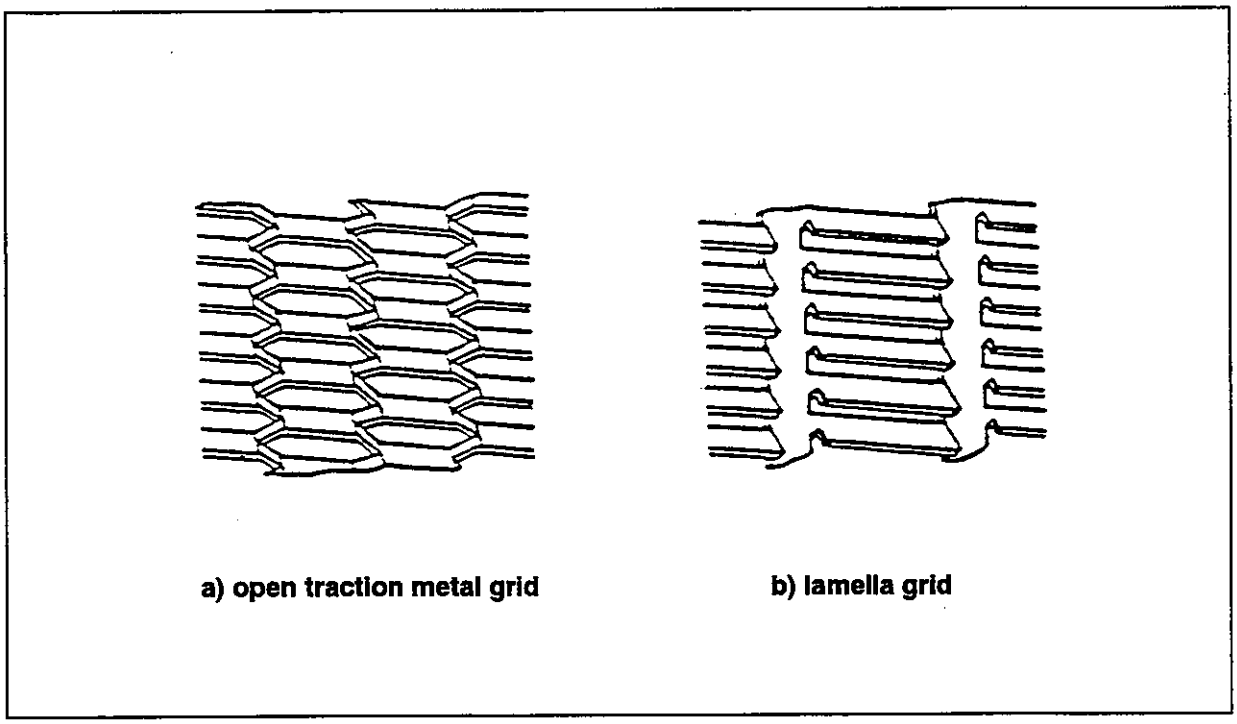

Fig. 17: Perspective drawings of two types of uncontrolled shading device systems [30].

Advantages of this system are :

- The "glass house" look is avoided and many design options are possible,
- the shading properties can be calculated,
- it has no movable components and thus no operating costs,
- serving as a mechanical and weathering protection, it can replace the glazing covering,
- it enables a low-cost system.

Disadvantages of this system are :

- only direct solar irradiation is controlled,
- during winter the high-angle diffuse radiation is not utilized, whereas in summertime the low-angle diffuse radiation will be transmitted,
- the facade is permanently shaded by the vertical parts of the grid structure ,
- the horizontal slats allow maximum transmittance for only one azimuth hour angle, the resulting hourly variations are of a sinuous character.

Movable lamella grids that are controlled according to the changing position of the sun might be the optimum solution, but optimum energy savings have to be compared to associated extra costs.

VENTILATED SYSTEMS

Overheating can be avoided by more than just shading devices. Another way is to move the extra heat gains to another location or to store the solar gains within the building construction.

If an air space is left between insulation layer and wall, it is possible to ventilate the system employing the heated air. This is illustrated in figure 18.

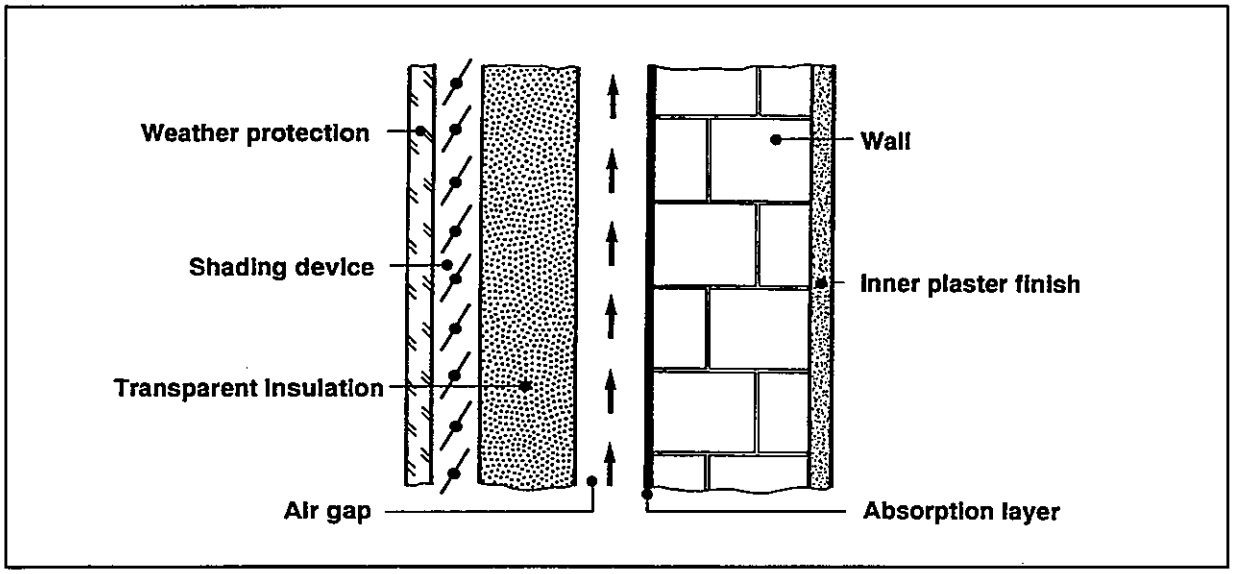

Fig. 18: Transparent insulation systems installation with air gap between insulation layer and wall.

In an open circuit, the heated air flows directly into the interior rooms. In a closed circuit, it passes through internal thermal storage. In principle, internal building components can store and transport heated air, if they are constructed as building components with a hollow core (walls and ceilings, compare figure 19). Such systems are currently being developed.

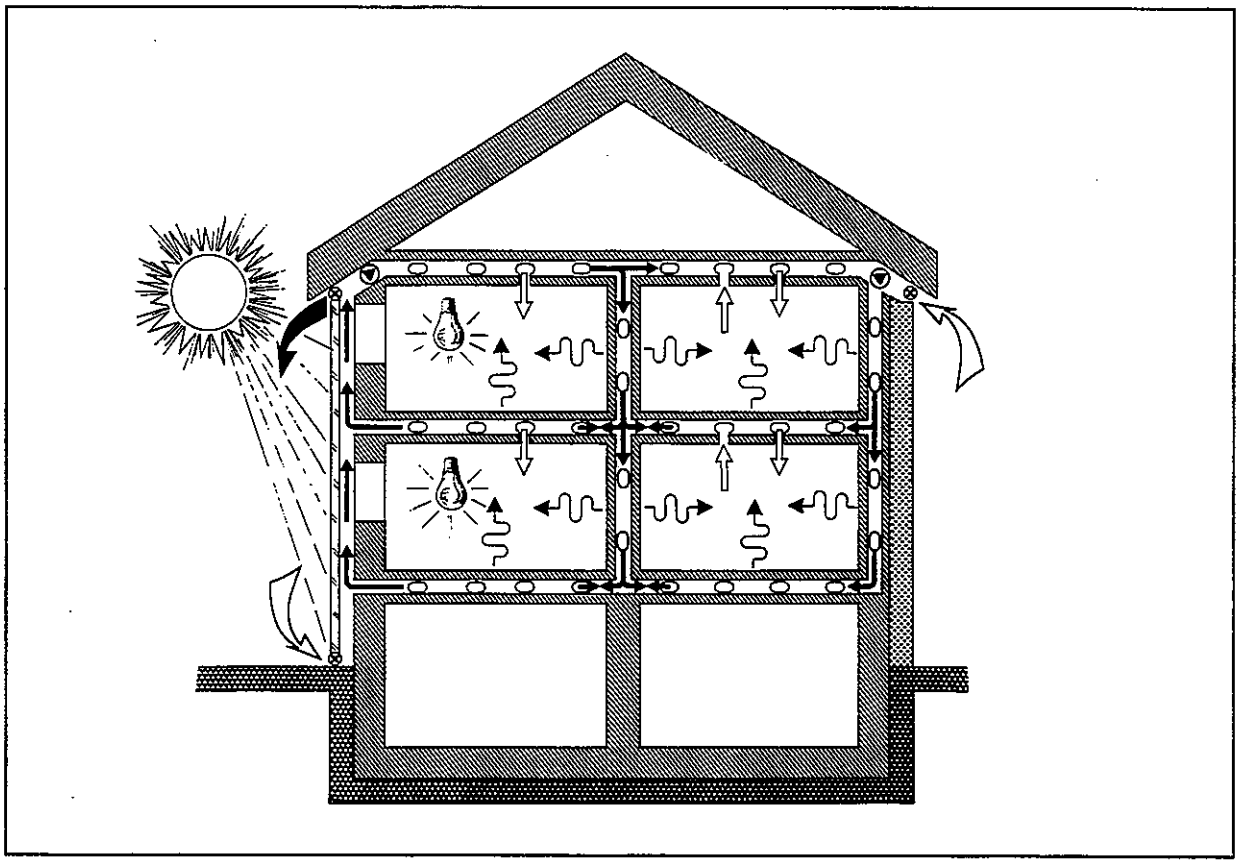

Fig. 19: Schematic representation of a hybrid system with air supplied hollow core slabs for thermal storage by interior building components.

WATER–COOLED SYSTEMS

Domestic water can be heated by running it through water pipes laid along the external wall surface. If there is not enough solar radiation for heating the water, it can thus at least be preheated. Such systems can be installed without solar shading devices, since solar radiation can also be used during summer, making the installations cost–effective. Additional pipes enhance the storage capacity of the external wall, and reduce the thermal stress the wall construction is exposed to. For this reason, lightweight building materials may also be employed for constructing water–cooled systems. For the actual construction, however, careful dimensioning is required.

7. MONITORING RESULTS

The thermal behavior of a wall with transparent thermal insulation is illustrated by the example of a winter day and night measurement in figure 20. Indicated are the time profiles of radiation intensity, outside and inside air temperatures and wall surface temperatures. Also shown are the heat flux density measured at the interior wall surface of a 200 mm concrete wall provided with a transparent insulating system (U-value: 1.3 W/(m^{2}K, diffuse transmissivity: 0.6). As can be seen, indoor air temperatures are rising only slightly after a strong peak of solar radiation while inside surface temperatures are substantially increased as there is a heat gain through the wall, peaking six hours after the solar peak. The maximum temperature of 43 °C of the exterior wall surface is reduced because of damping within the wall to about 30 °C at the interior surface. At noon and during the whole night, the heat flux within the wall is directed to the inside.

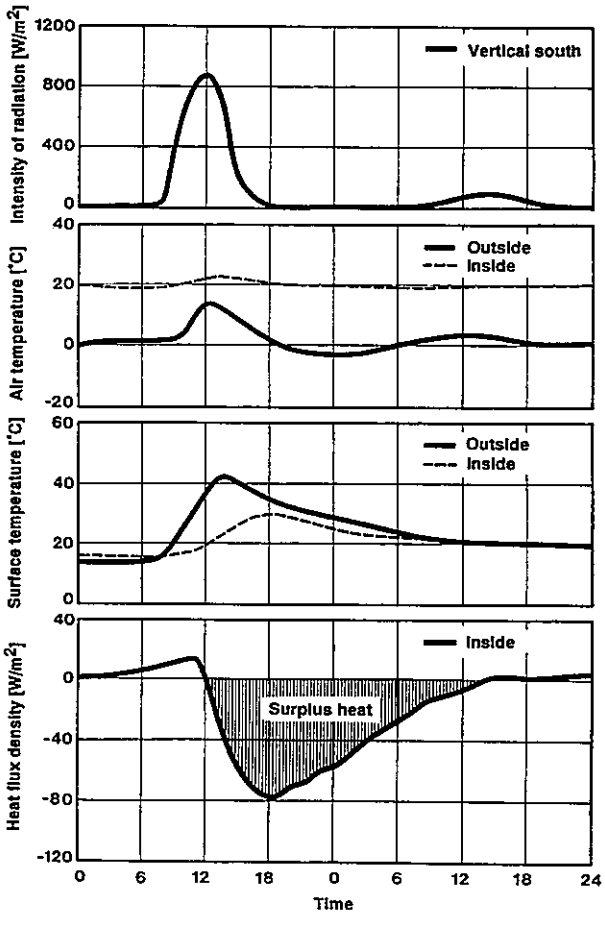

Fig. 20: **Measurement cycle (24 hours) of a 200 mm concrete wall with transparent insulation.**

WALL MATERIAL AND THICKNESS

The thermal capacity of the wall induces a damping of the temperature amplitude from the outside to the inside and a phase shift between the solar supplies from outside and the useful heat transmitted into the room, see [21–29]. Table 2 presents the measured phase shifts and ratios of amplitudes for five different wall constructions covered by the same transparent insulation (U–value of TIM–layer = 1.1 W/m²K, solar transmissivity = 0.5). Also compared are the wall's maximum surface temperatures.

Table 2: **Delay and temperature amplitude damping and thermal behavior of different test wall constructions, covered by the same TIM–system.**

Wall construction		Phase shift	Ratio of amplitudes	Max. surface temperature [°C]	
Material	Thickness [mm]	[h]	[-]	exterior	interior
Porous brick	365	14.0	0.04	73	24
	240	6.8	0.11	64	27
Limestone	240	6.2	0.14	53	26
Floating brick	240	5.6	0.19	51	27
Heavy concrete	200	4.0	0.46	43	31
	50	0.8	0.78	51	45
Cellular concrete	50	1.2	0.65	103	67

In Table 3 the effective U–values of various south–oriented wall constructions covered with TI materials are given (same TI material as in table 2). The effective U–values were obtained by way of experimental investigations.

Table 3: **Influence of different construction materials on the effective U–value of walls with transparent insulation (with surplus heat (N=1), without surplus heat (N=0).**

Construction material	Wall-thickness [mm]	U-value [W/m²K]	Effective U-value [W/m²K]	
			N = 0	N = 1
Vertical core brick	365	0.5	0.25	-0.3
Light brick	240	0.7	0.31	-0.15
Limestone	240	0.8	0.32	-0.22
Pumice concrete hollow block	240	0.8	0.31	-0.22
Heavy concrete	200	1.0	0.41	-0.30
Normal concrete	50	1.3	0.54	-0.16

Table 4 illustrates the influence of the insulating system on the thermal performance of a 200 mm south–oriented concrete wall. With solar radiation transmissivities ranging from 0.2 to 0.6, and U–values between 0.9 and 1.6 W/m²K, the exterior wall surface temperature is between 32 °C and 52 °C.

Table 4: **Influence of transparent insulating layer on the thermal behavior of a 200 mm south–facing concrete wall.**

Transmissivity [-]	U-value [W/m²K]	Max. surface temperature [°C] exterior	interior
0.6	1.0	52	33
0.6	1.1	46	32
0.5	1.1	44	30
0.5	1.6	38	29
0.4	0.9	40	29
0.3	1.2	32	26
0.2	1.0	33	26

Measurements on the solar transmittance of a lamella grid construction according to [30] are listed in Fig. 21. Results are based on measured data at an angle of incidence of 0° (horizontal to plane of lamella) and 90° (perpendicular to plane of lamella).

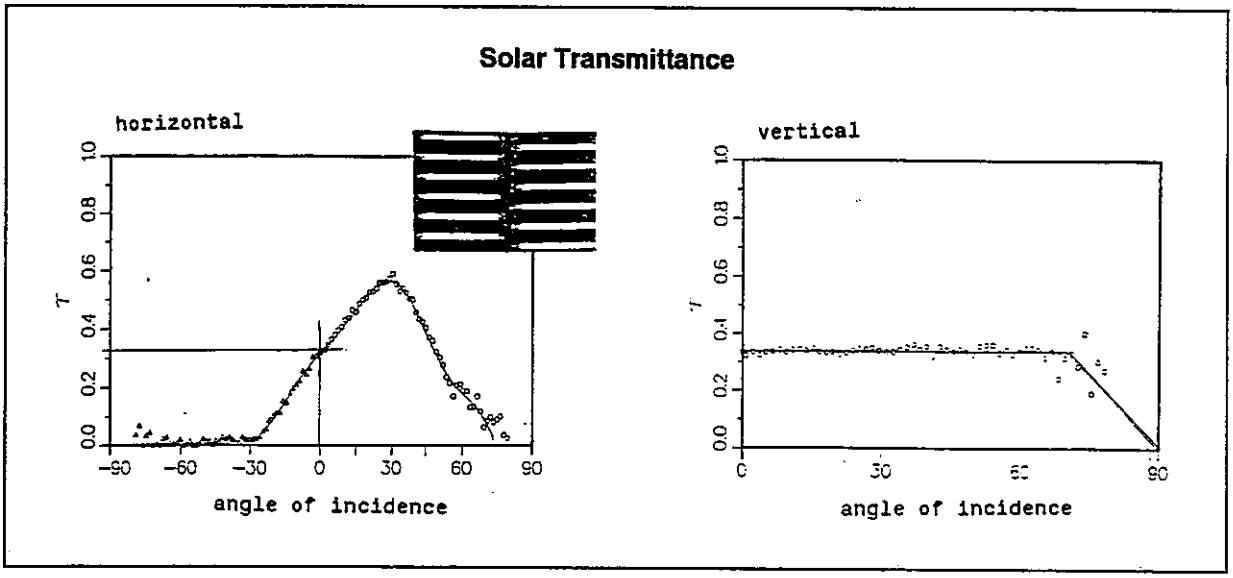

Fig. 21: **Measurements on lamella grid construction #3. The solar transmittance has been monitored for two extrema of the angle of incidence.**

8. SIMULATION OF TIM–SYSTEMS

Several investigations have been carried out to develop algorithms for simulating TIM–systems. Two aspects have been considered:

a. Algorithms for calculating light transmittance of TI–Materials;
b. Algorithms for calculating solar transmittance of TI–Materials;

Investigations of the first aspect will result in subroutines which are used for integration within daylighting simulation programs (see Appendix A). Subroutines of the second aspect already have been integrated in building energy analysis simulation programs.

a. Algorithms for calculating solar transmittance of TI–Materials

The thermal behaviour of TIMs can be translated into a calculation model in various ways. For detailed calculations, which are primarily directed to the level of behaviour of the material, specific computer programs are used and developed for research institutes in this field. For simulation of temperatures and heating loads within a total model of (part of) a building often less accuracy will suffice as regards the algorithms simulating the material.

On the basis of optical formulae (Fresnel and others), an hourly transmission coefficient for direct and diffuse radiation is calculated for each transparent element (optionally after making a shading calculation). Also the per layer amount of absorbed solar energy is calculated and according to a resistance model divided into an in–flowing source term and an out–flowing portion. More detailed computer models for (multi–zone) energy simulation of a building make use of this physical model for transparent elements.

Computer models based on homogeneous isotropic, planoparallel layer structures are unsuitable for several types of transparent insulation materials (for instance capillary and honeycomb structures). Moreover, the convection flows and the temperature dependence of thermal resistance are not modeled in detail. At a high temperature in a TIM wall, this may lead to inaccuracy. In general, algorithms determining solar transmittance of transparent insulation materials can be integrated

within a building energy analysis simulation program in a way, illustrated in figure 22, which represents a thermal model of walls covered by transparent insulation materials :

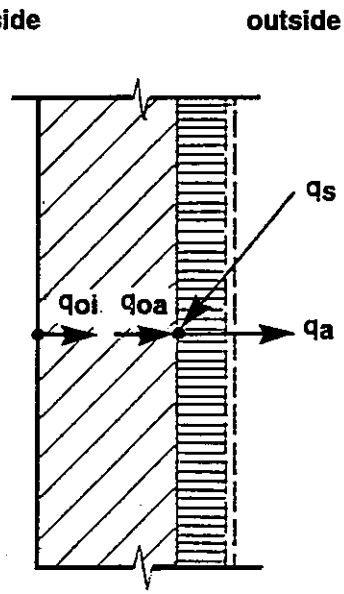

q_s : absorbed solar radiation

q_{oi} : interior heat flow of wall construction

q_{oa} : exterior heat flow of wall construction, excl. q_s

q_a : exterior heat flow of wall construction, incl. q_s

At the absorber surface following balance has to be fulfilled :

$$q_{oa} + q_s = q_a$$

Fig. 22: Schematic drawing of a thermal model of a wall covered by transparent insulation material according to [30].

Calculation of solar gain q_S is based on determination of solar transmittance, which is separated into a constant value for the diffuse radiation part and an angle dependent direct radiation part.

b. Algorithms for calculating light transmittance of TI–Materials

Concerning the daylighting behaviour of TIMs, the light scattering effects within each transparent insulation layer and the succeeding scattering characteristism of the complete element backside facing to room are of special importance.

The majority of algorithms developed concentrate on the energetic aspect of transparent insulation materials.

Overview about transparent insulation material modeling activities

1. Building daylighting analysis simulation

A simple algorithm for calculation of the angle dependent light transmittance (both sides) through TIM honeycomb material based on monitored material data has been derived according to [31]. The algorithm serves to calculate the angle distribution of radiation within the visible range behind of a TIM–window system. The basic formula for calculating the angle dependent total light transmission has been modified to establish a relationship to monitored data. It is intended to integrate the algorithm within the daylighting analysis simulation program SUPERLITE. A detailed description of the algorithm according to [31] is listed in Appendix A.

2. Building energy analysis simulation

Within the simulation support group of IEA TASK 13, Netherlands has prepared a report [32], called "Technology Simulation Set", in which integration of TIM–simulation on four different levels of simplifications into the building energy analysis simulation program SUNCODE–PC is described in detail (see Appendix B). Two activities have been carried out in Germany. The first activity was a participation within a Swiss research project, providing a subroutine for TIM–simulation. The source code of this subroutine is published within the report [30] (see Appendix C). The second activity has been taken within a national project establishing a simple algorithm for calculating the total solar transmittance of TI–Materials [33] as a stand alone PC–program (see Appendix D) and subroutines considering different

transparent material structures [34] (see Appendix E); especially for honeycomb systems, a PC-program (GWERT) [35] is available. As the total solar transmittance is a typical characteristic of window systems, this kind of simplification for calculating TI-Materials enables the use of such results as input for any building energy analysis simulation program. A TIM-system is then introduced as a special window system type. Such simplification is able to handle the energetic aspect of TIM-system in interaction with a building energy balance sufficient accurately but cannot provide exact results concerning dynamic temperature behaviour within a TIM-system. The main advantage however is the creation of an easy input by a minimum effort and optimizing of computation time.

The above described investigations provide a wide spectrum of possibilities to simulate TIM-systems. Main results and conclusions of several parameter sensitivity studies will be presented in the following section.

9. SIMULATION RESULTS

USE OF SURPLUS HEAT

Depending on radiation intensity and outdoor air temperature, transmission heat flow losses are more or less reduced. The direction of heat flux in winter may be temporarily reversed from the outside to the inside, the transparently insulated wall working as a heater and serving as heat storage. Its thermal capacity induces a damping of the temperature amplitude from the outside to the inside and a phase shift between the solar supplies outside and the useful heat transmitted into the room. The kind of insulation system, wall material and wall construction selected influences the way surplus heat is used. The amount of generated surplus heat and its useability are dependent on the storage capacity of the external walls, the phase shift of temperature amplitudes and the maximum interior wall surface temperature. Useability requirements have to be considered when determining the dimensions of insulation systems.

The effective heat flux density is the integral mean value of heat flow densities variable in time:

$$q_{eff} = \left(\sum_{i}^{nhr} q(t) \cdot \Delta t \right) / nhr$$

with : heat flux density q(t)
hours of observation nhr

The quotient of effective heat flow density (average of observation period) and the difference between the air temperatures on either side of the wall (q_i, q_e)is indicated as the effective U–value:

$$U_{eff} = \frac{q_{eff}}{\theta_i - \theta_e} = \frac{q_{eff}}{\Delta\theta}$$

This value assumes the heat gains (solar storage by TIM–system) to be useful. Further differentiation is possible: disregarding heat gains, an upper limiting value for the effective U–value is calculated using this equation for heat loss Q_L:

$$U_{eff\ (N=0)} = \frac{Q_L}{\Delta t \cdot \Delta\theta}$$

Including the heat gains Q_G (solar storage by TIM system), the lower limit for the effective U–value is obtained as follows:

$$U_{eff\ (N=1)} = \frac{Q_G + Q_L}{\Delta t \cdot \Delta\theta}$$

This approach for the examination of the wall construction should only be used when ideal boundary conditions are being assumed, since these values do not apply for actual constructions.

ORIENTATION

An overview of the energetic performance under different orientations is given in figure 23. It presents the mean of heating period of the effective U–values with surplus heat (N=1) and without surplus heat (N=0) of the 200 mm transparently insulated concrete wall. The calculations are based on a U–value of 1.1 W/(m²K) and a solar transmissivity of 0.46 under average German climate conditions in Stuttgart. The smallest losses and the largest gains were observed at south facades, the effective U–value being reduced from 1.0 to –1.7 W/(m²K). Significant reductions in heat losses were also obtained at north walls.

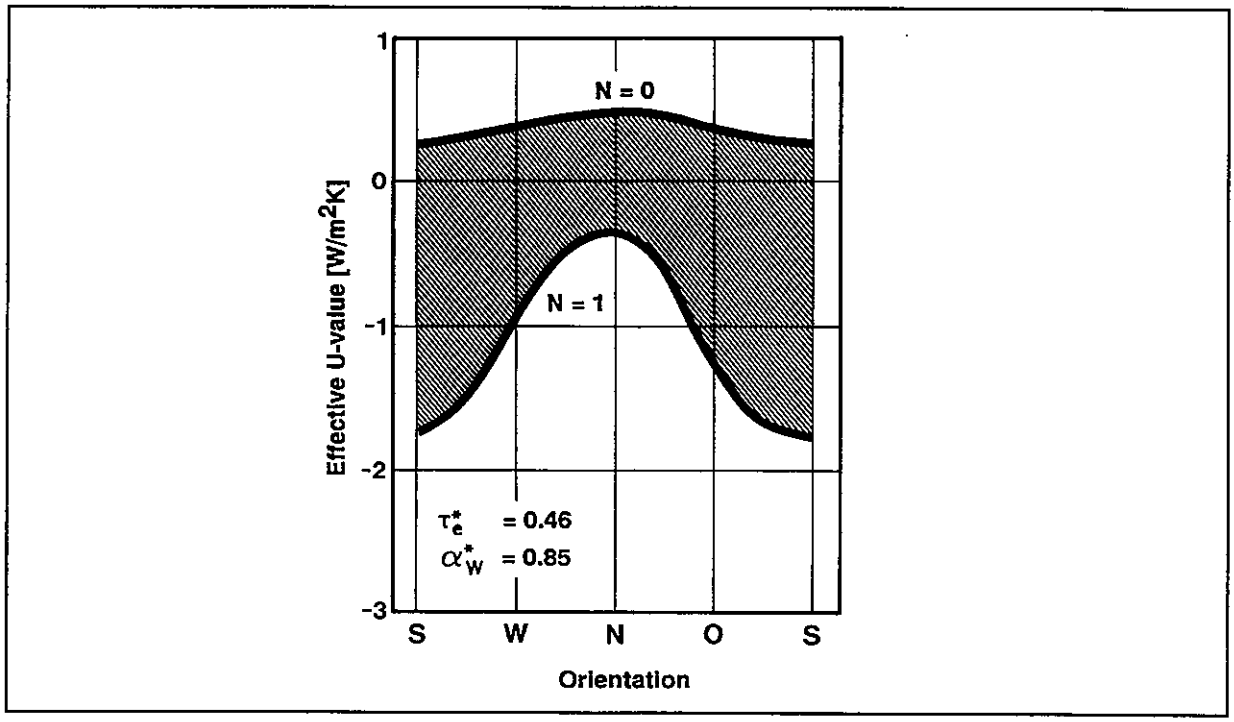

Fig. 23: The influence of orientation on the energetic performance of the wall with transparent thermal insulation (Example: 200 mm concrete wall).

The peak value of thermal exposure is approximately the same for south, east and west walls. However, there is a difference with regard to the time when maximum temperatures occur. As illustrated in Table 5, thermal stress peaks occur in summer for east and west walls, in spring and autumn for south walls.

Table 5: **Influence of orientation on the thermal behaviour of a wall with transparent insulation (200 mm concrete wall).**

Orientation	Season	Max. surface temperature [°C]	
		exterior	interior
South	Autumn	43	31
East	Summer	39	29
West	Summer	42	30

COLOUR OF ABSORPTION LAYER

The colour of the insulation material also influences the energetic performance of transparently insulated facades. The values of solar absorptance are 0.39 for white, 0.91 for black and 0.98 for selective black. Differences in selective tint more or less influence the solar absorptance. The impact of different solar absorptances on the energetic performance is illustrated in figure 24 for the 200 mm transparently insulated concrete mass wall.

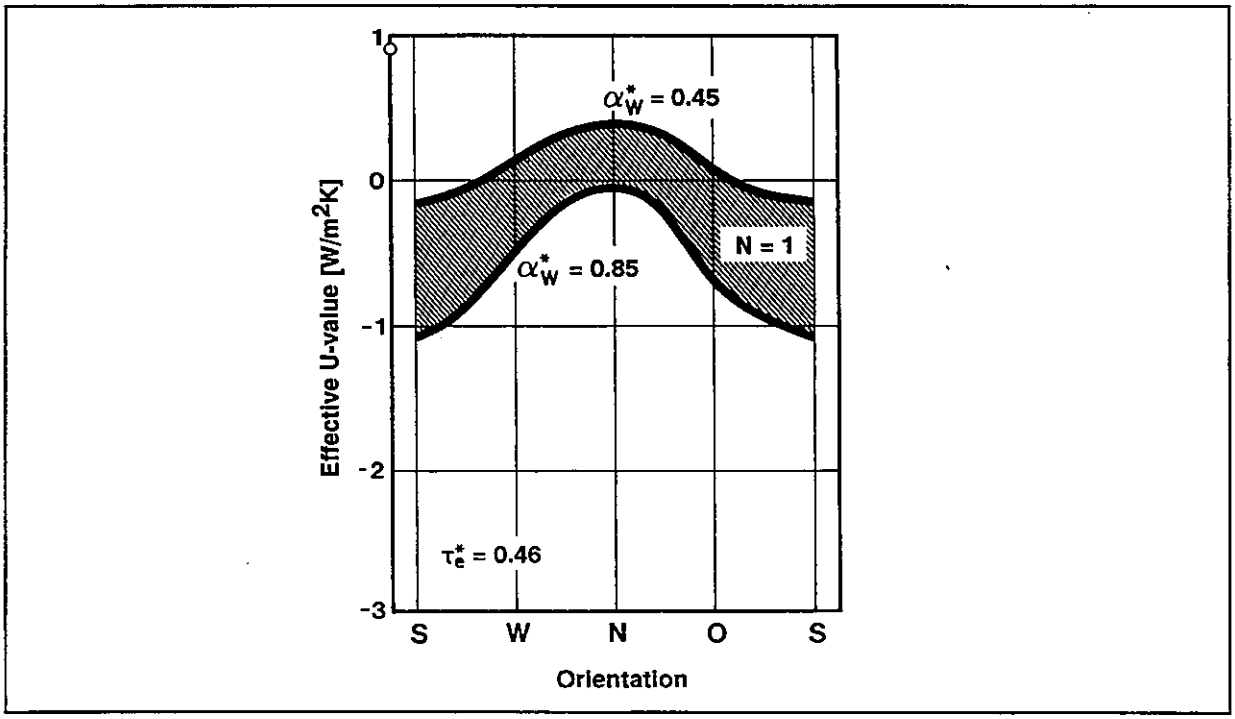

Fig. 24: **The influence of solar absorption on the energetic performance of a wall with transparent thermal insulation. (Example: 200 mm concrete wall).**

Thicker transparent insulation layers result in a lower 'U'–value. However, they are also the cause for a lower degree of transmissivity and a decrease in solar gains. The interdependence of the two effects leads to climate– and material–dependent optimum values of layer thickness. Figure 25 identifies various materials applied to a south–oriented, 200 mm concrete wall under moderate, central European climate. In cases where the degree of radiation transmission varies strongly due to the layer thickness, optimum values for materials with high scattering effects range even below 50 mm – under moderate climate conditions. In climates with stronger radiation, a higher degree of radiation transmission can compensate for lower levels of insulation, and vice versa.

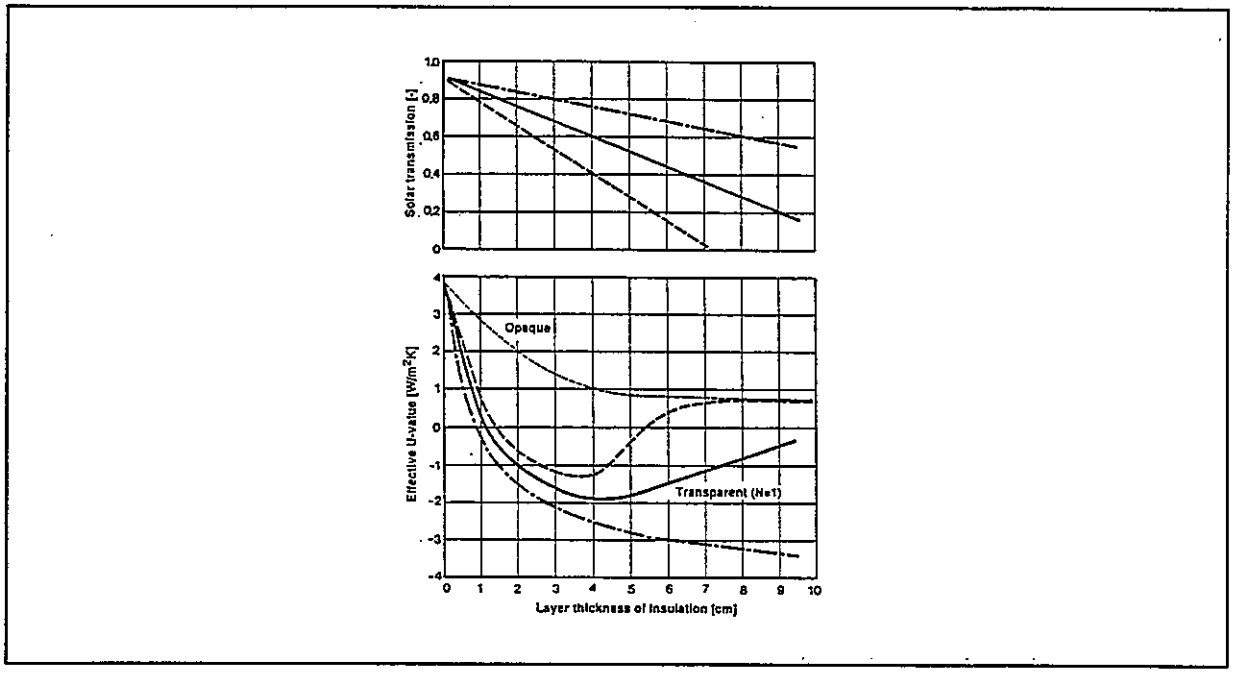

Fig. 25: Influence of layer thickness of different transparent insulating materials on the effective U–value (Example: 200 mm south oriented concrete wall).

If the surplus heat is disregarded, the effective U–values amount to half of the theoretical values. With surplus heat, gains are obtained for all constructions, the effective U–values being negative. The respective influences of different insulation layers are presented in Table 6. A visible reduction in the effective U–value is observed for radiation transmission degrees as low as even 0.3.

Table 6: **Influence of solar transmission of transparent insulation on the effective U-value of a 200 mm south facing concrete wall (N=1: with / N=0: no solar storage).**

Transparent insulation		Effective U-value [W/m²K]	
Transmission of solar radiation [-]	U-value [W/m²K]	N=0	N=1
0.6	1.0	0.14	-0.88
0.6	1.1	0.27	-0.84
0.5	1.1	0.41	-0.30
0.5	1.6	0.58	-0.13
0.4	0.9	0.35	-0.28
0.3	1.0	0.48	0.26

INFLUENCE OF CLIMATE

The solar contribution to heating achieved by using transparent thermal insulation can be summarised by way of the following definitions:

Insolation E [kWh/m²] :

$$E = \sum_i I_i \cdot \Delta t$$ with : solar irradiation I_i [kW/m²]

and **degree-day** DD [Kd] :

$$DD = \sum_{n=1}^{z} (20 - t_{amb,n})$$ with : average daily (n) ambient temperature $t_{amb,n}$ days of heating period (z)

The so called **degree-day insolation fraction** represents the impact of climate:

$$E_{DD} = \frac{\text{Insolation}}{\text{Degree-days}} = \frac{E}{DD} \quad [kWh/m^2Kd]$$

Heat flows from the room to the wall are positive quantities (**heat losses** Q_L).

$$Q_L = \sum_i q_i \cdot \Delta t \qquad \text{for heat flux } q_i > 0$$

Heat flows from the wall into the room are negative quantities (**heat gains** Q_G) :

$$Q_G = \sum_i q_i \cdot \Delta t \qquad \text{for heat flux } q_i < 0$$

Figure 26 shows the influence of climate conditions on potential heat gains and heat losses for different insulation systems and wall constructions, as compared to opaque insulation. The heat flow through the wall is plotted in relation to the ratio of insolation per degree day (degree day insolation fraction) in monthly values.

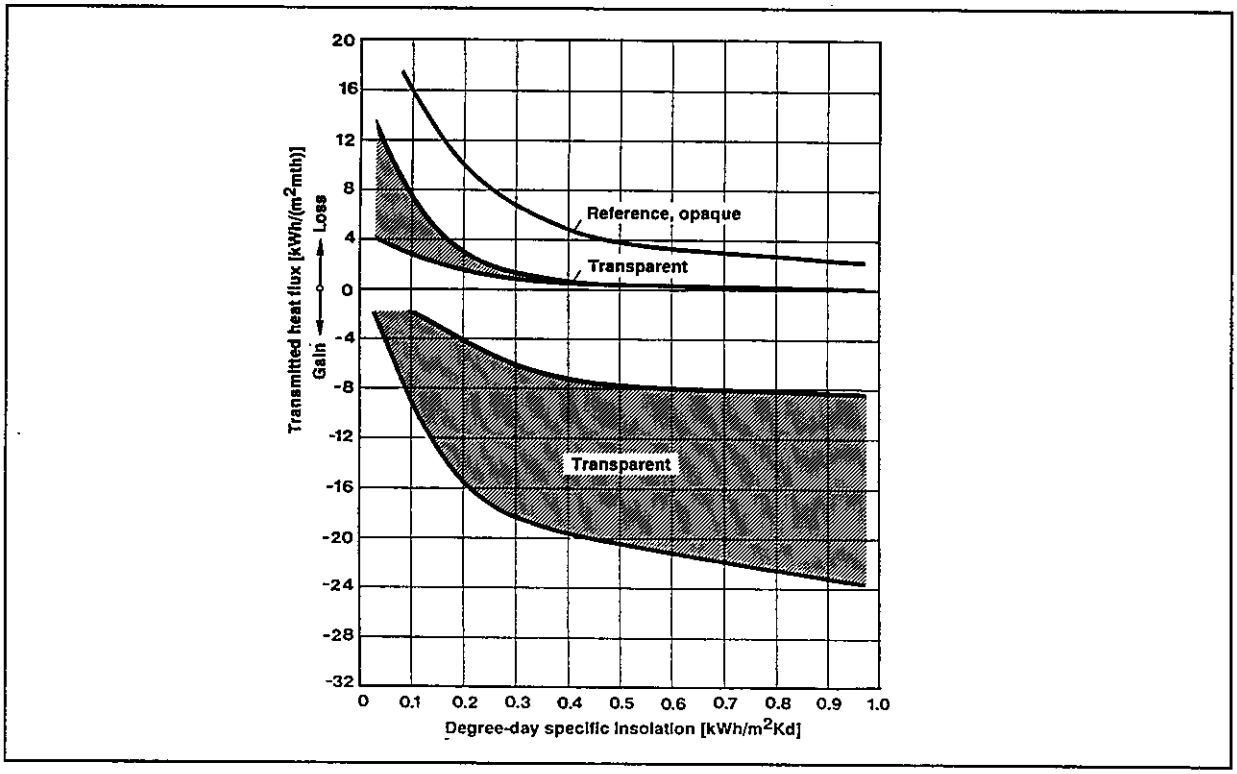

Fig. 26: Influence of climate on monthly heat gains and losses of transparently insulated mass walls.

Here, idealised interior boundary conditions are assumed, i.e. a constant temperature of 20 °C. The different, transparently insulated walls are presented in figure 26 (hatched section), as well as an opaquely insulated reference wall. At mean heating period temperatures the monthly heat loss of the opaquely insulated refe-rence wall is 13 kWh/m^2, or more than 100 kWh/m^2 per year. For walls equipped with transparent thermal insulation, the monthly heat transmission losses range between 2 and 6 kWh/m^2, counterbalanced by heat gains between 3 and 12 kWh/m^2. Due to the limited heat capacity of the external wall, heat gains can only be stored for one or two days. They are given off to the interior as surplus heat. Heat losses occur during prolonged periods of weak radiation, although in theory there is more than enough surplus heat to offset them. In figure 27, a hatched section separates the limiting values with and without surplus heat. Even in Shetland, where weak radiation pre-dominates, negative U-values can be obtained at mean heating period temperatures, implying that during the heating period, more heat is transmitted into the interior than given off through the wall.

Figure 27 displays the effective U-value of the 200 mm concrete wall, which depends on the degree day insolation fraction which is a function of climate. For evaluation, values characteristic for locations ranging from Shetland to Sicily are given. These values have been calculated for a transparent thermal insulation layer with a U-value of 1.1 W/(m^{2}K) and a solar transmission 0.5.

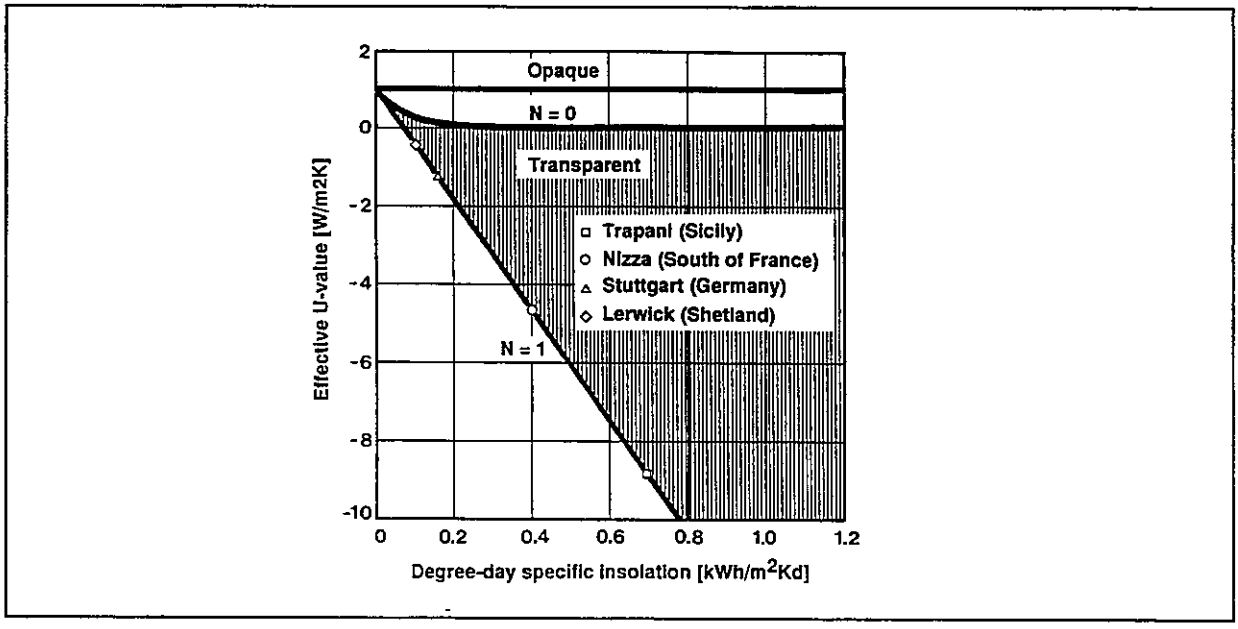

Fig. 27: **Influence of climate on the effective U-value of a transparently insulated wall (200 mm concrete wall).**

The solar contribution to the reduction of heat transmission losses SCT is given as :

$$SCT = \frac{\text{maximum HC} - \text{real HC}}{\text{maximum HC}}$$

where " maximum " means a heat consumption (HC) without solar gains. In figure 28. the relation of SCT is plotted versus monthly climate data for the range of different wall constructions and transparent insulating systems according to Tables 3 and 4.

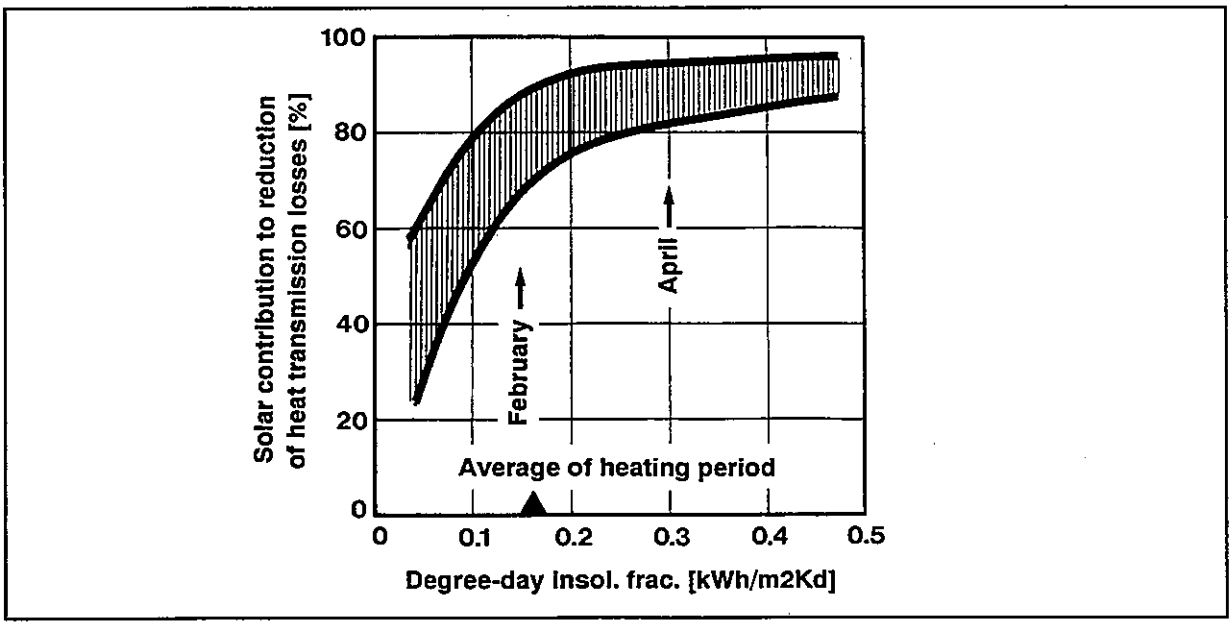

Fig. 28: Influence of climate on the solar contribution to reduction of heat transmission losses of transparently insulated mass walls.

Figure 29 shows the influence of climate conditions on the monthly solar fraction SFR of the different transparently insulated wall constructions.

$$SFR = \frac{\text{exploited insolation}}{\text{real insolation}}$$

Depending on climate, wall constructions and insulating systems, values of less than 0.1 and up to nearly 0.4 have been obtained.

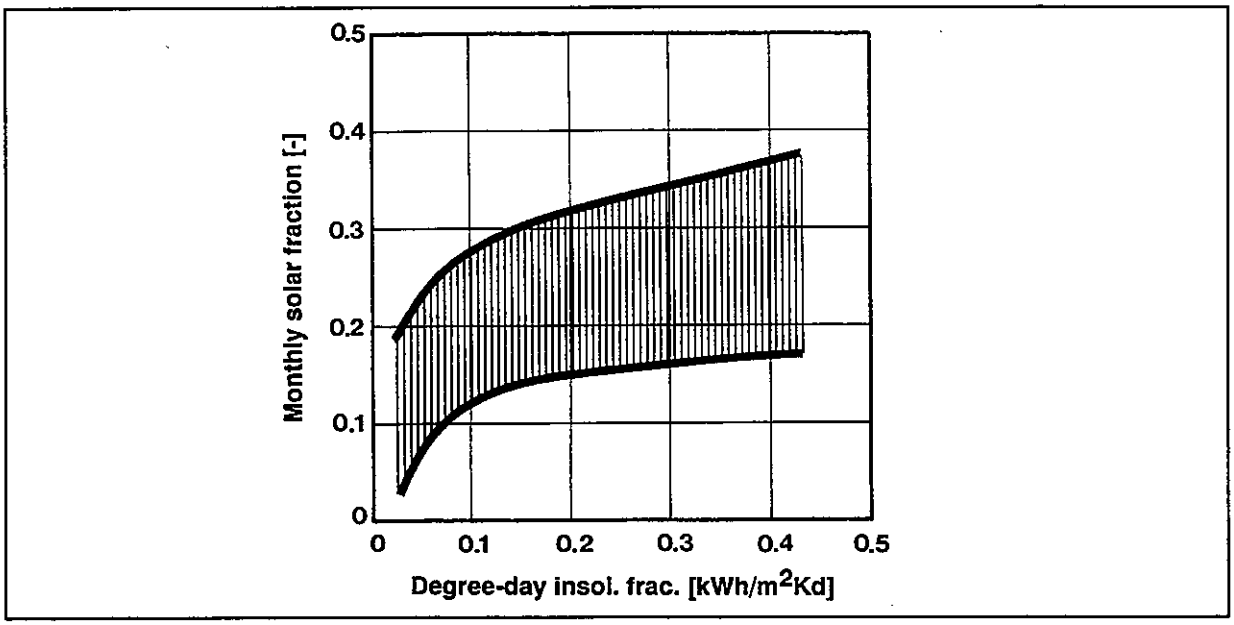

Fig. 29: Influence of climate on the monthly solar fraction SFR for a range of different wall constructions and insulation systems.

10. COST–BENEFIT RATIOS

The extra costs of a TIM–construction with solar controlled shading device compared to a conventional facade is in a range of 450 – 950 $ per m² facade area. The energy savings are 50 – 200 kWh/m²a in a middle European climate, compared to the insulation level according to actual requirements (U–value of exterior wall ca. 0.6 W/m²K). This is not cost effective. The only possibilities for improving this situation are either to try to increase the utilization of solar gains or to reduce the costs [36]. Sensitivity parameter studies have shown that the range for improving the TIM–system performance is relatively small, the most promising way remains in reducing the costs of a TIM–system.

The most promising economic solutions are TIM–systems with a minimum of movable components, i.e. metal facade with a lamella grid constant shading device. The extra costs of such a construction lie within 200 $/m² facade area. As this is a solar uncontrolled system the utilized energy savings are 30 – 40 % lower than obtainable by a controlled TIM–system.

11. CONCLUSIONS

ADVANTAGES

- In addition to the insulating effect, the TIM-system also provides heat gains from solar radiation.
- Solar heat gains are delayed, and therefore, compliment the immediate direct gains from windows.
- Compared to conventional wall construction, the interior wall surface temperature is warmer, thus improving thermal comfort.
- Higher wall surface temperatures reduce the risks of moisture penetration and the occurrence of surface condensation and mold.
- In combination with facade areas equipped with transparent insulation, TIM's lead to reduced heating loads.

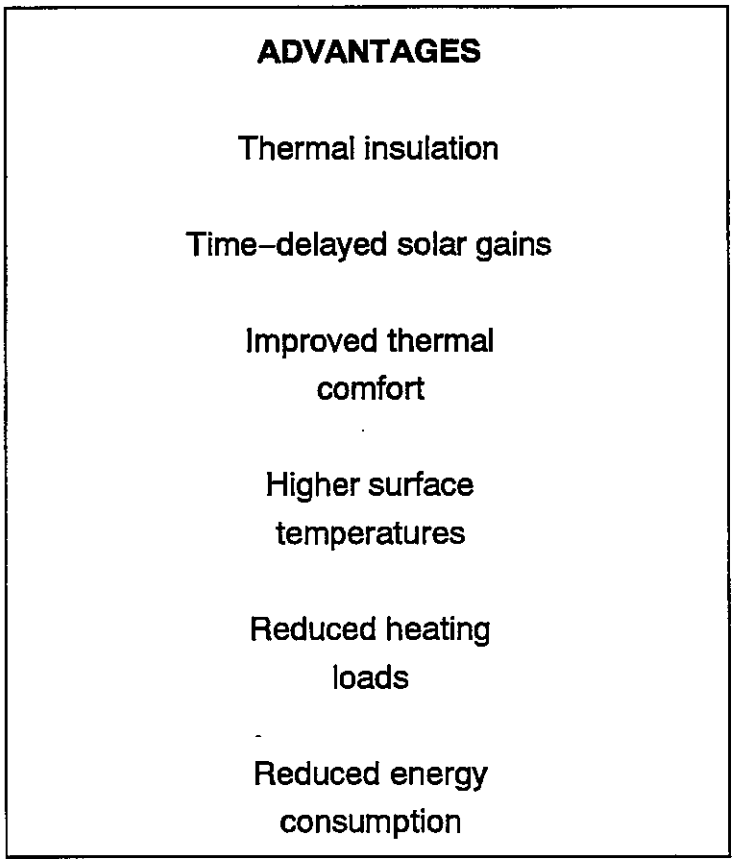

DISADVANTAGES

- The combination of various insulation systems and wall materials leads to different thermal performance of these wall constructions in relation to each other. An inappropriately designed system may result in an overheating of the insulation system and wall .
- During the warmer months of the year, it may become necessary to use solar shading devices to avoid overheating of interior spaces. This makes the system more expensive without enhancing its efficiency.
- Some materials have to be fitted to glass frames or have to be covered externally with glass panes. Hence, these materials have to be mounted to the building facade with the help of frame systems. Their application becomes more costly and may spoil the visual aspect of the building.
- Applications of this system to walls built out of highly insulating building materials and to thin walls of low storage capacity may result in high temperatures inside the wall .
- The fire behaviour of some materials is inappropriate.

EXPERIENCE FROM TESTS AND COMPUTER MODELING

The following issues have been identified:

- Massive concrete walls result in the highest solar utilization. Minimum wall thickness should be 15 cm to avoid overheating and to receive a time phase shift against direct gains through windows.

- Massive clay walls only achieve half of the solar utilization as concrete ones. The heat transmission through the wall is relatively low and high temperature on the exterior (absorption) surface causes high thermal losses to the ambient.

- Performance of lime brick walls are between that of concrete and clay.

- Exterior plaster layer covering a clay brick wall does not improve the overall system efficiency, but damps the maxima of absorber–temperatures.

- South orientation is very important. A deviation of only 45° from South reduces the total solar gains by 20 %. On the other hand north oriented TIM–walls will achieve a positive energy balance over the heating period if transparent insulation is thicker than 10 cm thickness. The diffuse radiation is sufficient to compensate the average losses of a heating period.

The solar gain utilization is coupled to a fast reacting back–up heating system, which is automatically sensible to occurance of internal gains. For storage of surplus gains, it is necessary to allow room temperatures up to 24°C. Buildings with a high envelope insulation level and of partially low mass construction do have sufficient storage mass. Although within highly insulated buildings, a competitive situation between internal gains, direct gains through windows and indirect gains by TIM–systems occurs, auxiliary heating displacing energy achieves ranges of 50 – 200 kWh/m² TIM facade and heating season.

Careful detailing and dimensioning can preclude damage to wall construction and thermal insulation exposed to the severest thermal conditions. In old buildings, wall construction has to be checked for inhomogeneities. In modern buildings, the phase change of temperature amplitudes and the variations of amplitudes in time have to be

adapted to requirements for use. For the dimensioning of the system, either of two strategies can be adopted:

(1) Optimisation of heat gains related to facade area

(2) Minimisation of heat consumption related to living space.

In general, the optimisation of heat gains related to facade area will always result in partial coverage with transparent thermal insulation. The smaller the amount of transparently insulated facade surface, the larger the heat gains related to facade area, because a larger quantity of the temporarily generated surplus heat can be used. Variations with opaque thermal insulation for remaining areas may lead to the same trend in terms of energy consumption.

12. References

[1] Platzer, W.J.: Transmittance characteristics of transparent insulation materials. Proc. 1st Int. Workshop TI1 " Transparent insulation materials for passive solar energy utilization ", 27.–28.Nov.1986, L.F. Jesch (Hrg.) (1987) p. 20–22.

[2] Platzer, W.J.: Komponenten und Materialien für die passive Nutzung der Solarenergie. Tagungsbericht 6. Int. Sonnenforum, Aug. 1988 Berlin, Band 1 (1988) S. 303–310.

[3] Platzer, W.J., Wittwer, V.: Total Energy Transmission of Transparent Insulation Materials. Proc. Workshop on Optical Property Measurement Techniques, Ispra, Italy, 27–29 Oct. 1987.

[4] Platzer, W.J.: Total Heat Transport Data for Plastic Honeycomb–type Structures. Solar Energy, Vol. 49., No. 5, pp. 351–358, 1992.

[5] Schreiber, E.; Boy, E. and Bertsch, K.: Aerogel as a Transparent Thermal Insulation Material for Buildings. Proc. of the First International Symposium on Aerogels. Springer Verlag, Berlin Heidelberg (1985).

[6] Wittwer, V.; Dengler, J., Platzer, W.: Transparent Insulation Materials. Proc. Symosium on Optical Material Techniques for Energy Efficiency and Solar Conversion XI, 19–21 May 1992, Toulouse.

[7] Wittwer, V.; Platzer, W.: Transparent Insulation Materials. Perspective in energy, 1991, volume 1, pages 59–69.

[8] Platzer, W.J.: Licht und Wärme; Entwicklungslinien bei TWD–Materialien. Sonnenenergie, Heft 2, Apr. 1992.

[9] Wittwer, V. et al.: Translucent Insulation Materials. Proc. INTERSOL 85, Montreal (1985).

[10] Hollands, K.T.: Designing honeycombs for minimum material and maximum transmission. Proc. of the 2nd Int. Workshop on Transparent Insulation, p. 40–42, Freiburg (1988).

[11] Rubin, M.; Lampert, C.M.: Transparent Silica Aerogels for Window Insulation. Solar Energy Materials 7 (1983), p. 393–400.

[12] Tewari, P.H. u.a.: Advances in Production of Transparent Silica aerogels for Window Glazings. Proc. of the First Int. Symposium on Aerogels, p. 31–37. Springer Verlag, Heidelberg und Berlin (1985).

[13] Platzer, W.J.: Directional–hemispherical solar transmittance data for plastic honeycomb–type structures. Solar Energy, Vol. 49., No. 5, pp. 359–369, 1992.

[14] Platzer, W.J.; Bennewitz, P.A.; Wittwer, V.: Measurement of hemispherical solar transmittance of structured materials like transparent insulation materials. Symposium Optical Materials Technology for Energy Efficiency and Solar Conversion IX. 12–13 March 1990, The Hague, Netherlands. Proceedings SPIE volume 1272, p.297–308.

[15] Platzer, W.J.; Bergkvist, M. : Bulk and surface light scattering from transparent silica aerogel. Symposium Optical Materials Technology for Energy Efficiency and Solar Conversion IX. 19–21 5.1992, Toulouse, France. Proceedings SPIE volume 1727, p.297–308.

[16] Dengler, J., Diegmann, V.; Platzer, W.; Wittwer, V.: Direkte Bestimmung von diffus–hemisphärischen Transmissions– und Reflexionsgraden von transparenten Wärmedämmungen, Fensterelementen und Abschattungs–vorrichtungen. 8. Internationales Sonnenforum, 30.6–3.7 1992, Berlin, Tagungsbericht Teil 1, S. 189–194.

[17] Lampert, C.M., Omstead, T.R. and u, P.C.: Solar Energy Materials 14 (1986) p. 161.

[18] Krochmann, J.: Lichttechnische und strahlungsphysikalische Daten von Isoliergläsern. XXXI/85 A. Berlin University (1985).

[19] Ortmanns, G. and Fricke, J.: Moderne Fenster. Physik in unserer Zeit 19 1 (1987) 1–7.

[20] Boy, E. und Meinhardt, S.: Self regulating, temperature-dependant solar screens. TALD – a temperature controlled variable transparent glass. Building Research and Practice 16 (1988), H. 4, S. 227–230.

[21] Boy, E.: Experimental Investigations of Passive Solar Energy Utilization of Transparent Insulated Walls. Proc. of the ISES Solar World Congress, Hamburg (1987).

[22] Boy, E. and Bertsch, K.: Transparente Wärmedämmung: Wärmedämmung und passive Solarenergienutzung in einem System.wksb 32 (1987) vol 22, p. 29–33.

[23] Boy, E.: Transparente Wärmedämmung im Praxistest – Zwischenergebnisse aus einer zweijährigen Untersuchungsperiode. Bauphysik 11 (1989), H. 2, S. 93–99.

[24] Goetzberger, A., Gertis, K.A. et al.: Transparente Wärmedämmung. Final Report on BMFT Project 03E–8411–A. IRB Verlag, T 1830, Stuttgart (1988).

[25] Grochal, P.; Hegen, D.; Boy, E.: Entwicklung eines fugenlosen transparenten Wärmedämmsystems. BMFT–Statusbericht 1989: "Energetische Optimierung der Solarapertur", S. 301–313. Fachinformationszentrum Karlsruhe (1989).

[26] Werner, H.: Zwillingshäuser des Fraunhofer–Instituts für Bauphysik. Untersuchung energiesparender Maßnahmen. TAB (1983), H. 1, S. 15–19.

[27] Platzer, W.J.; Wittwer, V.: Fortschritte bei transparenten Wärmedämmaterialien. 7. Internationales Sonnenforum, Deutsche Gesellschaft für Sonnenenergie, 9–12 Oct., Frankfurt, Tagungsbericht, Band 1, S. 527–532.

[28] Wittwer, V.; Platzer, W.J.: Transparent Insulation Materials. Symposium Optical Materials Technology for Energy Efficiency and Solar Conversion IX. 12–13 March 1990, The Hague, Netherlands. Proceedings SPIE volume 1272, p.284–296.

[29] Platzer, W.J.; Wittwer, V.: Transparent Insulation Materials. Materials Science for Solar Energy Conversion Systems, ISBN 0080409377, chapter 3.

[30] Wellinger, K.; Schneiter, P.; Schläpfer, B.: Transparente Isolation, Schlußbericht zum Forschungsprojekt 1987–1990, Schweizer AG, Hedingen, Juli (1990).

[31] Hennings, D.: Ein einfacher Algorithmus für die (beidseitig) winkelabgängige Licht–Transmission durch TWD–Wabenmaterial. Mitteilung an FHG–IBP, Kaiser Bautechnik, Duisburg, Sept. (1991).

[32] Eijdems, H.H.E.W.: Transparent Insulation Materials. IEA TASK XIII, Technology Simulation Set, National Institute for Social Housing in the Netherlands (NCJV), Ede, Feb (1993).

[33] Schreiber, E.; Boy, E.; Bertsch, K.: Heizenergieeinsparung durch Wände mit transparenten Wärmedämmschichten – Rechenergebnisse unter idealisierten Innenrandbedingungen. SA 4/85, Stuttgart (1985).

[34] Schreiber, E.; Heim, U.; Boy, E.: Zwischenbericht: Wärmetechnisches Verhalten transparenter Dämmschichten an Gebäudefassaden – Vergleich Messung/Rechnung. GB 14/86, Stuttgart (1986).

[35] Platzer, W.J.: Calculation Procedure for Collectors with a Honeycomb Cover of Rectangular Cross Section. Solar Energy, Vol. 48, No. 6, pp. 381–393, Pergamon Press Ltd., 1992.

[36] Platzer, W.J.: Transparente Wärmedämmung, eine neue Alternative im Hochbau. Energiewirtschaftliche Tagesfragen 40 Jg., Heft 3, März 1990, S.136–142

APPENDIX A

Dr. Detlef Hennings, Kaiser Bautechnik, Duisburg:

A simple Algorithm for Calculation of the Angle Dependent Light Transmittance (both sides) through TIM Honeycomb Material

Dr. Detlef Hennings, Kaiser Bautechnik / Intelligent Building

A simple algorithm for calculation of the angle dependent light transmittance (both sides) through TIM honeycomb material

State 30.09.91

The algorithms described as follows shall serve to calculate the angle distribution of solar radiation behind of a TIM–window system. The angle distribution on the front side of the window system to ambient is assumed to be known. The derivation of the angle dependent total transmission is related to monitored data. The distribution along angles is based on simple assumptions.

In detail the algorithm consist of:

1. The angle dependent total transmission is described by a formula of Ofer Novik which has been modified to be able to relate to monitored data.

$$t_{tot} = t_0 * 0.994^{(D/a * f_{eff} * \tan(T))}$$

where
- t_0 = transmission at 0°, typ 0.96...0.97
- D = thickness of TIM–layer, e.g. 100 mm
- a = average width of honeycomb, e.g. 3.4 mm
- f_{eff} = correction for effective honeycomb width, 1.1 ... 1.3, typ 1.20
- T = angle of irradiation related to normal

with the correction f_{eff} the function is related to monitored data, which is possible by only small resulting error.

2. The undisturbed transmitted beam is determined by :

$$t_{dir} = t_1^{(n * f_{eff})} * (T)$$

with
- t_1 = transmission through a honeycomb separation wall at irradiation angles of (90° – T)
- n = D/a * tan(T)

Except for very small angles of irradiation t_{dir} is very small (<0.01).

3. A part is assumed to be totally diffuse (isotrop) of the half space to inside:

$$t_{diff} = t_{ges} * (t_0 - t_{ges})$$

4. The rest (related to t_{ges}) is distributed equally on an azimuth ring with constant angle (T = irradiation angle) to normal inside :

$$t_{ring} = t_{tot} - t_{dir} - t_{diff}$$

The width of ring should be minimum 5°, however can be adapted to top according to the angle step differences of the whole model.

The assumptions 3 and 4 have been fixed arbitrarily for now and have not yet been proofed by experiment.

APPENDIX B

A. Poel and H. H. E. W. Eijdems, NCIV, EDE:

Modeling of Transparent Wall Covering Insulation Materials.

IEA
SOLAR R&D

INTERNATIONAL ENERGY AGENCY

solar heating and cooling programme

TASK XIII

advanced solar low-energy buildings

TECHNOLOGY SET: TRANSPARENT INSULATION MATERIALS

(draft)

Prepared by : ir. A. Poel
: ir. H.H.E.W. Eijdems
Date : Januari 1991

NCIV

N C I V , National Institute for Social Housing in the Netherlands

TASK XIII
ADVANCED SOLAR LOW ENERGY BUILDINGS

TECHNOLOGY SET: TRANSPARENT

INSULATION MATERIALS (draft)

TDE/BPo/PSc/077/r.097

Januari 1991
Projectnumber: 337218

prepared by: ir. A. Poel
ir. H.H.E.W. Eijdems

NCIV, National Institute for Social Housing in the Netherlands
Postbox 273
6710 BG EDE

Requested by the Netherlands Agency for Energy and the Environment (NOVEM) to furnish a Dutch contribution to Task XIII of the IEA Solar Heating and Cooling Programme (contractno 41.12.045.10)

CONTENTS

1. INTRODUCTION

This report gives an overview of properties of Transparant Insulation Materials (TIM) and ways of thermal modelling of walls provided with TIM at the outside. Based on literature searches, an condensed overview of the present level of progress in the classification of TIMs into various materials and their properties is given in chapter 2, in so far as they are of importance for the thermal simulation in respect of Task 13. Not included in this report are detailed discussions of chemical behaviour or optical properties. The collected data do not give a full picture and it is not clear yet how the properties of the materials as measured can be compared. Appendix 1 contains the most important data from the literature. At this moment a fair number of TIMs (between 30 and 50) of various sorts have been developed. The best known form is double or triple glazing. A number of these materials are being marketed commercially (Israel, Germany, Sweden, USA). In West-Germany (Fraunhofer Instituut, Freiburg) international workshops on TIMs have been taking place for several years.
In the literature on TIMs (lit. [1], [2] and [3] a division is made into four categories on the basis of their optically distinguishing characteristics. The materials are classified into:
- parallel layer structures (e.g.: double glazing and film);
- perpendicular structures (e.g.: honeycombs);
- hollow structures (e.g.: glass bulbs and stacked egg boxes);
- quasi-homogeneous structures (e.g.: aerogels).

Chapter 3 until 7 is giving information on possibilities of modelling TIM-walls. Four levels of detail are distinguished and there accuracy is discussed. Apart from the energy consumption due to the application of TIM-walls also the overheating aspect is of main importance. Therefore this comfort issue is also adressed in the modelling chapters. Finally chapter 8 containes some conclusions concerning the four modelling levels. More information on material properties and modelling aspects are incorporated as appendix I and II.

2. PROPERTIES OF TRANSPARENT INSULATION MATERIALS

2.1. General remarks

The main parameters of TIM constructions for assessing the energy behaviour are the U value (thermal transmittance) and the Fsg value (solar gain factor); being the total of solar energy passing the glazing per m2 (transmission as well as the inward flowing portion of the absorpt solar energy in the glazing) devided by the total incident solar energy on the glazing per m2. The Fsg value depends on the transmittivity and the absorptivity of the material for solar radiation. In the case of traditional building materials it is assumed that the thermal conductivity coefficient can be approximately considered irrespective from the thickness and the temperature of the construction. This does not automatically apply to TIM constructions. Particularly in the case of honeycomb structures the thermal conductivity increases considerably with rising temperature. The more homogeneous aerogels display this effect to a lesser extent. In Appendix I (Figures I.1 - I.4) there are a number of relevant characteristic graphs from various literature sources.
The non-linear relation between the thermal conductivity coefficient and the layer thickness cannot generally be modelled within the scope of traditional computer models. Neither is this necessary as the thickness of the modelled construction remains constant during a calculation. This property does mean that for most TIMs an energetic optimum can be found in the relation between U value and Fsg value as a function of the thickness.

The transmittivity (tau) for solar radiation of the material is dependent on the absorption and the thickness, the surface structure and the angle of incidence of the incident radiation. For most TIMs this relation, too, differs from that for normal clear window glass. In the Figures I.4 - I.6 of Appendix I the transmittivities of Aerogel, AREL honeycomb, respectively, and clear window glass are plotted against the layer thickness. For a honeycomb structure the decrease of the transmittivity as a function of the layer thickness is distinctly less considerable than for glass and Aerogel. Within the ranges in which the various materials are used (aerogel 10 - 30 mm, glass 4 - 10 mm, honeycomb 40 -100 mm) the transmission curve as a function of the thickness is practically linear.

For the various TIMs the influence of the angle of incidence on the transmittivity is given in Figures I.7 - I.10 of Appendix I.
The characteristic kink at psi = 60 degrees in the transmission curve of window glass is far less persistent in other materials. This shows that transmission by TIM of direct solar radiation is different from that in the case of glass. Depending on the orientation of the plane in which TIM is positioned, the distribution and the intensity of transmitted direct radiation over a period of one day (or one year) will differ from that of glass having the same Fsg value. As compared with glass many types of TIM transmit more radiation in the case of small angles of incidence and less in the case of relatively large angles of incidence. For vertical surfaces this means that when the sun is in a low position TIM will transmit more radiation (for instance during the winter and in the morning or evening).

Diffuse radiation and direct radiation when the sun is in a high position are transmitted by TIM to a lesser extent. It should be born in mind that the transmission curve will change by covering TIM with, for instance, sheets of glass.
Finally annexed are tables containing properties of materials derived from the various literature sources. Comparison of the data from these tables is no simple matter. Sometimes different values are reported for the same materials. Moreover, the conditions under which the measurements were carried out are not always the same. Within the scope of this IEA task it is not of primary importance to understand the exact behaviour of a specific TIM. Primary emphasis is on the possibilities of energy saving under acceptable conditions of comfort within a realistic design. To this end it is of importance, however, that the characteristic properties of TIM are properly understood and modelled, especially in relation to the aspect of overheating. On the other hand, for the determination of the potential of TIM in the low energy design there is no absolute need for these properties to characteristic of a particular product, but the values assumed must be realistic or attainable in the near future. In this investigation use will as much as possible be made of results from IEA task 10 (Table I.1, Appendix I). For, they provide the best possible guarantee for drawing unambiguous conclusions about the properties of the materials. Moreover, this approach contributes to the harmonization of the various IEA tasks.

Most publications do not directly reveal any classification by performance. From an energetic point of view a construction having a good U value and a moderate solar gain factor may display a performance equal to that of a construction having a moderate U value and a very good solar gain factor. The performance of TIM is governed by the climate (temperature as compared with radiation intensity) and the construction positioned behind it. Therefore, on account of the radiation effect, the orientation of the plane in which the TIM is placed is also of importance.

2.2. Overview of properties

On the basis of a simplified approach Table 1 shows a classification by performance for TIM constructions. This classification is to serve as an aid in the designing of a house. The thermal resistance and transmittivity for diffuse solar radiation (tau, dif) are from Table I.1 (Appendix I). All materials are assumed minimally to be covered on the exterior with a layer of clear window glass. To that end the transmittivity of a number of materials was multiplied by the value 0.77 (transmittivity for single glass according to Table I.4, Appendix I). The Fsg factors (Fsg, ti) from Table 1 were determined or estimated on the basis of data from the other sources.

type	name	De	Dti	Di	R,ti	tau,dif	Fsg,ti
		[mm]			[m2K/W]	[-]	[-]
A	DOUBLE CLEAR GLAZING	6	11	4	0.14	0.62	0.70
A	DOUBLE GLAZING LOW-E	4	14	4	0.56	0.51	0.60
A	HIT GLAZING	6	70	6	1.26	0.58	0.63
C	GLASSBULBS	4	32	4	0.60	0.24	0.30
C	P-FOIL	3	60	3	0.70	0.57	0.62
B	PC-HONEYCOMB	4	100	0	0.94	0.58	0.63
B	PC-CAPILLARY	4	100	0	1.26	0.45	0.50
B	PMMA-CAPILLARY	4	40	0	0.61	0.56	0.62
C	PMMA-FOAM	4	32	0	0.54	0.35	0.37
B	POLYSTROL-HEX	4	80	0	0.66	0.62	0.68
D	AEROGEL GRANUL. EVAC.	4	10	4	0.74	0.65	0.70
D	AEROGEL MONOL. EVAC.	4	15	4	1.83	0.55	0.60

Type A = parallel layer structures
Type B = perpendicular structures
Type C = hollow structures
Type D = quasi-homogeneous structures
Di = thickness of inside cover
Dti = thickness of TIM structure
De = thickness of outside cover
R,ti = heatresistance of TIM-construction including covers (m^2K/W)
tau,dif = transmittance for diffuse solar incidence
Fsg,ti = solar gain factor for diffuse solar incidence

Table 1: Thermal and optical properties of characteristic TIMs used as window(s)

In Figure 1 the solar gain factors (Fsg,ti) of the various constructions in Table 1 (excluding double clear glazing) are plotted against the thermal transmittance (U,ti). U,ti is derived by using the following formula $U,ti = (R,ti + 0,17)^{-1}$ in which 0,17 is the sum of interiour and exteriour surface resistances. The constructions in the top left-hand corner of the graph combine a low U value with a high Fsg value and consequently display a better performance than the constructions in the bottom right-hand corner.

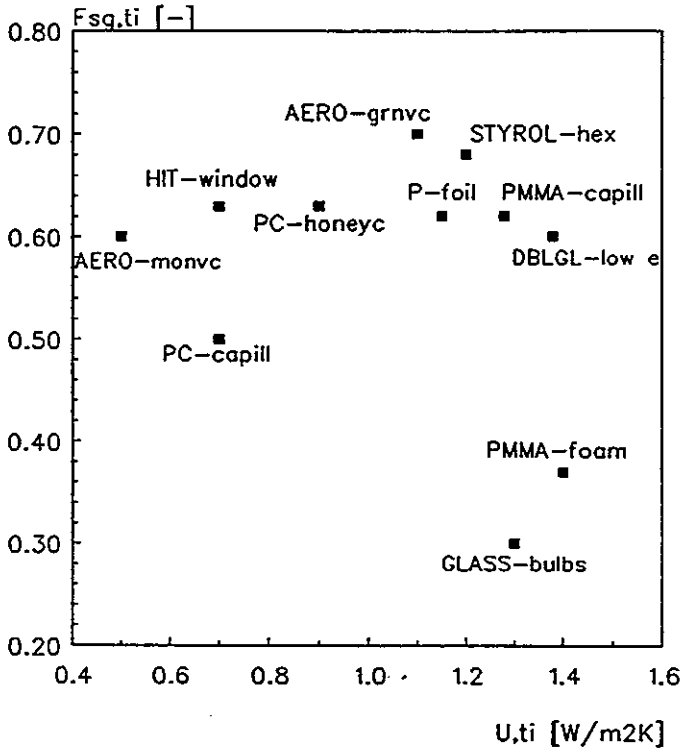

DBLGL-low e	=	Double glazing with low-e coating
HIT-window	=	High Insulation Technology window; 2 UP-coated films in double glazing construction (Geilinger AG)
GLASS-bulbs	=	Glass bulbs in double glazing cover (Grunzweig und Hartmann AG)
P-foil	=	P-layer insulation (Schweizer AG)
PC-honeyc	=	Polycarbonate honeycomb 100 mm. (Arel Energy)
PC-capill	=	Polycarbonate capillairy 100 mm. (Okalux)
PMMA-capill	=	Polymethylmetacrylate capillairy (Okalux)
PMMA-foam	=	Polymethylmetacrylate foam (A. Hohnholz)
STYROL-hex	=	Hexagonal polystyrol honeycomb (BASF AG)
AERO-grnvc	=	Aerogel granulat evacuated (BASF AG)
AERO-monvc	=	Aerogel monolith evacuated (Airglass AB)

Figure 1: Graphical representation of the Fsg value as a function of the U value

3. MODELLING OF TIM-WALLS ON FOUR LEVELS OF DETAIL

The thermal behaviour of TIMs can be translated into a calculation model in various ways. For detailed calculations, which are primarily directed to the level of behaviour of the material, specific computer programs are used and developed by and for research institutes in this field. In combination with measuring results characteristic properties of materials can be derived. For simulation of temperatures and heating loads within a total model of a building often a less high accuracy will suffice as regards the algorithms simulating the material. Figure 1 is a schematic representation of a vertical section of a wall covered with a TIM construction with electric analogue for the most important thermal resistances and source terms. The more detailed computer models for (multi-zone) energy simulation of a building make use of this physical model for transparent elements. On the basis of optical formulae (Fresnel and others) an hourly transmission coefficient for direct and diffuse radiation is calculated for each transparent element (optionally after making a shading calculation). Per layer also the amount of absorbed solar energy is calculated and according to a resistance model divided into an in-flowing source term and an out-flowing portion. On this modelling level all computer models are based on homogeneous isotropic, planoparallel layer structures. For several TIMs this model is not suitable (for instance in the case of capillary and honeycomb structures). Moreover, the convection flows and the temperature dependence of thermal resistance are not modelled in detail. At a high temperature in a TIM wall this may lead to inaccuracy. If the thermal conductivity coefficient is chosen on the safe side, then the heat gain and the overheating are lower in reality than calculated by the models because the thermal resistance of TIMs decreases with increasing temperature.

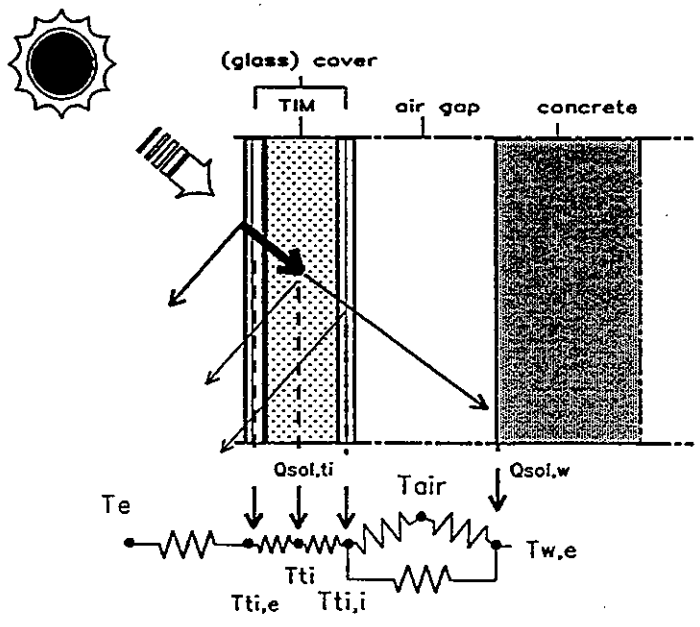

Te = outside air temperature
Qsol,ti= absorbed solar energy in the TIM construction
Tair = mean air gap temperature
Qsol,w = absorbed solar energy at the mass wall surface
Tti,e = mean temperature of the outer TIM covering layer
Tti = mean temperature of the transparant insulation material
Tti,i = mean temperature of the inner TIM covering layer
Tw,e = outer surface temperature of the mass wall

Figure 2: Simplified model for a TIM construction with electric analogue

As within this study use was made of the computer model Suncode-PC the present description must be considered to be within the scope of the possibilities of this model. The methodology described, however, is not bound by a particular computer program. Further, the TIM layer referred to in this description is always coupled to a mass wall by an air cavity. Given below are in order of decreasing accuracy and increasing simplicity four levels on which a TIM can be simulated within an existing calculation model.

- level 1: programming the TIM characteristic on a high modelling level in a separate subroutine or as separate program;

- level 2: making use of existing routine for transparent elements (for instance window section in Suncode) and approaching the TIM behaviour as closely as possible by means of conventional window input parameters;

- level 3: employing existing routine for walls and including the TIM characteristics in the input parameters of the outer surface (film coefficient, absorptivity for solar radiation);

- level 4: stationary calculation of the U value and an Fsg value for the composite construction of TIM layer and mass wall.

These four modelling options will be further described in the following four chapters. Simplifications in the physical model are effected with reference to the schematic representation in Figure 2. So the modelling according to Figure 2 is on level 2.

4. SOFTWARE MODIFICATION FOR TIMs (LEVEL 1)

programming the TIM characteristic on a high modelling level in a separate subroutine or as separate program

In principle this option provides the best possibility for a specific TIM to be accurately included in a calculation. The heat resistance of the TIM layer in a dynamic model can be calculated as a function of occurring temperatures. The transmittivity and the absorptivity of the TIM layer can be calculated as a function of the angle of incidence of the solar radiation, taking account of the optical properties of the material. The dynamic effect of the mass wall is completely included in the calculation. This option, however, is very elaborate, calls for access to and knowledge of the source code and the structure of the calculation model. Moreover, for an approach to be successful, formulae must be available which accurately define the behaviour of the various types of TIMs. Considering the importance of TIMs for future energy saving in buildings and the need for assessing the effect of applications in the design phase, it is desirable yet for the existing programs to include algorithms for reliable simulation of the behaviour of TIMs. But adaptation of existing software to new materials falls beyond the scope of the present investigation (objective of IEA task 12). This option will therefore not be further discussed.

5. MODELLING OF TIMs AS GLASS CONSTRUCTION (LEVEL 2)

making use of existing routine for transparent elements (for instance window section in Suncode) and approaching the TIM behaviour as closely as possible by means of conventional window input parameters

If within a simulation model a window element can be placed in front of a mass wall, it is possible for the TIM layer to be modelled as a window. In this way the phase shift in solar gain through the massive wall is completely taken into account in a dynamic calculation. In modelling a window it should first of all be checked whether the thermal resistance, mean transmittivity and solar gain used by the program are in agreement with the desired value. Secondly, it may be tried to approach the angle dependent transmission curve of a specific TIM.

Normally window elements in front of a wall can be modelled in two different ways. The first option consists in modelling it as separating element between an inside space and the climate outside. Alter-natively, it can be modelled as outer construction layer of a Trombe wall. For a TIM to be placed on an outside wall by using the first option an additional zone need be defined which represents the air cavity in the TIM wall. If the Trombe construction is not ventilated with inside air, then the two options within the program lead to identical results. As an additional "zone" is used for the aircavity this often offers wider scope for modelling ventilation patterns and the like, it was decided in this description to choose this option. Figure 3 is a schematic representation of a section of a TIM wall with electric analogue.

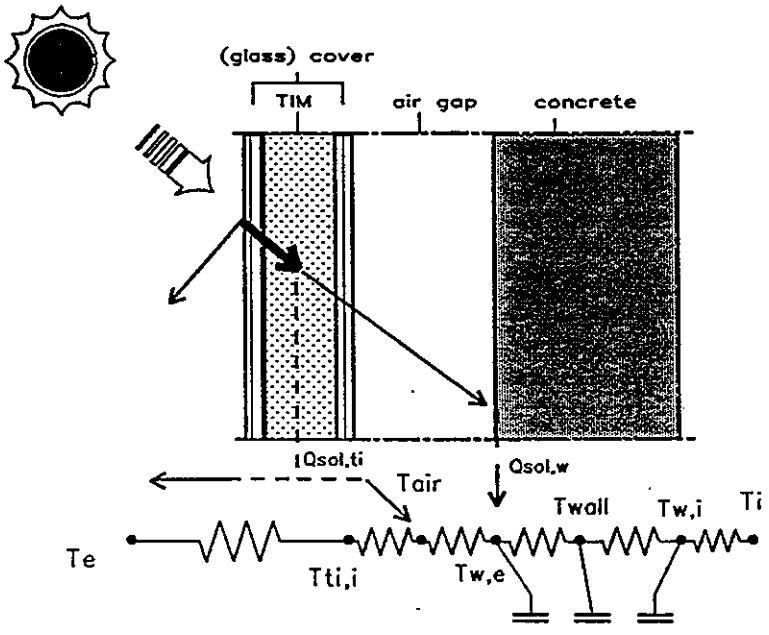

Te = outside air temperature
Qsol,ti= absorbed solar energy in the TIM construction
Tair = mean air gap temperature
Qsol,w = absorbed solar energy at the mass wall surface
Tti,i = mean temperature of the inner TIM covering layer
Tw,e = outer surface temperature of the mass wall
Twall = mean temperature of the mass wall
Tw,i = inner surface temperature of the mass wall
Ti = inside air temperature

Figure 3: Model for a window element in Suncode with electric analogue

Some simulation codes permit introducing window elements which are built up of one or more identical glass layers. For each type of window a number of parameters may be given.

For the entire window they are: the thermal transmittance (U), a shading coefficient (SC) and the number of glass layers (a). For the glass layers the extinction coefficient (K), the refraction index (n) and the layer thickness (t) are given. In Appendix I are the formulae which are used within the code Suncode for calculating the conduction and absorption by the glass. It is not possible to use a temperature dependent U value for the TIM layer. But the same can yet be varied as a function of time (hourly over the day and per season). Within this study a constant lambda value has been used for the TIM which occurs at a temperature of 10 degrees C.
In this way "safe" results are obtained such that the energetic effect is slightly underrated, whereas the overheating is somewhat overrated. The best agreement between model and reality is achieved for TIMs which consist of parallel layer structures or quasi-homogeneous structures.

When a TIM is modelled as window element, a number of steps must be distinguished. First of all it should be ensured that the transmittivity and solar gain factor calculated by the program have the desired average value over the year (or heating season) (in accordance with Table 1. In the second place it may be tried to approach the angle dependent transmission curve (for instance from Appendix I) of the modelled TIM as closely as possible. A dilemma to this approach is that of most TIMs no suitable parameters have been published (yet) which are directly applicable as input for conventional computer programs. Moreover, most TIM constructions are composed of several non-identical layers. In order that the TIM behaviour may yet be reasonably accurately approached in calculations, the influence of the input parameters of the glass has been investigated. The object envisaged is achieving a transmission curve which corresponds to the desired TIM by variation within the program of the number of layers, the layer thickness, the index of refraction and the extinction coefficient. As a result, the above input parameters do lose their physical meaning. The shading coefficient is a parameter which is of linear influence on the amount of incident radiation (SC = 1.0 implies that 100% of the radiation on a particular surface will reach the window). As the SC in the program may also have a value higher than 1.0, this parameter can be used as scale factor. This means that if the form of the transmission curve corresponds to the desired form, but the magnitude does not, then the simulated curve can be scaled up linearly to the desired absolute value using the inverse SC (see Figure 4).
In Appendix II of the present report the transmission and the solar gain curves are presented as a function of the angle of incidence for various input parameters.

The advantage of modelling TIMs as window elements are:

- the simple input of the program using existing input parameters;
- the possibility of introducing sun shading provisions;
- the calculation of transmission and absorption by the program as a function of the angle of incident radiation.

Moreover, a considerable disadvantage is that the temperature dependence of the thermal conductivity coefficient is not taken into account. A sensible choice of the lambda value will lead to the results being on the safe side (underrating energy saving, overrating overheating).

The method outlined above is, of course, only a makeshift means of arriving yet at a reasonably accurate approach of the physical behaviour on the basis of the scanty data available on a particular TIM. Probably in the near future the necessary parameters will be determined and/or published which can be directly used as input. There will be need for a validation of the accuracy of results by modelling on this level on the basis of better algorithms (other computer models) and measuring data.

At present the only validation available consists in a comparison of the measured with calculated angle dependent transmission curve, account being taken of the annual average solar gain and transmission coefficients.

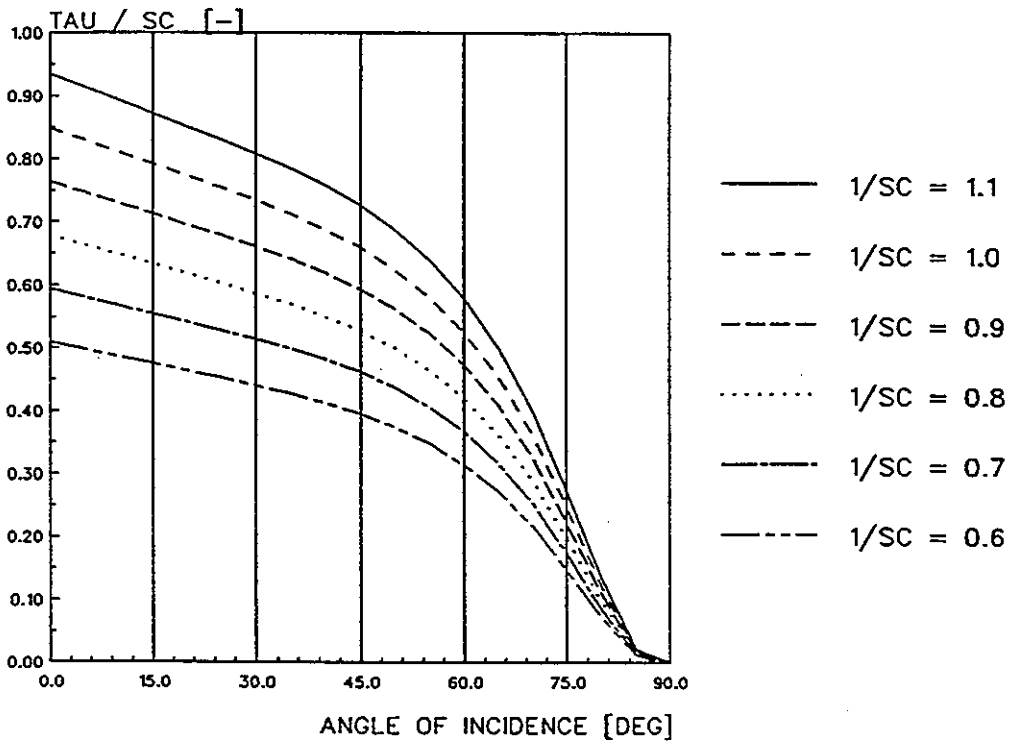

Figure 4: Effect on a transmission curve of variation of the shading coefficient within Suncode

6. MODELLING OF TIMs AS SURFACE RESISTANCE AND ABSORPTIVITY (LEVEL 3)

employing existing routine for walls and including the TIM characteristics in the input parameters of the outer surface (film coefficient, absorptivity for solar radiation)

A simpler way of modelling a TIM as outside insulation on a wall consists in adaptation of the surface resistance and the absorptivity in the case of incident radiation of the outside surface of a wall. To this end the surface resistance at the outside of the wall is increased by the total thermal resistance of the TIM construction plus air cavity. At the same time the absorptivity is reduced by multiplication by the average solar gain factor of the TIM construction. Figure 5 shows a schematic representation of this modelling. As compared with the preceding option this method has the disadvantage that in computer programs the solar gain of the TIM layer is no longer angle dependent, solar shading cannot be put in and the U value of the TIM layer can no longer be varied as a function of time and/or season. In the Suncode program the surface resistance values are put in as constants for the whole calculation. No distinction is made as regards the effect of transfer by radiation or convection.

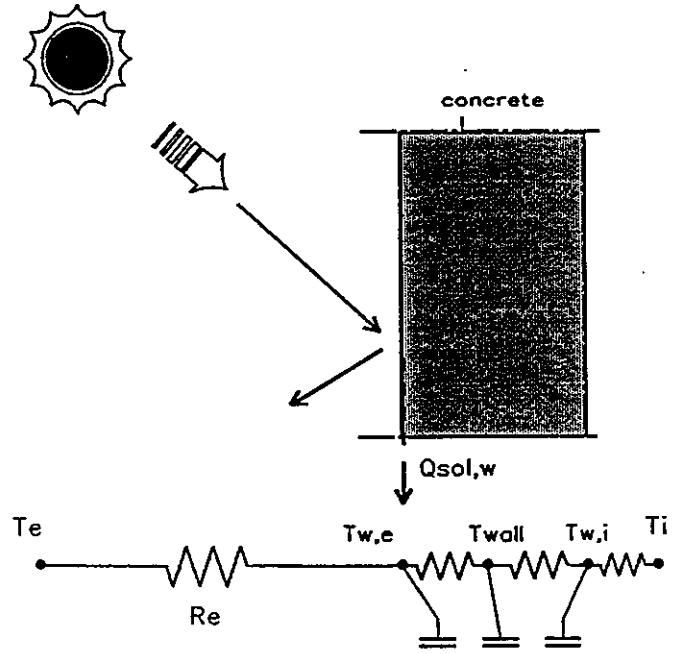

Te = outside air temperature
Qsol,w = absorbed solar energy at the mass wall surface
Tw,e = outer surface temperature of the mass wall
Twall = mean temperature of the mass wall
Tw,i = inner surface temperature of the mass wall
Ti = inside air temperature
Re = outer surface resistance of the mass wall

Figure 5: Model for a TIM construction as surface resistance and absorptivity with electric analogue

The results of the modelling procedures on level 2 and level 3 (Figures 3 and 5) were compared on the basis of a simple building model (shoebox from [13]). The annual heat and cooling loads were calculated as well as the hourly heat flows and temperatures of TIM constructions and mass walls. The calculation was first carried out with TIMs as window elements (level 2). On the basis of this calculation the average Fsg factors of the TIM construction over the heating and the cooling season were determined (orientation dependent).

Then the calculation was again made for the same building.
In this second calculation the TIM constructions (windows within the model) were modelled on level 3 by summation of the original surface resistance, the total thermal resistance of the TIM construction and the resistance of the cavity into one fictitious surface resistance. Per TIM wall the original absorptivity for solar radiation of the mass wall was subsequently multiplied by the seasonal average Fsg factor of the TIM construction.
In the re-calculation the mass wall was defined as outside wall. Figure 6 shows the surface temperatures of a south-facing wall in the two calculations for a sunny winter day. The temperature differences both at the inside surface (lines 1 and 3) and at the outside surface (lines 2 and 4) are negligible.

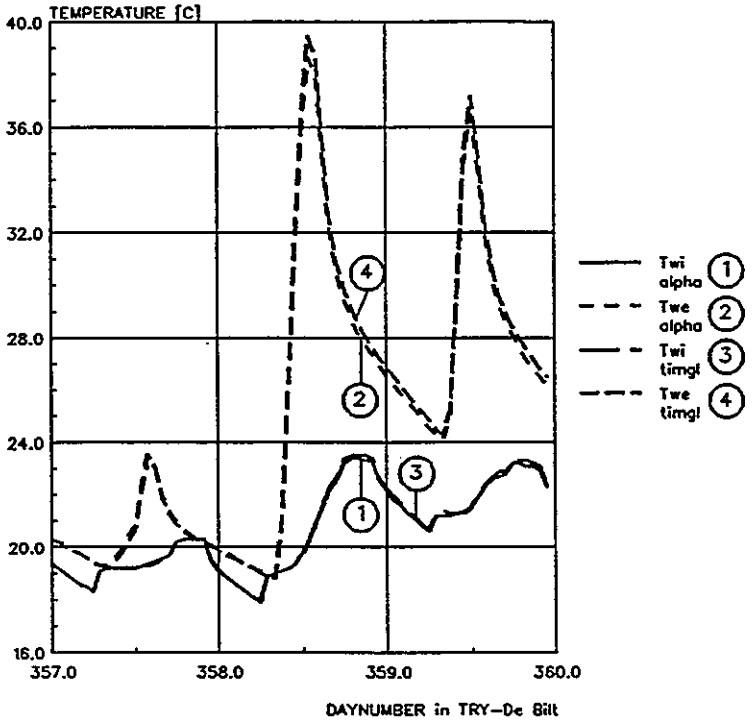

Twi,alpha (curve 1) = Surface temperature at the inner side of the mass wall for TIM construction modelled on level 3 (alpha,e & abs,e)
Twe,alpha (curve 2) = Surface temperature at the outer side of the mass wall for TIM construction modelled on level 3 (alpha,e & abs,e)
Twi,timgl (curve 3) = Surface temperature at the inner side of the mass wall for TIM construction modelled on level 2 (window element)
Twe,timgl (curve 4) = Surface temperature at the outer side of the mass wall for TIM construction modelled on level 2 (window element)

Figure 6: Surface temperatures of a south-facing TIM wall

The same results were found for a north-facing wall and a summer situation (not shown).

For use of season controlled sun shading the calculation can be carried out per season, provided that the Fsg factors for each season are known.

The advantages to this way of modelling are the simplicity and the limitation of the number of zones for calculating a complex building (with many TIM walls). This is of importance for rapidly calculating a number of variants from a design study.

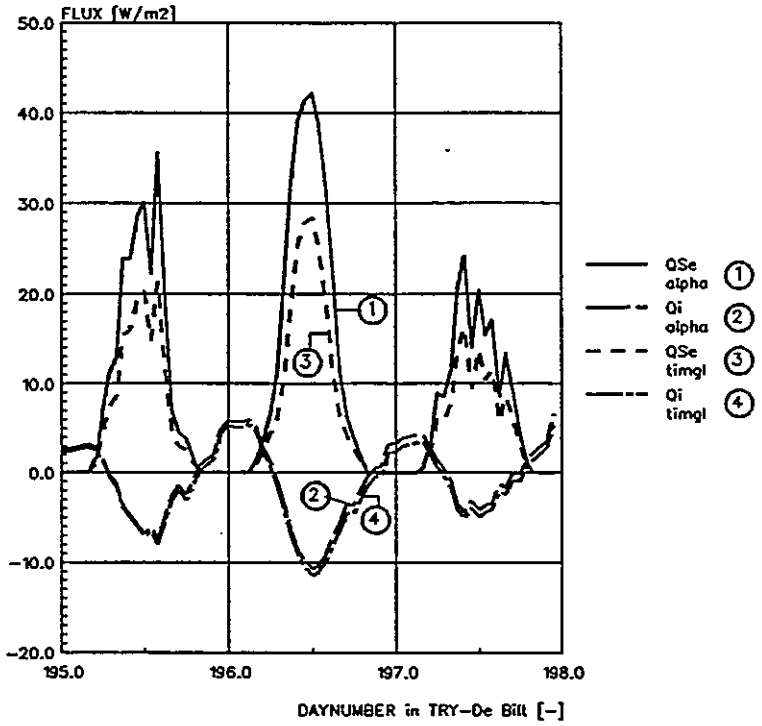

QSe,alpha (curve 1) = Absorbed solar energy at the outer surface of the mass wall for TIM construction modelled on level 3 (alpha,e & abs,e)

Qi,alpha (curve 2) = Net heat flux at the inner surface of the mass wall for TIM construction modelled on level 3 (alpha,e & abs,e)

QSe,timgl (curve 3) = Absorbed solar energy at the outer surface of the mass wall for TIM construction modelled on level 2 (window element)

Qi,timgl (curve 4) = Net heat flux at the inner surface of the mass wall for TIM construction modelled on level 2 (window element)

Figure 7: Heat flows at a south-facing TIM wall

Figure 7 illustrates the heat flows for the two models (levels 2 and 3) on both sides of the wall. Here there is a distinct difference in the amount of radiation incident on the outer surface of the wall (between the lines 1 and 3). This occurs due to the fact that the convective portion of the radiation absorbed in the TIM is in case of level 2 modelling not taken into account as incident radiation but as convection and conduction on the wall whereas level 3 modelling calculates this convective and conductive portion as incident radiation. This, of course, is of hardly any influence on the heat transfer at the inside surface (lines 2 and 4) nor on the net heat flow at the outside surface (lines 5 and 6). Figure 7 shows that the two modelling ways lead to virtually identical net heat flows at the surfaces.

Finally, in Figure 8 the yearly heat and cooling loads and the extent to which the temperature exceeds the 25 degree-Celcius limit are plotted for the two modelling ways (next to the basic variant). Here, too, they are in good agreement with each other.

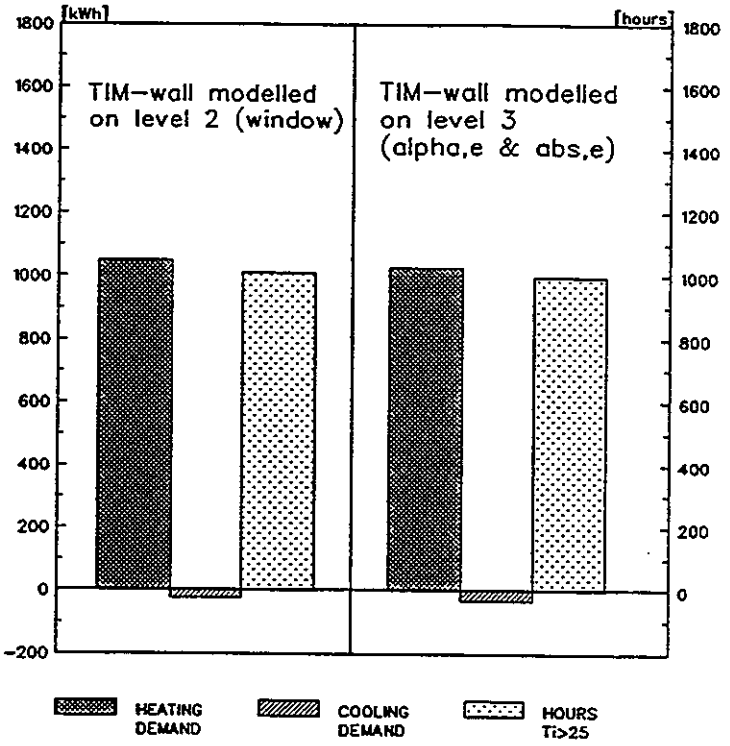

Figure 8: Comparison of the yearly heat load and the cooling load and overheating of the Dutch shoebox model with TIM modelled on level 2 and level 3

7. MODELLING OF TIMS ON THE BASIS OF U VALUES AND Fsg FACTORS DETERMINED BY STATIONARY CALCULATION (LEVEL 4)

stationary calculation of the U value and an Fsg value for the composite construction of TIM layer and mass wall

The simplest way of modelling a TIM layer on a mass wall is by means of a composite heat resistance and a solar gain factor. In this way of modelling the temperature effect on the U value, the influence of the angle of incidence of incident radiation as well as the dynamic effect of the mass wall will be disregarded. This approach is therefore not suitable for carrying out overheating calculations for the inside climate. The parameters do appear to be suitable for simple energy saving calculations based on the heating season. Figure 9 gives the electric analogue for calculating the solar gain factor for the overall construction.

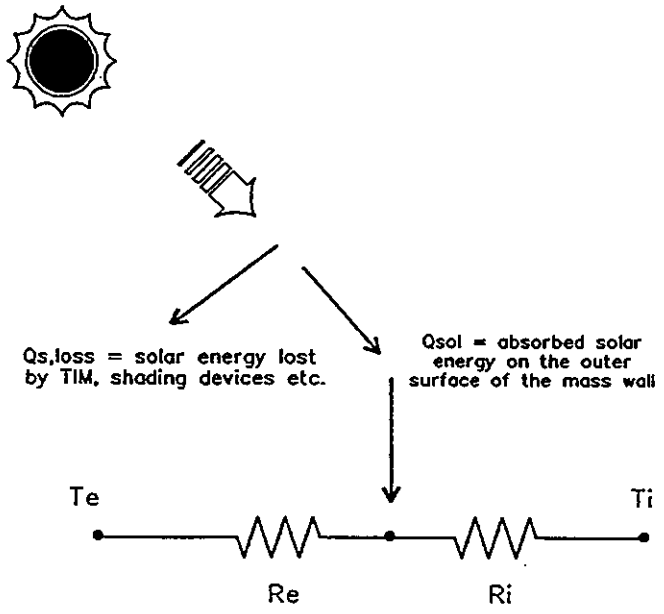

Qsol = solar incidence on the outer surface of the mass wall reduced by the solar gain factor of the TIM construction
Re = total heat resistance between the outer surface of the mass wall and the outside air
Ri = total heat resistance between the outer surface of the mass wall and the inside air

Figure 9: Model for stationary calculation of a TIM construction

On this level the total Fsg factor of TIM construction and mass wall (Fsg,ti+w) is determined by stationary calculation based on the Fsg factor of the TIM construction (Fsg,tim) and ratio of the thermal resistance (as indicated in Figure 9) according to the following formula:

$$Fsg,ti+w = Fsg,tim * Re/(Ri + Re) \qquad (I)$$

In this approach the dynamic effect of the mass wall is disregarded. In this case a comparison between this model (level 4) and level 2 is again made on the basis of a calculation with the Dutch shoebox model from [13] with north- and south-facing TIM walls.
The Fsg factor for the TIM construction has been derived from the quotient of the total solar gain via the TIM window and the incident radiation performed by the program (Suncode-pc). The yearly average Fsg factor for the TIM construction in this specific calculation is Fsg,tim = 0.64. In this calculation the term Re/(Re+Ri) is equal to 2.085/(2.085 + 0.384) = 0.84. So the value for Fsg,ti+w = 0.54. From the monthly heat flux on the inner surface of the TIM wall as a result of the solar load and the monthly incident radiation on the outer surface there is derived the monthly average Fsg factor for the total TIM wall. A good indication for the difference between the models on the levels 4 and 2 is obtained by a further consideration of the factor Re/(Ri+Re) from Formula I. Provided that a representative value for the U value and the Fsg tim is determined, the accuracy of a season calculation of energy consumption as far as the TIM wall share is concerned depends on the factor Re/(Ri+Re), which disregards the dynamic behaviour of the wall behind the TIM.
The value of this factor for level 2 is determined by taking the quotient of the monthly average Fsg,ti+w and Fsg,tim; for from Formula I it follows that:

$$Re/(Ri + Re) = (Fsg,ti+w)/(Fsg,tim) \qquad II$$

In Figure 10 this quotient is given for each month for the south-facing TIM wall and the north-facing TIM wall. For comparison the quotient determined by stationary calculation is given as a constant.

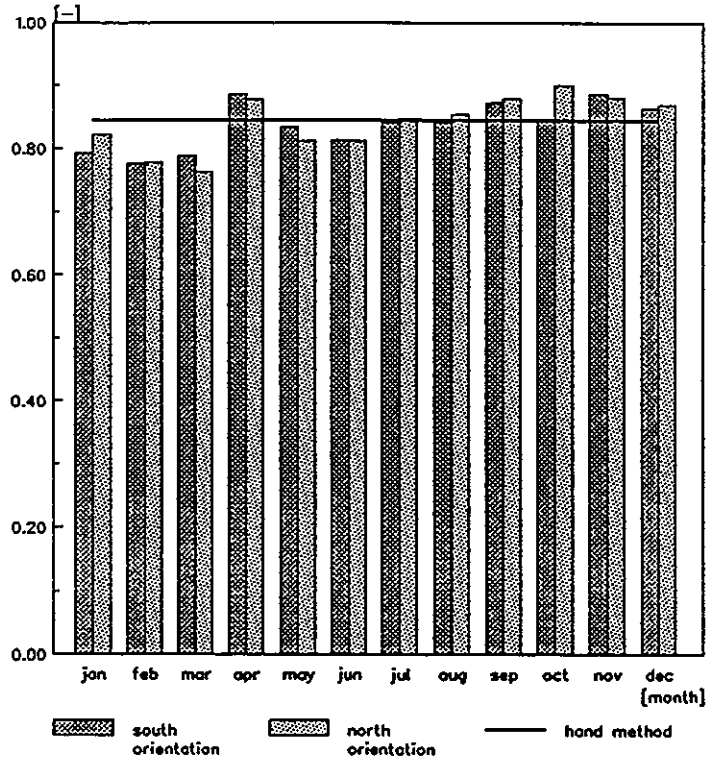

Figure 10: Re/(Ri + Re) from Formula I as monthly average for a south-facing wall and a north-facing wall on model level 2 and as a constant

Over the heating season the deviation of the "dynamic" from the stationary value for Re/(Re + Ri) and hence for Fsg ti+w is smaller than 2 [%]. On a monthly basis the greatest deviation is over 7 [%].

This way of modelling is unsuitable for the determination of temperature effects. For illustration two calculations of the inside temperature have been carried out with the Dutch shoebox model for a number of cold, sunny days from the month of April of the TRY for De Bilt in the Netherlands. In the second calculation the mass wall between the TIM construction and the interior is modelled by thermal resistances without thermal capacity. The resulting loss of thermal mass of the TIM wall is modelled in an extra internal partition wall in the interior. Figure 11 gives the hourly calculated inside temperatures for the two modellings. In the first calculation (Ti, dynamic: TIM wall) the temperature does not exceed 25 degrees C, but in the second calculation (Ti, station : TIM wall) it clearly does.

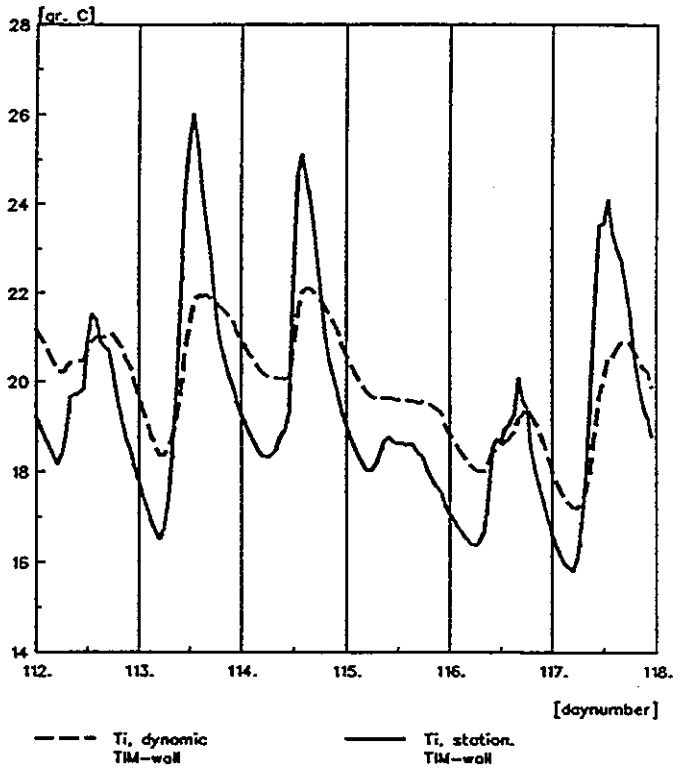

Figure 11: Variation in air temperature calculated with SUNCODE for the TIM wall modelled on level 2 (dynamic) and level 4 (stationary)

8. CONCLUSIONS CONCERNING MODELLING

Proper modelling of all the relevant thermal properties of transparent insulating materials in computer programs for energy and temperature calculations is only possible if for each type of TIM specific algo-rithms are developed and implemented (detail level 1). This falls beyond the scope of IEA task 13.
Modelling TIMs as window element within a dynamic simulation model (detail level 2) will lead to a good approximation of the yearly average transmittivity (and the Fsg factor) for direct normal and diffuse radiation. Varying the input parameters of the glass even makes it possible to simulate the transmission curve (and the Fsg curve) for a specific TIM as a function of the angle of incident radiation. This is the most successful for TIMs composed of planoparallel layers or quasi-homoge-neous structures. In this way acceptable results are obtained both as far as energy and comfort calculations are concerned. It is true that omitting a temperature dependent heat conduction coefficient of the TIM will lead to a deviation. By a sensible choice of the lambda value, however, safe results are obtained (underrating of the energy saving and overrating of the overheating). The method described in this report with respect to model level 2 can be adopted for those computer models, in which the input parameters for glass constructions can be modelled adequately detailed.

A simpler way of modelling a TIM construction can be realized by an adapted surface resistance and absorptivity in the case of solar radiation of the outer surface of part of a wall (detail level 3). When the average Fsg factor of the TIM is known for a particular orientation and/or season (for instance by a calculation according to the window model), it is possible in this way to make a reliable energy or temperature calculation. Here, too, the considerations apply as regards the temperature independent lambda value, as mentioned with level 2. The simplicity of the modelling thus permits rapid calculation of a building with a large number of TIM elements (for instance for design studies).

Finally, the simplest modelling (detail level 4) is done by characterization of a TIM on the basis of a stationary U value and Fsg factor. By this method the energy consumption based on the heating season can be determined with sufficient accuracy for properly insulated buildings with adequate thermal capacity. For temperature calculations this modelling option is unsuitable.

LITERATURE

[1] Jesch, L.F., e.a.,
"Transparant Insulation Materials for passive solar energy utilisation", Proceedings of the first International Workshop on TIM's,
Birmingham, 1987.

[2] Jesch, L.F., e.a.,
"Transparant Insulation in solar energy conversion for buildings and other applications", Proceedings of the 2nd International Workshop on TIM's,
Birmingham, 1988.

[3] Jesch, L.F., e.a.,
"Transparant Insulation Technology for solar energy conversion", Proceedings of the 3rd International Workshop on TIM's,
Birmingham, 1989.

[4] Zegers, F.T.S., C. J. van der Leun,
"Vlakke Plaatcollectoren met transparante Isolatie", 2e herziene druk,
Ecofys, Utrecht, mei 1989.

[5] Woon|Energie, Ecofys,
"Ontwikkelingen in transparante isolatiemateriaken voor toepassingen in zonne-energiesystemen",
Gouda/Utrecht, juni 1988.

[6] Dijk van, H.A.L., e.a.,
"Translucente thermische isolatie in gevels; een verkenning",
TPD, Delft, februari 1990.

[7] Normcommisie 351 74,
NVN 5125 "Energiegebruik in gebouwen - Verwarming van woningen",
Nederlands Normalisatie Instituut, Delft, november 1987.

[8] Haaster van, P.H., e.a.,
"Testset ten behoeve van de fysische kwaliteit van eenvoudige rekenmodellen voor het energiegebruik van woningen",
Bouwcentrum, Rotterdam, november 1988.

[9] Commision of the European Communities,
"Test Reference Years TRY, Weather Data Sets for Computer Simulations of Solar Energy Systems and Energy Consumption in Buildings",
CEC DG XII, Brussels, 1985.

[10] Svendsen, S.A.,
"Solar Walls and Transparant Insulation, The Use of Airglass in Passive Solar Heating", Invited paper at the Second Workshop in the Feasibility Phase of IEA Solar Heating and Cooling Programma Task XIII Advanced Solar Low-Energy Buildings,
Thermal Insulation Laboratory, TU of Denmark, Copenhagen, 1989.

[11] DeLaHunt, M.J., e.a.,
"Suncode-PC, A Program User's Manual",
Ecotope inc., Seattle 1985.

[12] Henning, S.,
"Airglass-Silica Aerogel, A transparant heat insulator", document D7:1990,
Swedisch Council for Building Research, Stockholm 1990.

[13] Poel, A, H.H.E.W., Eijdems,
"Dutch Shoebox for IEA Task XIII", working document, the Netherlands, TDE/HEy/PSc/066/r.783,
NCIV, Ede, October 1990.

[14] Poel, A, H.H.E.W., Eijdems,
"Properties of transparent insulating materials and their application in buildings", working document, the Netherlands,
TDE/HEy/PSc/066/r.784,
NCIV, Ede, October 1990.

[15] Poel, A, H.H.E.W., Eijdems,
"Modelling of transparent insulating materials on walls", working document, the Netherlands, TDE/HEy/PSc/066/r.789,
NCIV, Ede, October 1990.

[16] Poel, A, H.H.E.W., Eijdems,
"Influence of transparent insulating materials on energy consumption and comfort in houses",
working document, the Netherlands, TDE/HEy/PSc/069/r.904,
NCIV, Ede, October 1990.

[17] Bloomfield, D.,
"Design tool evaluation: Benchmark test cases", technical report no. T.8.B.4., Building Research Establishment, Garston, Watford, England, May 1989.

APPENDIX I : OVERVIEW OF MAIN PROPERTIES OF TRANSPARANT INSULATION MATERIALS

Material properties of TIM's gathered from literature are presented in this appendix.

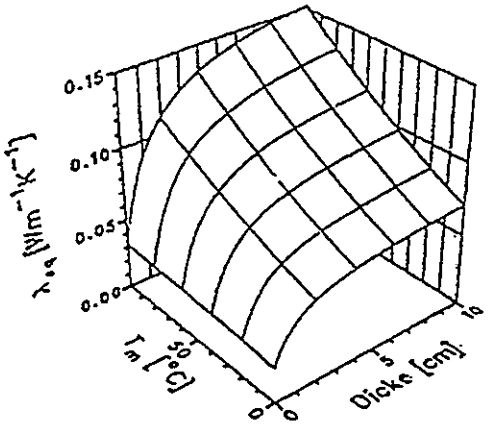

a. Polycarbonate (PC) capillary (1.7 mm cell diameter).

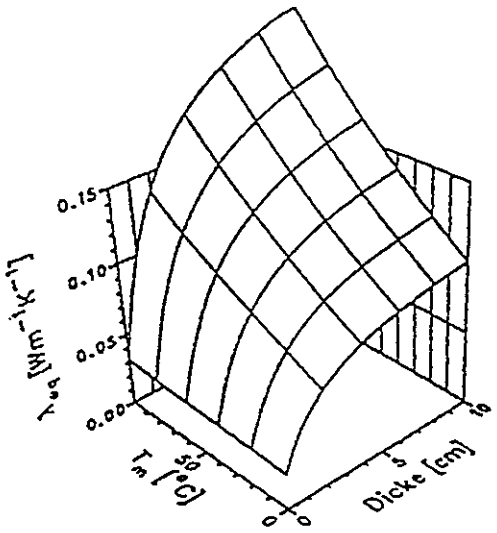

b. PC honeycomb (4.0 mm cell diameter).

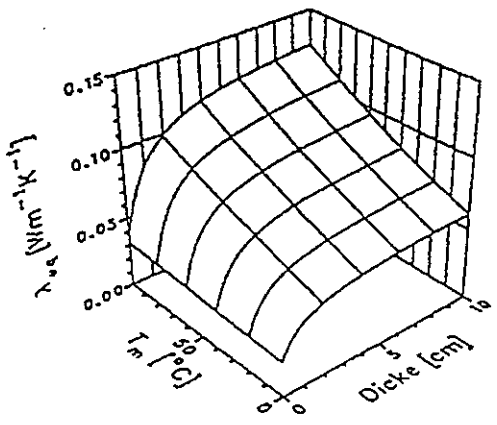

c. Polymethylmetacrylate (PMMA) foam 2-10 mm. cavities

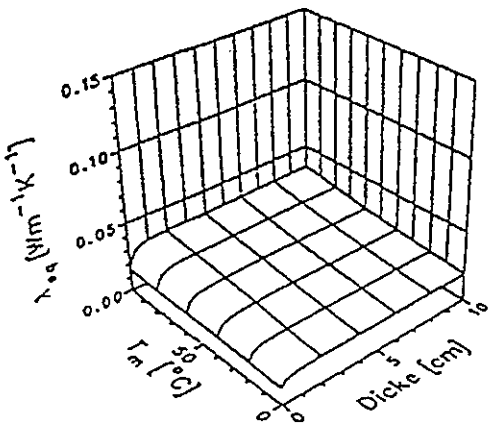

d. Aerogel-Granulat (air, 1 atm)

Figure I.1 : Examples of the equivalent thermal conductivity as function of temperature and layer thickness

source : lit [6] (research data from the Fraunhofer I.S.E., Platzer W., Freiburg 1989)

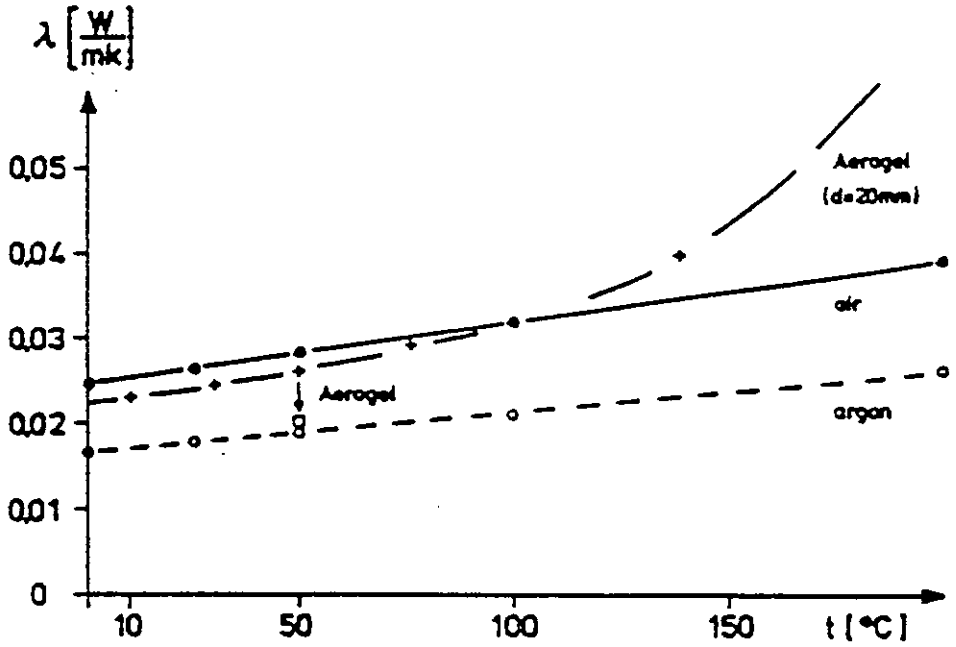

Figure I.2 : Thermal conductivity for granular aerogel as function of temperature

source : lit [1] (page 25 : "Aerogels - a new class of materials", Mielke M. and Wolff B., Ludwigshaven - FRG, 1986)

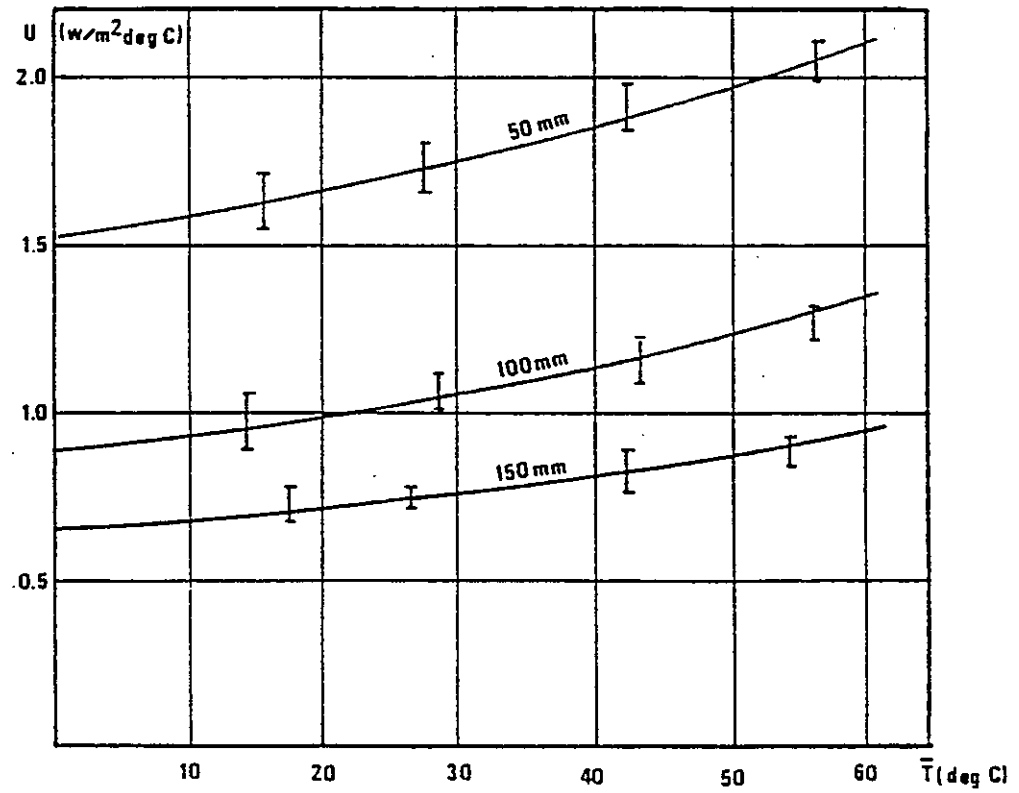

Figure I.3 : Heat Loss Coefficient of honeycomb slabs (both surfaces protected) as a function of thickness and mean temperature)

$\bar{T}$ = Mean honeycomb temperature (average of hot and cold boundary surfaces)

source : lit [1] (page 50 : "Application of honeycomb materials in active and passive systems", Novick O., Yavne - Israel, 1986)

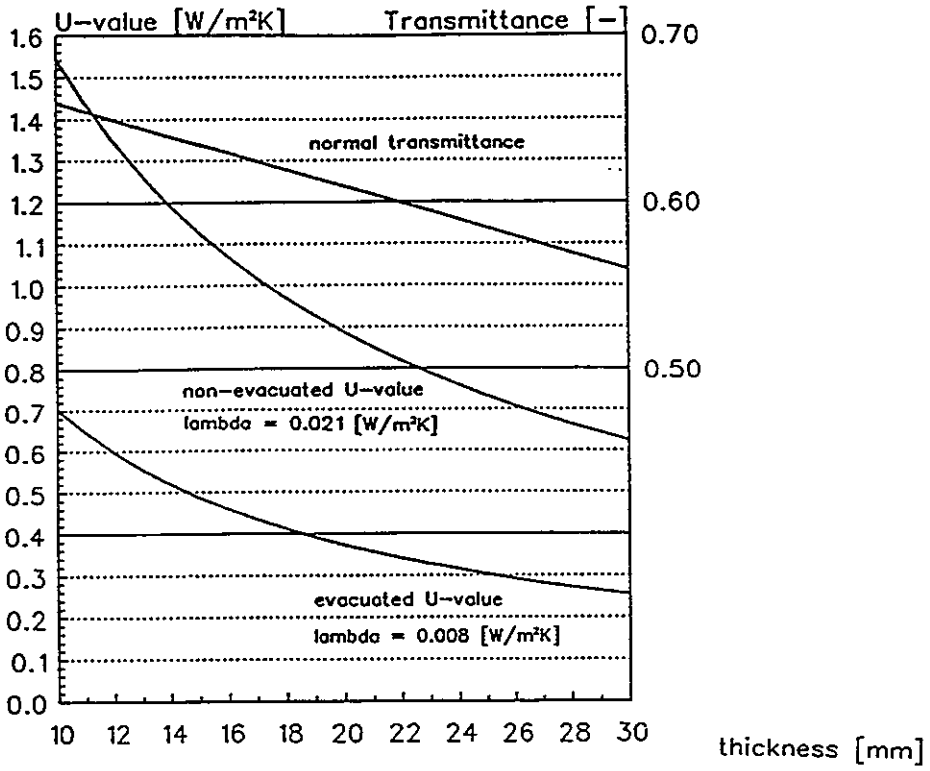

Figure I.4 : Aerogel window panes (including glass cover at both sides): U-value and normal transmittance

source : lit [2] (page 17 : "Aerogel window panes - energy savings in houses", Andersen N.B., Taastrup - Denmark, 1988)

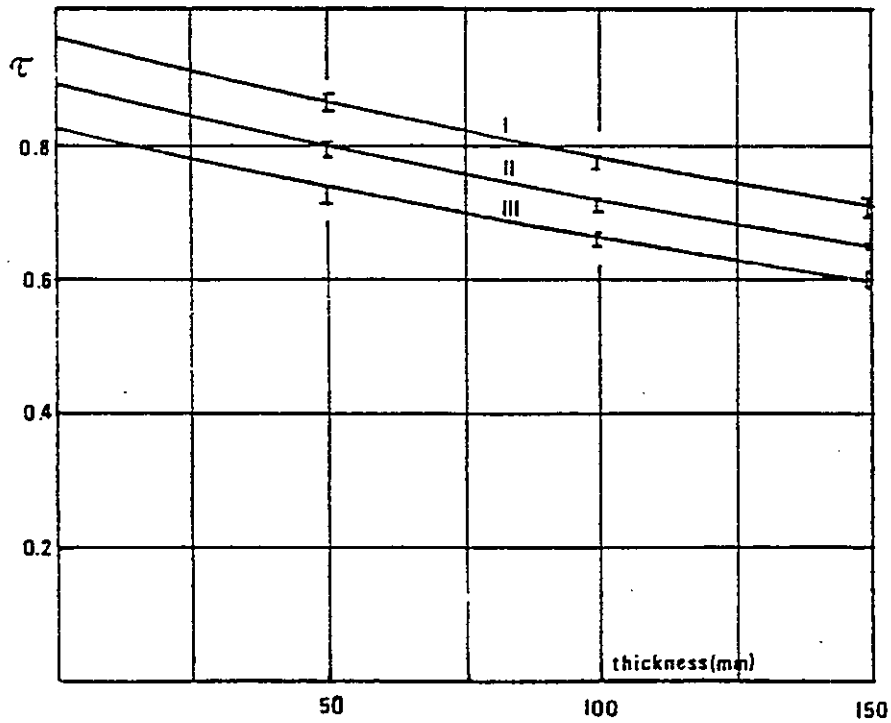

Figure I.5 : Transmission of diffused light (solar spectrum, air mass 2) as a function of honeycomb thickness

I = Unprotected honeycomb
II = Front shielding (low iron glass)
III = Total enclosure (Thermolake modules)

source : lit [1] (page 50 : "Application of honeycomb materials in active and passive systems", Novick O., Yavne - Israel, 1986)

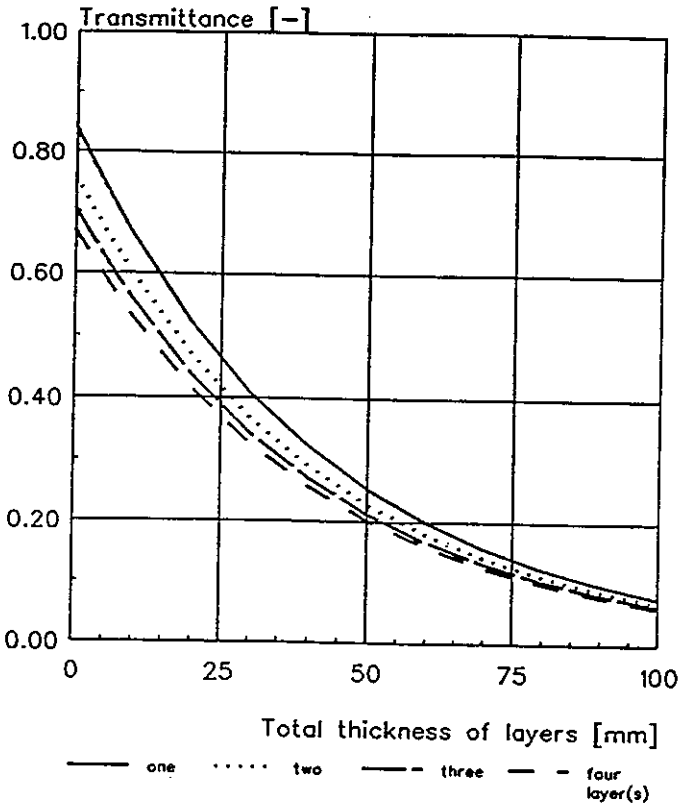

Figure I.6 : Transmission of diffused light as a function of thickness for clear floating glass

source : lit [12] (transmittance formula's taken from the SERIRES computermodel Suncode-PC (manual page 6-10), Wheeling T. and L. Palmiter, Ecotope, Seattle 1985)

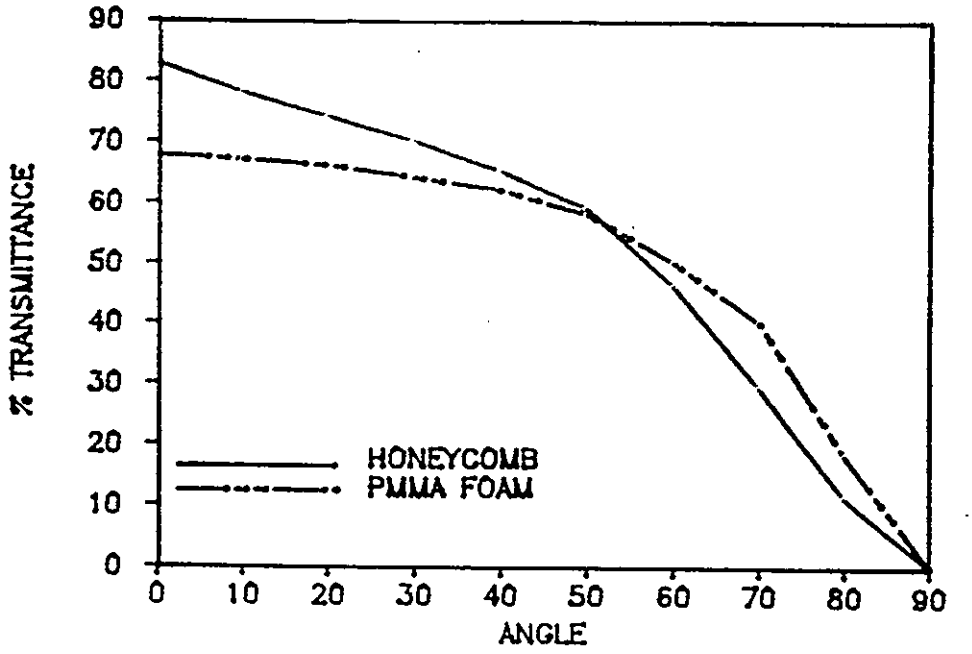

Figure I.7 : Transmittance versus incidence angle of two transparant insulation materials: honeycomb and PMMA foam

source : lit [1] (page 39 : "Energy saving potential of transparant insulation in new houses and in retrofit applications", Jesch L.F., Birmingham - UK, 1986)

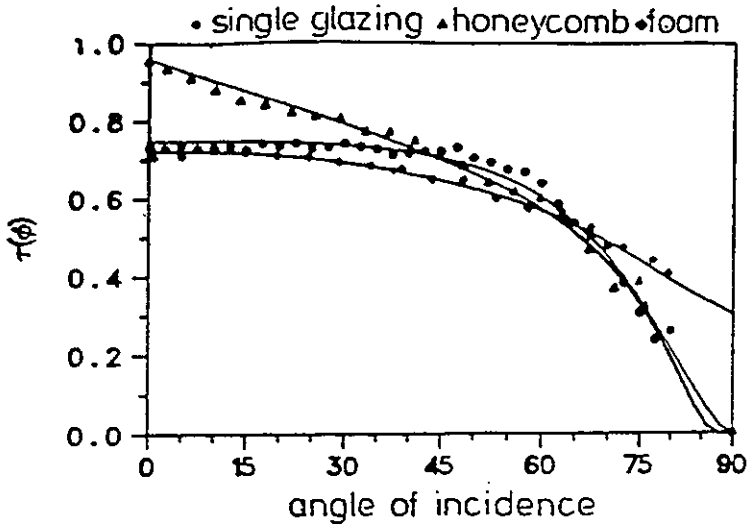

Figure I.8 : Transmittance in dependence on the angle of incidence

source : lit [2] (page 3 : "Transparant insulation materials", Wittwer V., Freiburg - FRG, 1988)

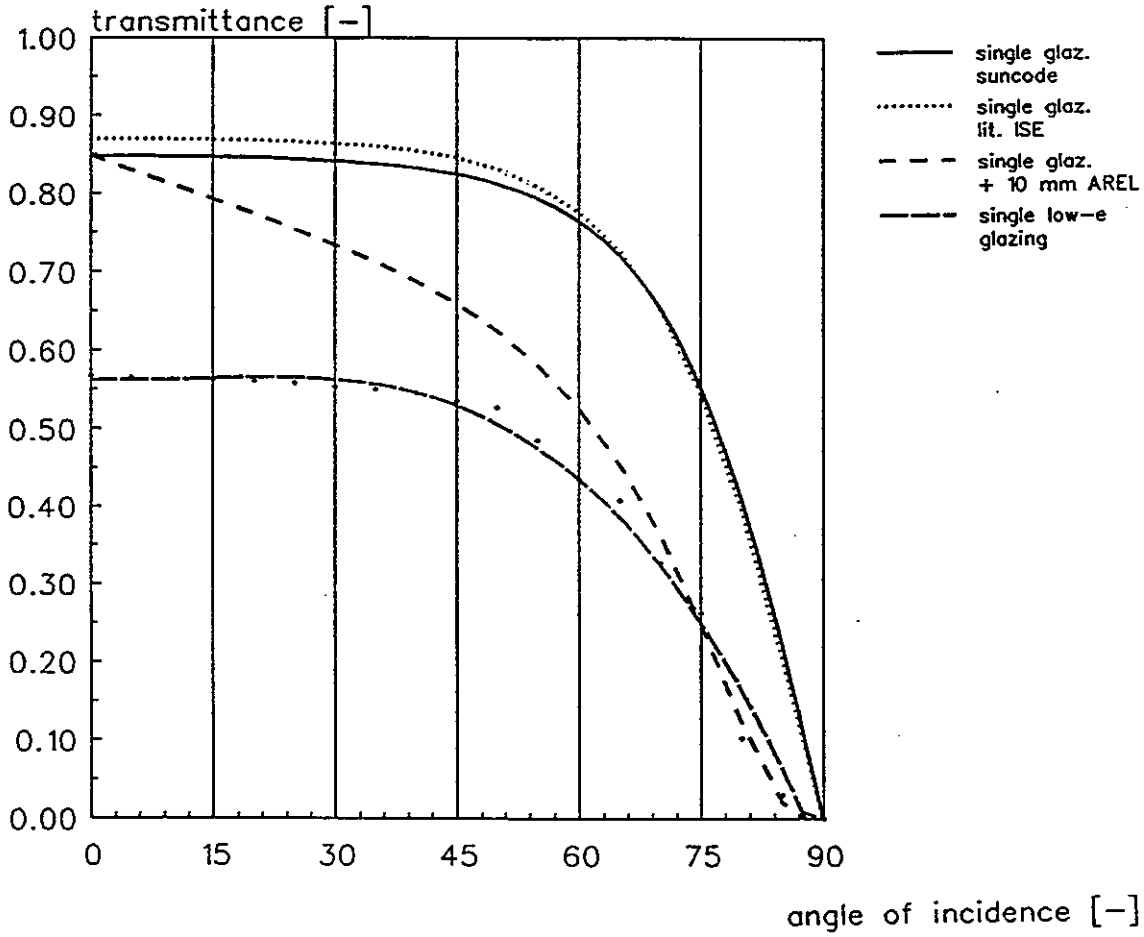

Figure I.9 : Transmittance in dependence on the angle of incidence

source : research data from the Fraunhofer I.S.E.
lit [12] (transmittance formula's taken from the SERIRES computermodel Suncode-PC (manual page 6-10), Wheeling T. and L. Palmiter, Ecotope, Seattle 1985)

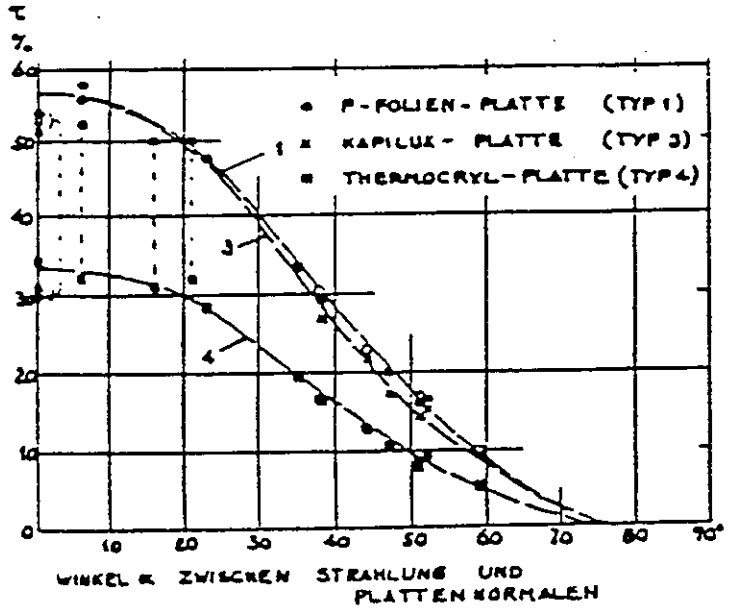

Figure I.10 : Solar energy transmission of TI materials

source : lit [2] (page 10 : "P-Layer insulation (P-Folienplatte) a new transparent thermal insulation material", Peter R.W., Zurich, 1988)

Type of transparent insulation	Solar transmittance $(\tau\alpha)_e$		Heat loss coeff.	Savings
	normal	diffuse	W/m²K	kWh/m² year
One layer of glass	0.84	0.74	5.7	65
Two layers of glass	0.75	0.65	3.1	101
One layer of glass with low emissivity	0.64	0.47	3.1	85
One layer of glass, selective absorber	0.86	0.76	2.8	122
One layer of glass, two layers of Teflon foil, selective absorber	0.77	0.64	1.2	179
One layer of glass, Isoflex (30 mm)	0.61	0.36	1.9	110
One layer of glass, Honeycombs (100 mm)	0.77	0.52	1.2	168
Granular silica aerogel between two layers of glass (20 mm)	0.55	0.35	1.2	135
Monolithic silica aerogel between two layers of glass (20 mm) evacuated	0.68	0.55	0.6	211

Table I.1.a : Data for typical transparant insulation materials used on a solar wall

Type of double glazed sealed unit	Solar transmittance direct and indirect (heat) with normal insolation (%)	Heat loss coef. (W/m²K)
Ordinary	76	3.1
Low energy panes type 1 Low energy panes type 2	72 65	1.9 1.4
Aerogel panes ordinary glass Aerogel panes low iron	70 75	0.4 0.4

Table I.1.b : Typical data for ordinary panes, low-energy panes and aerogel panes.

source : lit [11] ("Solar Walls and Transparant Insulation, The Use of Airglass in Passive Solar Heating", Svendsen, S.A., Copenhagen, 1989)

PRODUCTNAME	MATERIAL	MANUFACTURER	COMPOSITION WITH	THICKNESS MM	TRANSMITTANCE (DIFFUSE) %	U-VALUE W/M2K	NOTE
Aerogel	Aerogel-Granulat	BASF-AG	glass-glass	4 - 12 - 4	52	1.4	
			"	2 - 40 - 2	27	.5	
			"	4 - 10 - 4	65	1.1	evacuated
Aerogel	Aerogel-monolith	Airglass AB	glass-glass	4 - 15 - 4	55	.85	
				15	55	.5	evacuated
				100	44	.19	
Arel	PC honeycomb	Arel Energy	-	50	85	1.4	
				100	75	.9	
Glassfelt	Glassfelt	Grunzweig und Hartmann AG	glass-glass	6 - 21 - 6	24	1.8	
				6 - 40 - 6	19	1.1	
Glassbulb	Glassbulbs	Grunzweig und Hartmann AG	glass-glass	4 - 32 - 4	24	1.3	
IIIT	UP coated films(2x)	Geilinger AG	-	82	58	.7	
Honeycombs	Innerblinds	Watershed Energy Systems	-	93.7	68	1.79	
Hostaflon profile	Hostaflon	Hoechst	-	20	50		
				30		1.6	
Isoflex	PVC corrugated	HDW-Isoliertechnik	-	35	55	1.51	
Isoflex	Cellulose acetate	Isoflex AB	glass-corrugated sheet-film	4 - 10	72	2	
				4 - 20	61	1.7	
				4 - 30	56	1.47	
Isopalux	Glass capillary	INSA	glass-Isopalux-glass	6 - 100 - 6	50	1.1	
Iplus neutral R	Low-E glazing	Interpane	glass-glass	4 - 14 - 4	51	1.38	
Isocryl (small)	PMMA foam	IMC Acrylguss	-	16	50	1.91	
				20	45	1.67	
Isocryl (big)	PMMA foam	IMC Acrylguss	-	16	59	2.12	
				32	46	1.4	
				80	20	.7	
Kalwall panel	Fiber sandwich	Kalwall Solar Components	-	70	60	2.27	
				70	30	1.36	
				70	10	0.95	
Okalux Solar	PC capillary	Okalux	-	10	69	2.7	
				60	63	1.0	
				100	58	.7	
Okapane	PMMA capillary	Okalux	-	12	85	2.55	
				40	73	1.28	
P-film sheet	Film structure	Schweizer AG	acryl-structure-acryl	3 - 60 - 3	57	1.15	
Rodaplus X 560-3	PVC profile	Rodeca	-	60	65	1.45	
Styrolux	Polystrol	BASF AG	-	108	49	1.1	
Styrolux (hex)	Polystrol	BASF AG	-	80	81	1.2	
Thermocryl	PMMA foam	A.Hohnholz	-	18		1.75	
				80		.5	
Ultramid	Polyamid	BASF AG	-	98	60	.7	

Table I.2.a : Transparent insulation materials; Main properties of materials

source : IEA Solar Research and Development, Task 10 - Fraunhofer Institut, february 1990.

(no composite constructions)

PRODUCTNAME	MATERIAL	MANUFACTURER	THICKNESS MM	SOLAR TRANSMITTANCE %	THERMAL CONDUCTIVITY W/MK	MATERIAL HEAT RESISTANCE M2K/W	NOTE
Airglass	Aerogel	Airglass	12.5	80	0.01-0.02	0.63	see T.I.M.
Arel	PC honeycomb	Arel	50 - 100	85-75	0.1-0.13	0.77	see T.I.M.
Dutacryl	PMMA profile		16	75	0.19	0.17	double
Edimet	PMMA		3	92.3	0.21	0.014	
Float glass			3	85-89	0.8	0.004	
Granular Aerogel	Aerogel	BASF	12 - 20		0.02-0.023	0.87	see T.I.M.
Hostaflon	PTFE	Hoechst	0.05	88	0.23	-	
Isocryl	PMMA-foam	IMC Acrylguss	12 - 24	80-50	0.035-0.044	0.55	see T.I.M.
KBE-plan	GRP		1 - 1.2	90			
KBE-solar	GRP		20	75-80			
Kynar	PVDF		0.1	93	0.26	-	
Lexan	PC	G.E.	1 - 3	90-84	0.21	0.014	
Low-E glass			4 - 12 - 4	70		0.17	double
Low-iron glass			4	89-92	0.8	0.004	
Luran	ASA		3.2		0.18	0.018	
Makrolon	PC	Bayer	4.5	80	0.21	0.021	
Marlex	PE	Phillips	0.1	92	0.3-0.4	-	
Mylar	PETP		0.13	87	0.24	-	
Okapane solar	PC capillary	Okalux	40 - 100	80-65	0.078	1.28	see T.I.M.
Okapane solar	PMMA capillary	Okalux	60 - 100	63-58	0.046-0.078	1.28	see T.I.M.
Plexiglass	PMMA	Rohm & Haas	16	85	0.2-0.25	0.064	
Polyester	PETP		0.13	87	0.24	-	
Polylux	PC	Bauphysik	5.5	86	0.21	0.026	
Qualex	PC			80	0.21		
Sunlite Premium	GRP	Kalwall	0.635-1.016	90-85	1.5		
Sunlite Regular	GRP	Kalwall	0.635-1.016	90-85	1.5		
Tedlar	PVF	DuPont	0.1	90-92	0.167	-	
Teflon	FEP	Dupont	0.025-0.05	95-96	0.25	-	
Thermoclear	PC profile	GE	(4)-8-(10)	0.76	0.21	0.09-0.16	double
Thermoclear	PC profile	GE	(10)-16	0.61	0.21	0.20-0.25	triple
Vedrilser	PMMA	Vedril	1.5	92	0.16	0.009	

Table I.2.b : Collector, wall and window glazing; Main properties of materials

source : IEA Solar Research and Development, Task 10 - Fraunhofer Institut, february 1990.

Transluzente Isolation	Dicke (mm)	Λ (W/m²K)	k *) (W/m²K)	Licht-transm. (%)	τ_{Global} (%)	$q_{Wärme}$ (%)	g • τ • q (%)	g/k (τ /k)
3-fach Isolierverglasung	30		1.9	72	62	6	68	.36 (.33)
"HIT"-Fenster	90		0.65	56	31	9	40	.62 (.48)
P-Folienplatte Typ 1	64.1	1.30	1.15	78	57			(.50)
"Kapilux"-Wabenplatte Typ 3	84.3	0.918	0.85	78	57			(.67)
Thermocryl-Platte Acrylschaum, Typ 4	66.4	1.053	0.964	61	33			(.34)
P-Folienplatte (extrap.)	90	0.93	0.82		49			(.60)

*) 1/k = 1/Λ + 1/8 + 1/23 m² K/W

Table I.3 : Comparison between transparant insulation materials.

source : lit [2] (page 10 : "P-Layer insulation (P-Folienplatte) a new transparent thermal insulation material", Peter R.W., Zurich, 1988)

TIM	d(m)	τ_{dif}	g_{dif} ***)
PMMA capillairen*)	0,10	0,70 ± 0,03	0,78 ± 0,05
PC honingraat*)	0,10	0,75 ± 0,03	0,82 ± 0,05
PMMA schuim*)	0,015	0,55 ± 0,03	0,57 ± 0,02
aerogelkorrel tussen 2 PMMA platen (3 mm)*)	0,020 +0,006	0,37 ± 0,03	0,42 ± 0,03
PMMA plaat*)	0,003	0,77 ± 0,03	0,81 ± 0,03
Monolytisch aerogel, 14 mm, tussen 2 glasplaten (3 mm)	0,014 +0,006	0,55 ****)	0,6 ****)
Glas:**)			
enkel glas	0,004	0,77	0,79
dubbel blank glas		0,62	0,7
warmtereflect.dubb.glas		0,5	0,6
idem argon gevuld		0,5	0,6

*) : measurements data of Fraunhofer-ISE
**) : data of TPD
***) : g_{dif} = (actual solar heat gain)/(total solar incident) derived for TIM incl. surface resistances
****) : estimated values

Table I.4.a : Comparison between direct transmittance and total solar heat gain

source : lit [6] ("Translucente thermische isolatie in gevels; een verkenning", Dijk van, H.A.L., e.a., TPD, Delft, februari 1990)

materiaal	dikte (m)	gemeten: τ_{dif} (-)	$R_{10°C}$ m^2K/W	afgeleid: E_t (1/m)	λ_{eq} (W/mK)
Capillaire struktuur:*)					
PC (1,7 mm)	0,025	0,70	0,40	14	0,063
PC (1,7 mm)	0,096	0,58	1,27	5,7	0,076
PC (3 mm)	0,10	0,69	1,09	3,7	0,092
PMMA 7N (3 mm)	0,10	0,70	1,03	3,5	0,097
Honingraat struktuur:*)					
hexagonaal PS	0,080	0,80	0,70	2,8	0,11
sinusoidaal PS	0,093	0,66	0,78	4,5	0,12
rechthoekig PC	0,050	0,84	0,55	3,5	0,091
rechthoekig PC	0,10	0,75	0,93	2,9	0,11
verbeterde rechthoekig PC	0,10	0,75	1,03	2,9	0,097
PMMA schuim:*)					
type <A>, ca. 2,5 mm holten	0,016	0,49	0,33	45	0,048
type <C>, ca. 5 mm holten	0,016	0,59	0,30	33	0,053
	0,048	0,31	0,77	24	0,062
	0,080	0,20	1,25	20	0,064
type <C>, gecacheerd	0,016	0,54	0,29	39	0,056
Aerogel:					
korrels, tussen glas *)	0,014	0,55	0,50	43	0,028
(dikte en eigenschappen	0,024	0,43	1,00	35	0,024
inclusief 2x2 mm glas)	0,044	0,27	2,00	30	0,022
monolytisch aerogel **):					
in lucht, 1 atm.	0,010	0,88	0,48	13	0,021
in vacuüm (0,1 atm.)	0,010	0,88	1,3	13	0,008
(dikte en eigensch. excl.glas)					
gegranuleerde aerogel**):	0,020	0,50	0,95	35	0,021
(dikte en eigensch. excl.glas)					
Glas:***)					
enkel blank glas	0,004	0,77	0,005		
dubbel blank glas		0,6	0,18		
warmtereflecterend dubbelglas		0,5	0,39		
idem, argon gevuld		0,5	0,60		
dubbelglas met 2 warmtereflec-terende folies		0,3	1,50		

PC : polycarbonaat;
PMMA: polymethylmetacrylaat;
PS : polystyrol

*) : derived from measurements data of Fraunhofer-ISE
**) : derived from data of the Danish BRI
***) : data of TPD

Table I.4.b : Selection of thermal-optical properties

source : lit [6] ("Translucente thermische isolatie in gevels; een verkenning", Dijk van, H.A.L., e.a., TPD, Delft, februari 1990)

Material	Thickness (cm)	τ^{dif}	Λ^{10oC} ($Wm^{-2}K^{-1}$)
Single glass			
normal float	0.4	0.78	
low iron	0.4	0.84	
Double glazed window			
float	1.6	0.67	5.20
low iron	1.6	0.75	5.20
PMMA-type foam			
type A1K	1.6	0.58	3.60
type A2K	1.6	0.65	3.10
type (C)	1.6	0.60	3.50
type (C) film cover	1.6	0.58	3.50
Capillary structure			
PC	6.0	0.63	1.45
PC	10.0	0.60	0.79
Honeycomb structures			
Sinusoidal PS	10.8	0.66	1.28
hexagonal PS	4.3	0.75	2.21
hexagonal PA	9.8	0.61	0.97
sinusoidal PVC	10.8	0.45	1.12
hexagonal PVC	10.8	0.48	0.92
AREL/PC	10.0	0.71	1.10
Aerogel windows			
GRA 12968c	1.2	0.52	1.67
GRA 12968c	2.0	0.44	1.00

Remarks:

τ dif : Hemispherical-hemispherical global transmittance

$\Lambda 10^{o}C$: Heat loss coefficient at 10°C (without heat transfer to air as included in k/U-value

PC : Polycarbonate
PS : Polystyrene
PA : Polyamid
PVC : Polyvinylchloride

Commercial availbility:
PMMA-foam: IMC Acrylguss-GmbH, Remscheid. FRG
Capillaries: OKALUX, Marktheidenfeld, F.R.G
PC-Honeycombs: AREL Energy Ltd., Yavne, Israel

Table I.5 : Material data.

source : lit [1] ("Transmittance characteristics of TIM's", Platzer W., Wittwer V., Fraunhofer Institut SES, Freiburg november 1986.)

Material	D[cm]	Λ_{10}[W/m^{2}K]	k_{10}[W/m^{2}K]	τ_{dif}	g_{dif}
OKALUX PMMA HW	9.8	0.89±0.03	0.77±0.03	0.76±0.05	-
" PMMA HW	3.8	1.75±0.03	1.36±0.03	0.82±0.05	-
" TPX	10.0	2.03±0.05	1.51±0.05	0.49±0.05	0.53±0.05
" TPX	4.0	3.25±0.11	2.10±0.11	0.61±0.05	-
" TPX	1.2	5.74±0.26	2.92±0.26	0.72±0.05	-
" PC1	10.0	0.92±0.03	0.80±0.03	0.69±0.05	0.71±0.05
" PC1	8.0	1.13±0.03	0.95±0.03	0.73±0.05	0.74±0.05
" PC1	6.0	1.37±0.03	1.11±0.03	0.76±0.05	-
" PC1	1.5	4.07±0.15	2.42±0.15	0.79±0.05	-
" HFL	6.0	1.45±0.03	1.17±0.03	0.61±0.05	0.69±0.05
" HFL	4.0	1.91±0.05	1.45±0.05	0.65±0.05	-
" HFL	2.2	3.04±0.10	2.01±0.10	0.74±0.05	-
" PMMA 7N	10.0	1.08±0.03	0.91±0.03	0.70±0.05	0.78±0.05
" PMMA 7N	5.0	1.78±0.04	1.37±0.04	0.76±0.05	-
" PMMA 7N	4.0	1.94±0.05	1.46±0.05	0.83±0.05	-
" PMMA 7N	2.3	2.89±0.08	1.95±0.06	0.82±0.05	-
" PMMA 7N	1.5	3.40±0.11	2.16±0.07	0.79±0.05	-
" PMMA 7N	1.0	4.20±0.15	2.46±0.08	0.76±0.05	-

Table I.6.a : Measurements for capillary structures.

Material	k_t[W/m^{2}K]	$g_d(0°)$ 1)	g_{dif}	g_{eff}(+glass)	efficiency
OKALUX TPX	1.30	0.80	0.53	0.59	0.36
" HFL	0.83	0.95	0.58	0.67	0.49
" PC1	0.84	0.95	0.71	0.73	0.55
" PMMA 7N	0.93	0.95	0.78	0.76	0.57
" PMMA HW	0.81	0.95	0.82 2)	0.78	0.59

1) The optimal transmittance was used here for capillaries parallel to the incoming light; the transmittance for TPX was reduced because of bad quality of the surface cut and because of rippled cell walls

2) Estimated value from transmittance

Table I.6.b : Selection criteria for a high-temperature flat-plate collector.

Material	D[cm]	Λ_{10}[W/m^{2}K]	k_{10}[W/m^{2}K]	τ_{dif}	g_{dif}
Kaiser	6.0	1.41±0.04	1.14±0.04	0.79±0.05	-
"	8.0	1.15±0.03	0.96±0.03	0.74±0.05	-
"	10.0	0.97±0.03	0.83±0.03	0.75±0.05	-
"	12.0	0.81±0.03	0.71±0.03	0.71±0.05	-
AREL	5.0	1.81±0.05	1.39±0.04	0.81±0.05	0.87±0.03
"	10.0	1.07±0.03	0.91±0.03	0.75±0.05	0.82±0.03

Table I.6.c : Measurements honeycomb-structures (PC).

source : lit [1] ("Transparant Insulation Materials",Platzer W., Wittwer V., TI 3, Fraunhofer Institut SES, Freiburg september 1989).

DENSITY	70 – 250 kg/m^3
REFRACTIVE INDEX	1.015 – 1.055
HEAT TRANSFER COEFFICIENT	0.021 W/mK 20°C
—·— —·— —·—	0.2 W/mK 300°C
—·— —·— —·— EVACUATED	0.008 W/mK 20°C
GRAIN SIZE (TYPICAL VALUES)	3.5 nm
PORE SIZE (TYPICAL VALUES)	10 – 20 nm
SPECIFIC SURFACE AREA	700 m^2/g
VELOCITY OF SOUND	120 m/s
ACOUSTIC IMPEDANCE	10^4 – 10^5 kg/m^2 s
DIELECTRIC CONSTANT	1.14 FOR POWDER
	< 1.08 FOR PLATE
CHEMICAL COMPOSITION	99.99 % SiO_2
NON DEFORMING	UP TO 750°C
RESITANT TO RADIOACTIVITY AND UV	60 × 60 × 2 cm^3
MAXIMUM SIZE	
CAN BE DYED	

Table I.7 : Properties of Airglass-Silica Aerogel.

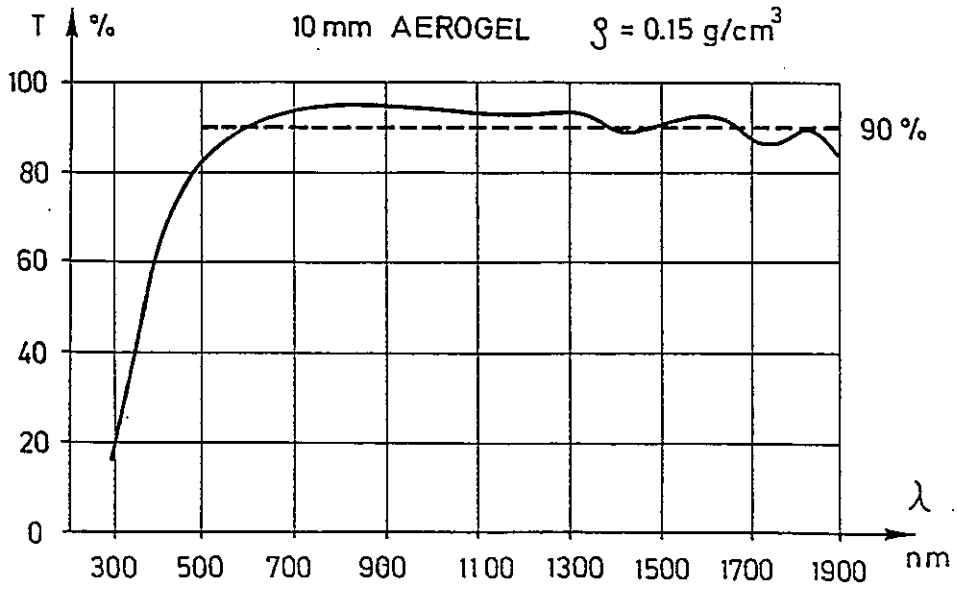

Figure I.11 : Transparancy of aerogel. (Only the unscattered light has been measured.)

source : lit. [13] ("Airglass-Silica Aerogel, a transparant heat insulation", Henning S., Swedisch Council for Building Research, Stockholm 1990.)

APPENDIX II: TRANSMITTANCE AND SOLAR GAIN FACTOR AS FUNCTION OF GLAZING PARAMETERS IN SUNCODE-PC

Within the computermodel Suncode-PC a window is characterized by its size, location in a surface and materialproperties of panes. The surface is used for determination of orientation and shading by sidefins and overhangs. The windows are assumed to be composed of one or more (equal) layers of glazing material. The glazing layers are characterized by a shading coefficient (SC; for modelling shading devices, etc), layer thickness (t), extinction coefficient (K) and index of refraction (n).
For normal clear floating glass the material coefficients are well known (n = 1.526, K = 0.0197 1/mm). The transmittance and solar gain factor are calculated from the angle of incidence as function of number of layers and layer thickness and the above mentioned material coefficients. The formula's used by the Suncode glazing algoritm are presented below (see also Figure 1). These formula's are valid for uncoated planoparallel layerconstructions of glass and plastics plates or foils (thickness > 0.0001 m).

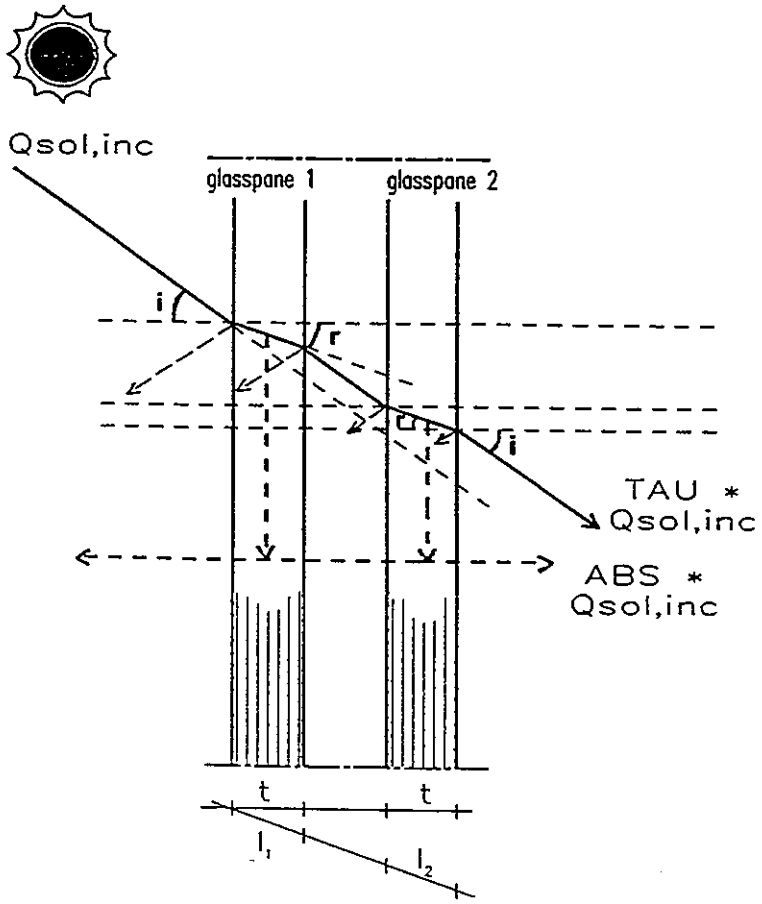

Figure 1: Scedule for calculation of transmittance and absorption within Suncode

Suncode formula's for calculation of glazing:

a = number of layers
t = thickness of single layer
n = index of refraction
K = extinction coefficient
i = angle of incidence
r = angle of refraction
l = length of path of the rays inside the glazing

$p = 2a - 1$; used for calculating multiple layer interactions

$x = \{(n-1)/(n+1)\}^2$; Fresnel reductionparameter for reflections at the outer glazing surface for normal incidence

$r = \arcsin\{\sin(i)/n\}$

$l = (a*t)/\cos(r)$

$v = \{\tan(i-r)/\tan(i+r)\}^2$; Fresnel reductionparameter for reflections at the outer glazing surface in the plane parallel to the plane of incidence

$u = \{\sin(i-r)/\sin(i+r)\}^2$; Fresnel reductionparameter for reflections at the outer glazing surface in the plane perpendicular to the plane of incidence

$y = \{(1-u)/(1+p*u) + (1-v)/(1+p*v)\}/2$; if $|i| > 0$
$y = (1-x)/(1+p*x)$; if $i = 0$

$$TAU = y * e^{-K*l}$$

total transmittance of all layers in the window

The above formula is used for calculation of the transmittance for direct and diffuse solar radiation. For diffuse radiation the angle of incidence is a constant (default = 60 deg.).

$w = \{(1-u)/(1+u) + (1-v)/(1+v)\}/2$; if $|i| > 0$
$w = (1-x)/(1+x)$; if $i = 0$

$q = e^{-(K*l/a)}$; fraction of solar intensity at the inner surface of a glazing layer in accordance to the intensity at the outer surface (1-q = absorbtivity of a single layer)

$z = w*q$

coeff.	1-layer	2-layers	3-layers	4-layers
A1	0.23	0.17	0.13	0.11
A2	0.00	0.63	0.47	0.39
A3	0.00	0.00	0.76	0.62
A4	0.00	0.00	0.00	0.83

$$ABS = (1-q)*(A_1 + A_2*z + A_3*z^2 + A_4*z^3$$

interior entering part of absorbed solar radiation

In the above formula for the interior entering part of absorbed solar radiation no term is included for reflections at the outer surface of the outer pane. This can clearly be seen if the coefficients for a single layer window are subtituted in the formula. According to us this indicates an error in the Suncode glazing algoritm. In the graphs of this appendix this omission is visualized for the solar gain factor not being zero at an angle of incidence of 90 degrees.

For modelling other materials then glass the extinction coefficient and index of refraction of this specific material should be known. For many of the transparent insulation materials these parameters are not (yet) known or public available. Strictly the suncode glazing algoritm is not suitable for calculating composite constructions of TIM and covering layers. For planoparallel multi-layerstructures filled with air the angle of incidence of the rays is equal for each transition of air to glass. The same aplies for the angle of refraction at the transition of glass to air. This effect is not applicable for a double glazing unit filled with airglass transparent insulation material. This latter will act like an ideal mirror for rays striking the surface at an angle of incidence above 75 degrees.

During the feasibility phase of this IEA task we faced two problems:

1) is it possible to get a global approach of TIM-behaviour by varying the glazing parameters within Suncode ?
2) which values of glazing parameters will give the best fitting for a specific TIM ?

To the first point the transmittance and solar gain factor curves of the 'glazing'-material as function of the angle of incidence are of interest. It is possible to change the shape of these curves by varying glazing parameters. If a TIM-like shape can be reached the first problem is solved.

The second point depends on the availability of transmittance and solar gain measurement data for several TIM's. If these data are available a statistical regression analysis might give the best fitting parameters and indication about the reliability of the fysical model for simulating TIM's. Since the glazing formula's are quite complex and due to a lack of available measurement data we can find an intermediate solution by a graphical approach. Therefore the transmittance and absorption formula's of the Suncode glazing algoritm are calculated for various sets of inputparameters and presented as graphs in this appendix. Variations were carried out for one, two, three and four layer-constructions in layerthickness (Figures 3, 4, 5 and 6), index of refraction (Figures 7, 8, 9 and 10) and extinction coefficient (Figures 11, 12, 13 and 14). The shading coefficient was not varied, because this parameter within Suncode has a lineair influence on transmittance and solar gain factor and can be used as a scaling parameter in the fitting proces (rotation round

the 90 degrees point at the horizontal axis; see Figure 2). A known transmittance curve of a specific TIM should be scaled up and/or down by the inverse shading coefficient and copied to a transparency. From the graphs in this appendix the best fitting curves can be found for transmittance and accompanying solar gain curves. The matching glazing parameters are in the graphtitle.

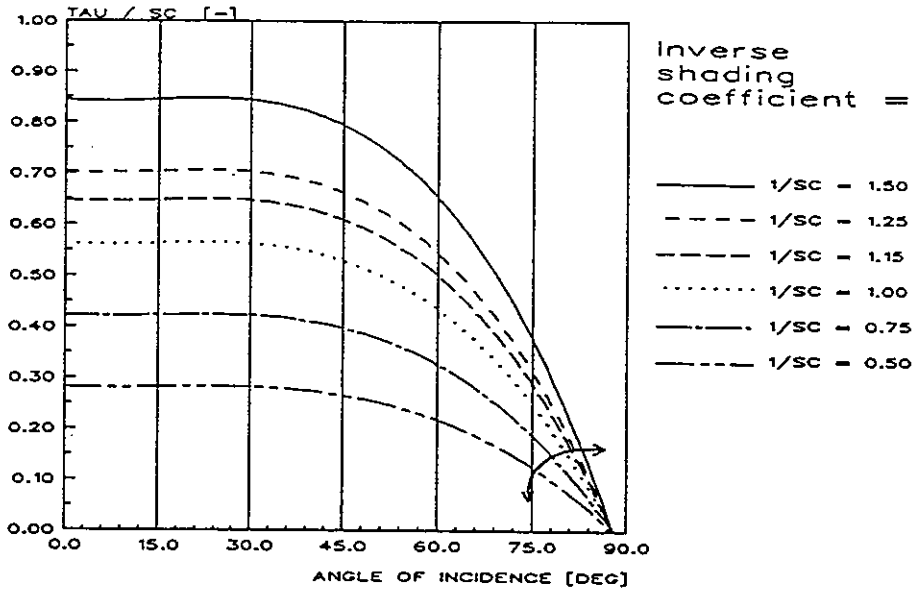

Figure 2: Example of scaling up or down the transmittancecurve with the inverse value of the Suncode shading coefficient

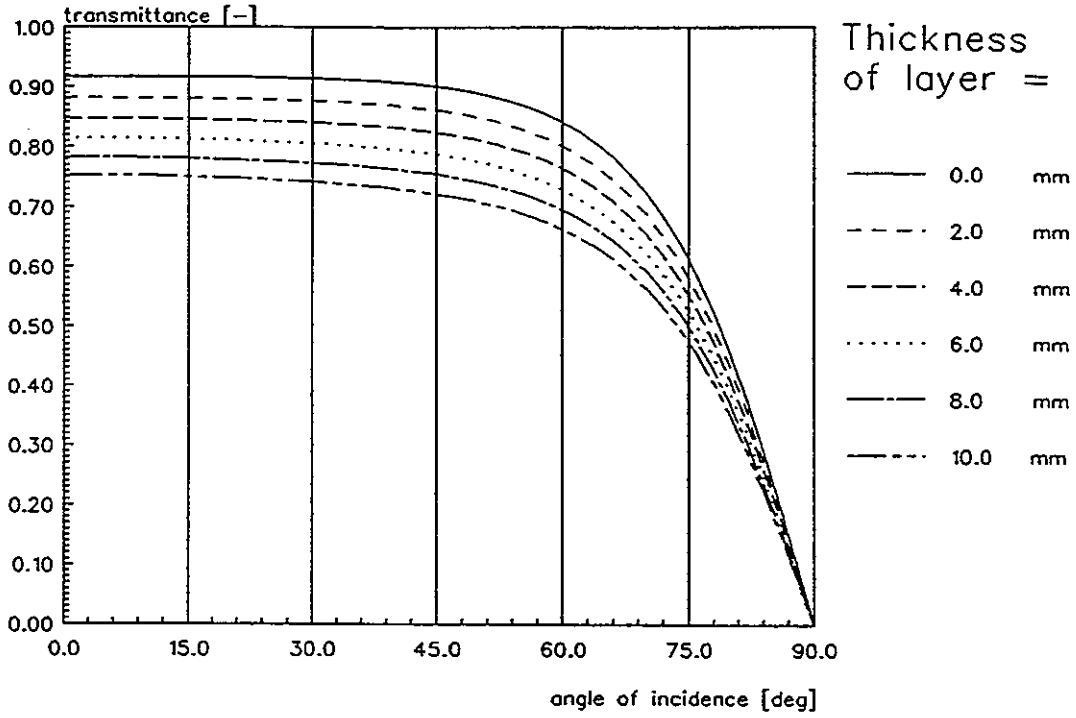

a. Transmittance

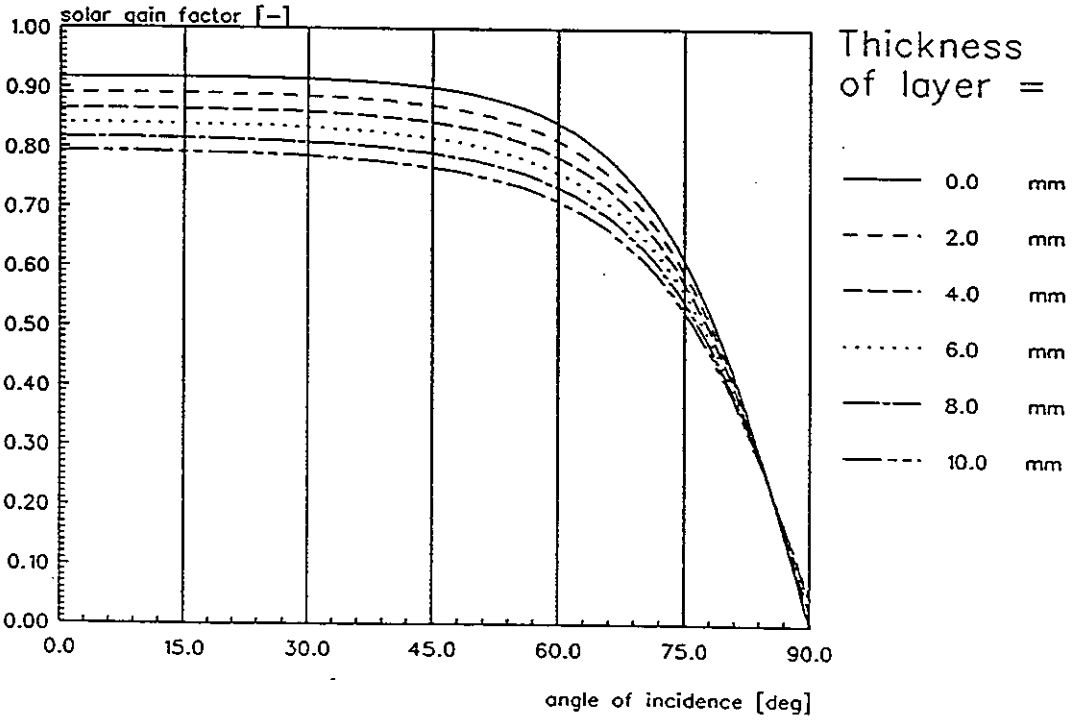

b. Solar gain factor

Figure 3: One-layer-glazing with variable layerthickness (n = 1.526, K = 0.0197 1/mm)

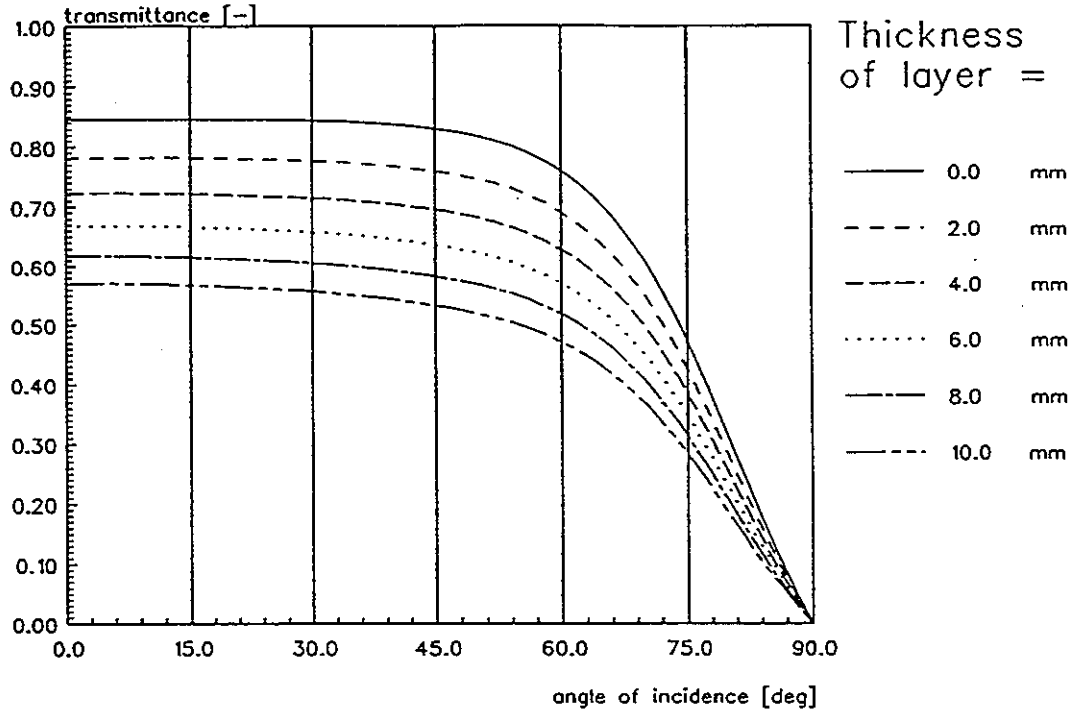

a. Transmittance

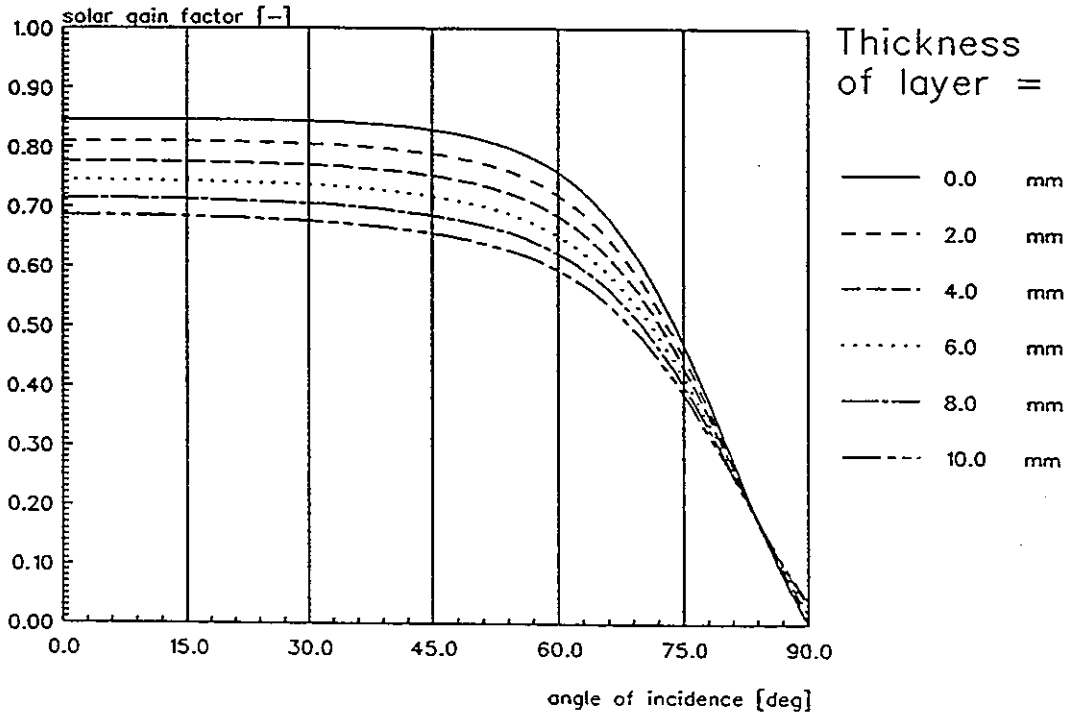

b. Solar gain factor

Figure 4: Two-layer-glazing with variable layerthickness (n = 1.526, K = 0.0197 1/mm)

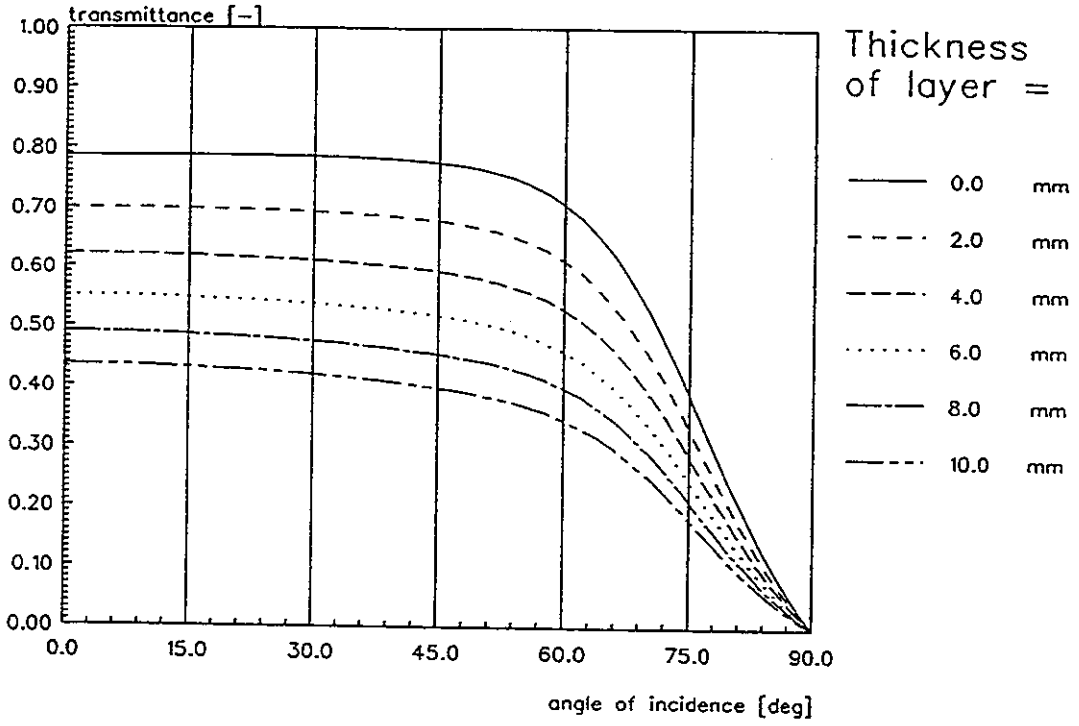

a. Transmittance

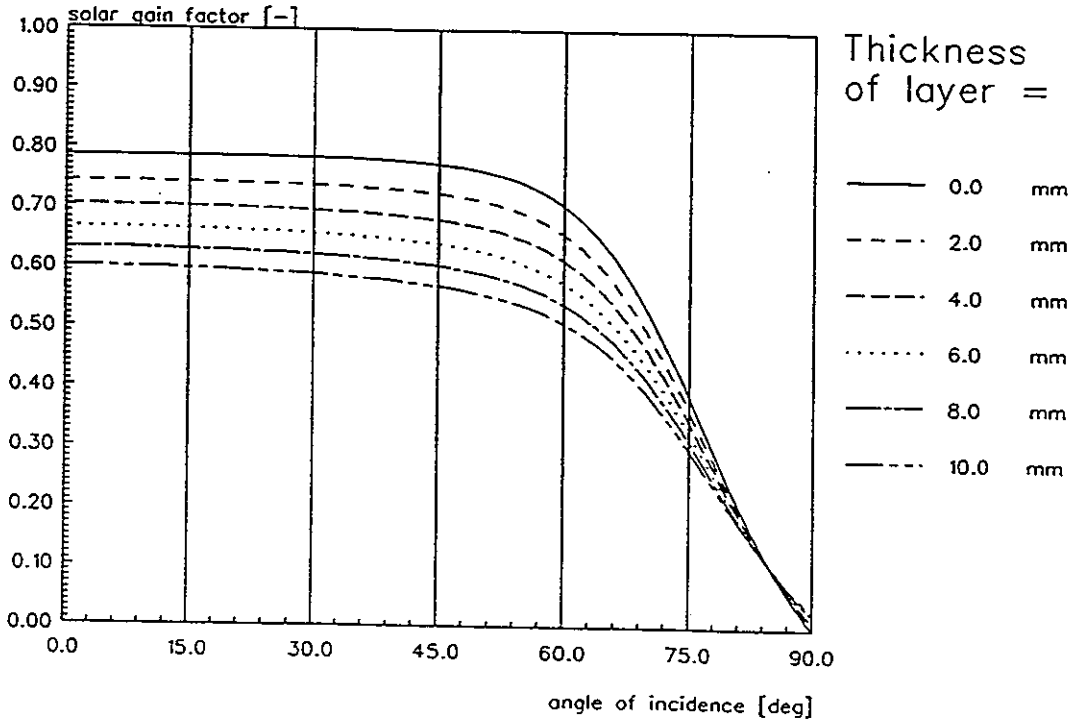

b. Solar gain factor

Figure 5: Three-layer-glazing with variable layerthickness (n = 1.526, K = 0.0197 1/mm)

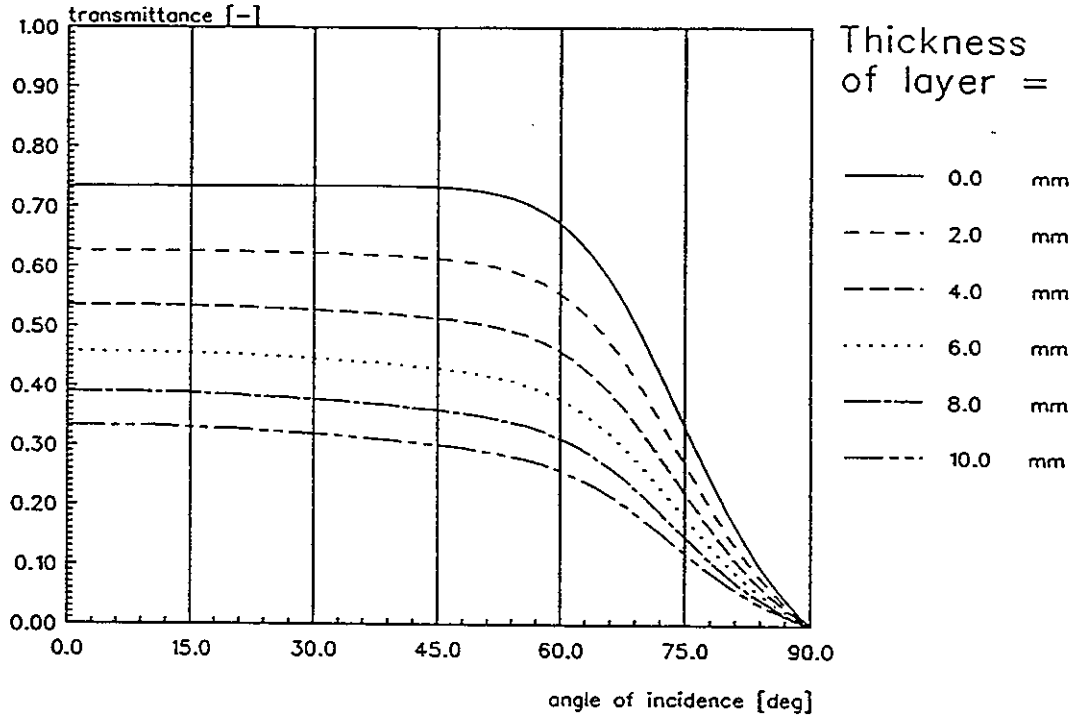

a. Transmittance

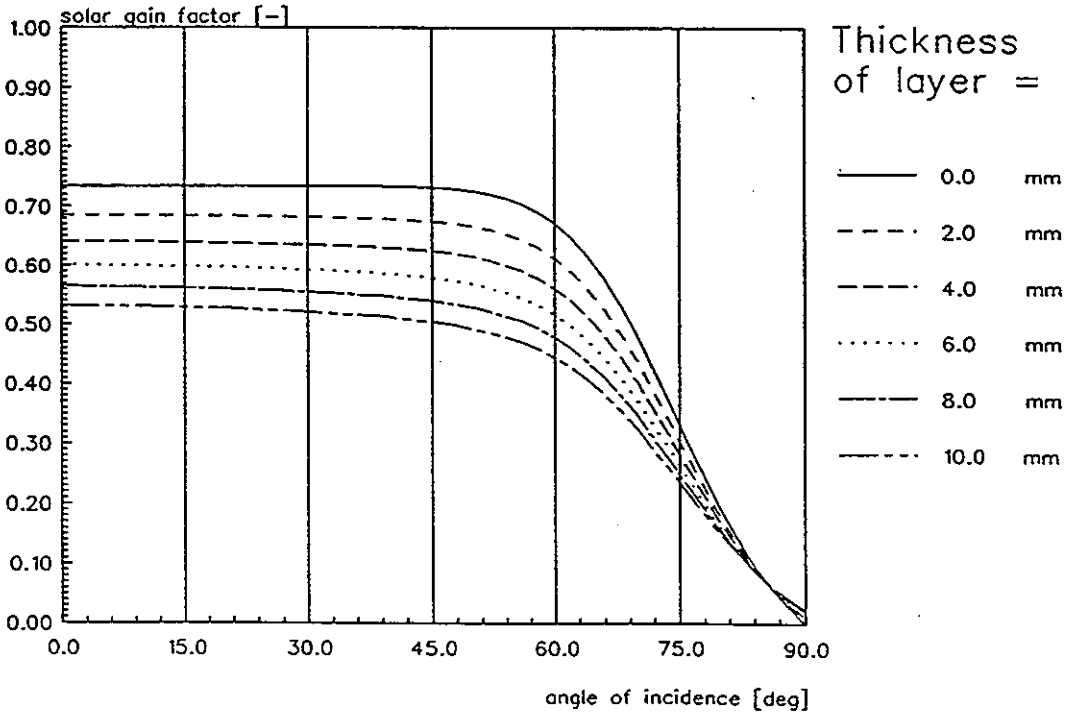

b. Solar gain factor

Figure 6: Four-layer-glazing with variable layerthickness (n = 1.526, K = 0.0197 1/mm)

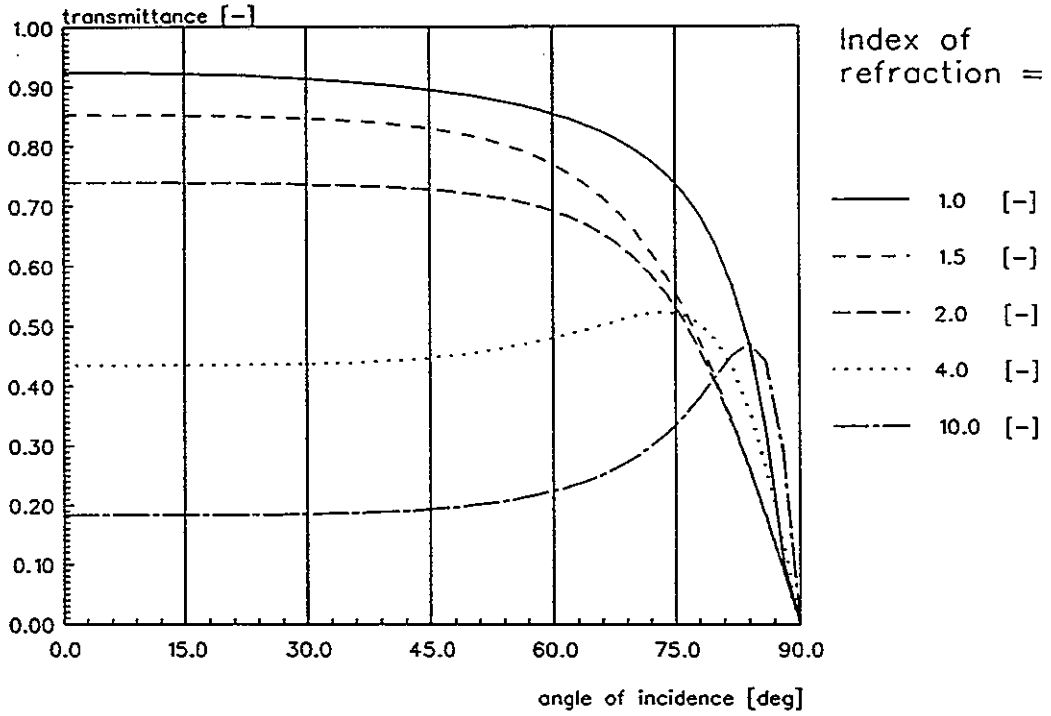

a. Transmittance

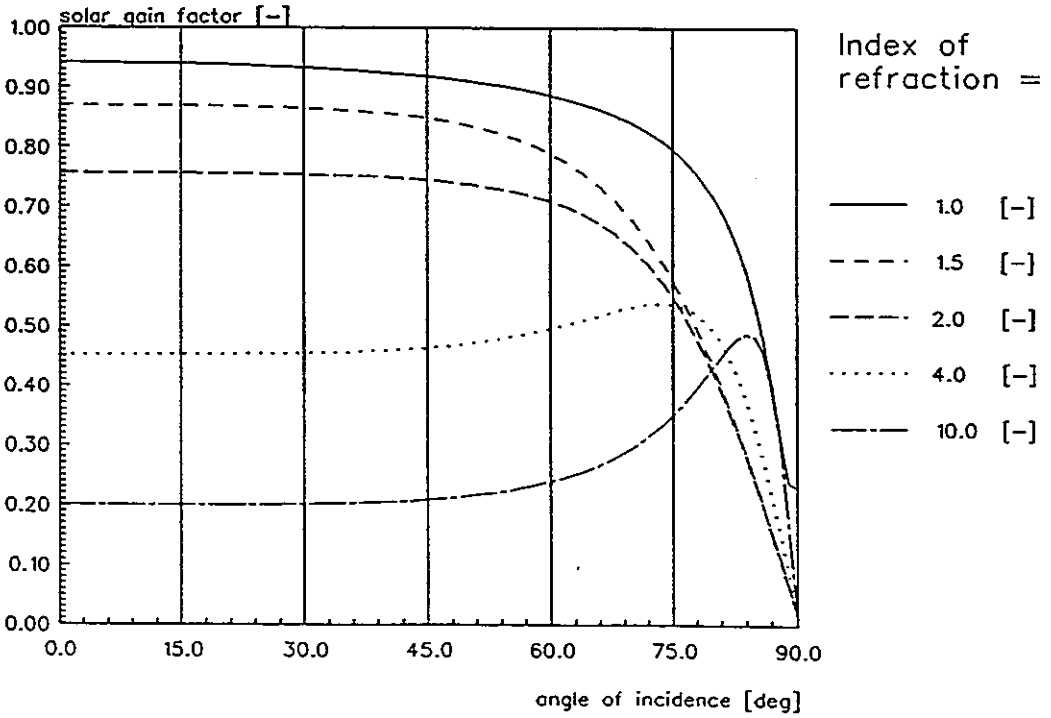

b. Solar gain factor

Figure 7: One-layer-glazing with variable index of refraction (t = 4 mm, K = 0.0197 1/mm)

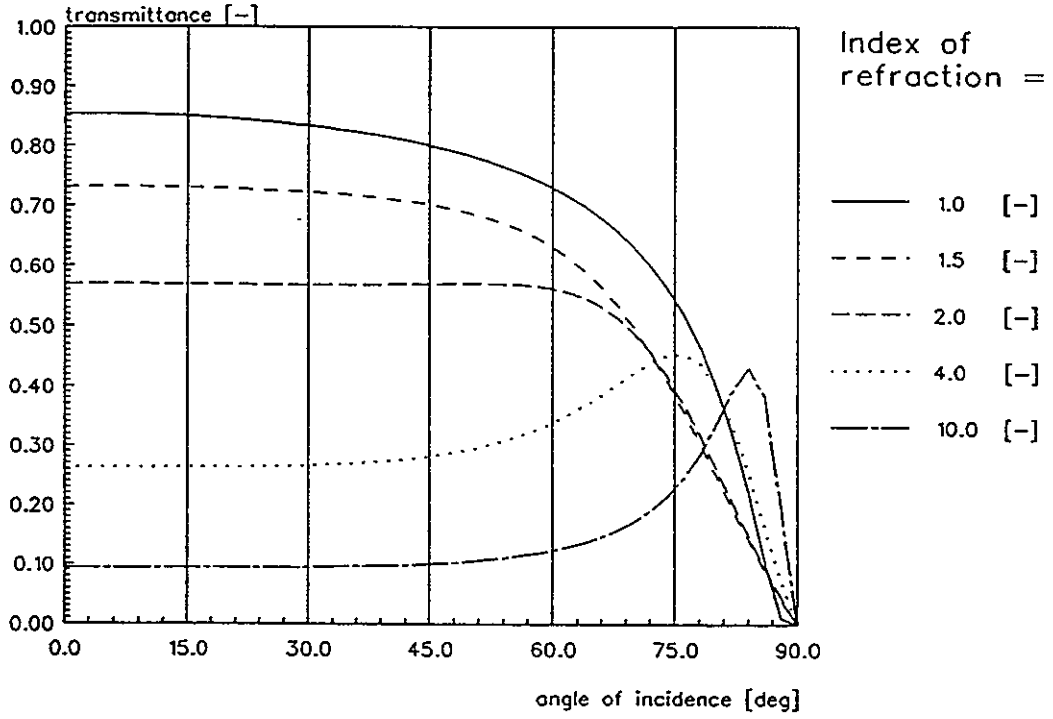

a. Transmittance

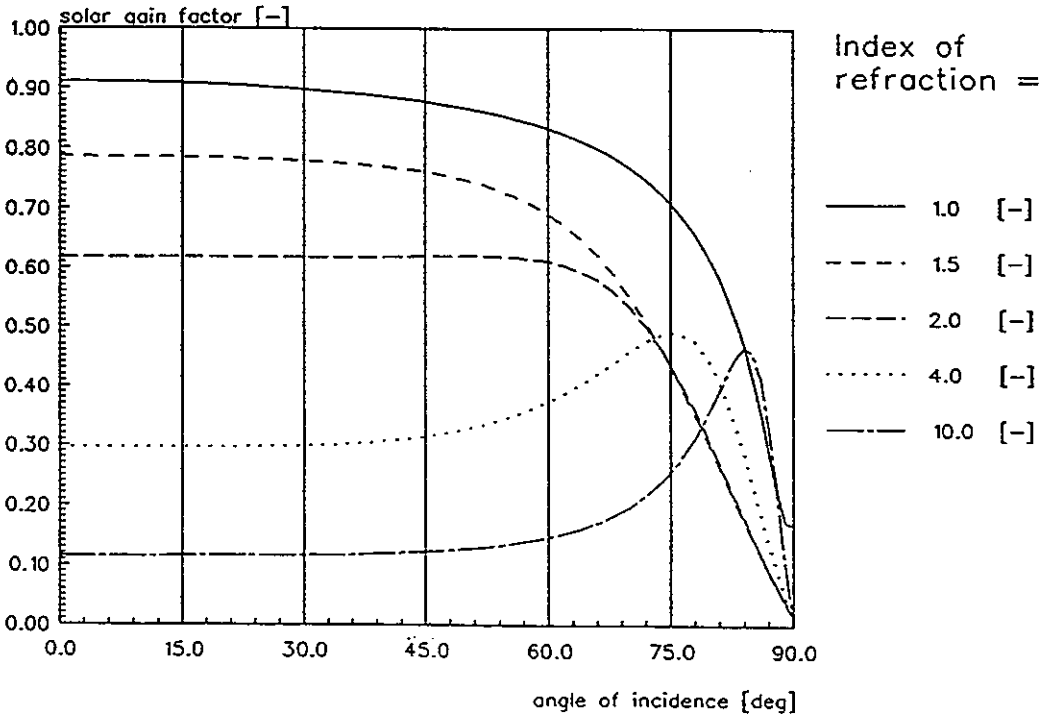

b. Solar gain factor

Figure 8: Two-layer-glazing with variable index of refraction (t = 4 mm, K = 0.0197 1/mm)

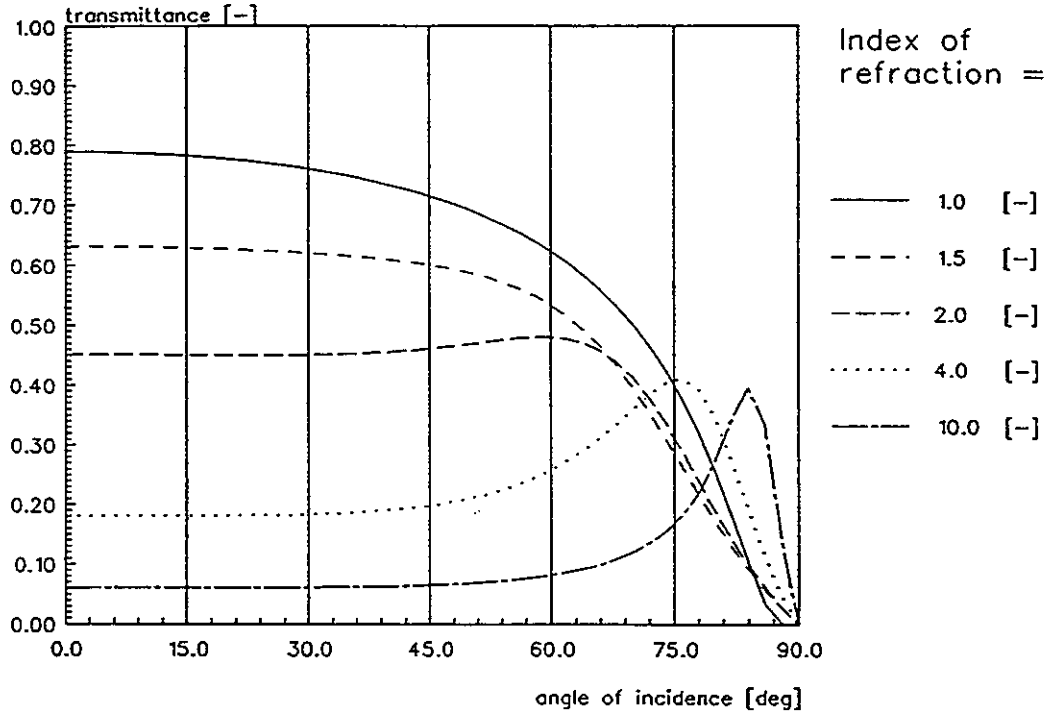

a. Transmittance

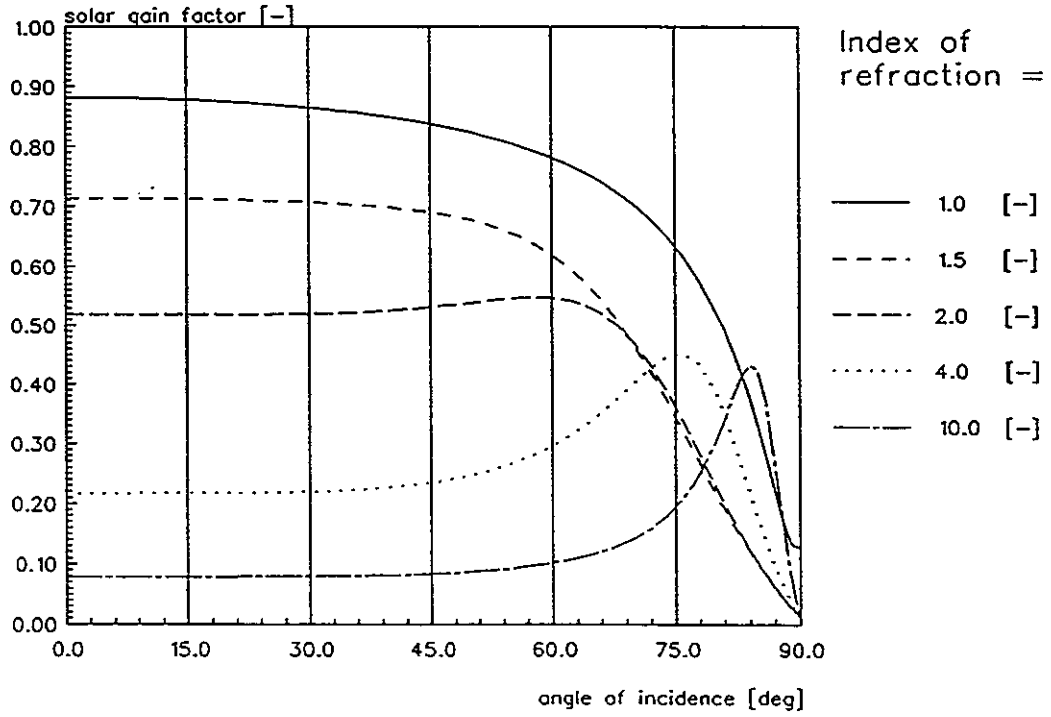

b. Solar gain factor

Figure 9: Three-layer-glazing with variable index of refraction (t = 4 mm, K = 0.0197 1/mm)

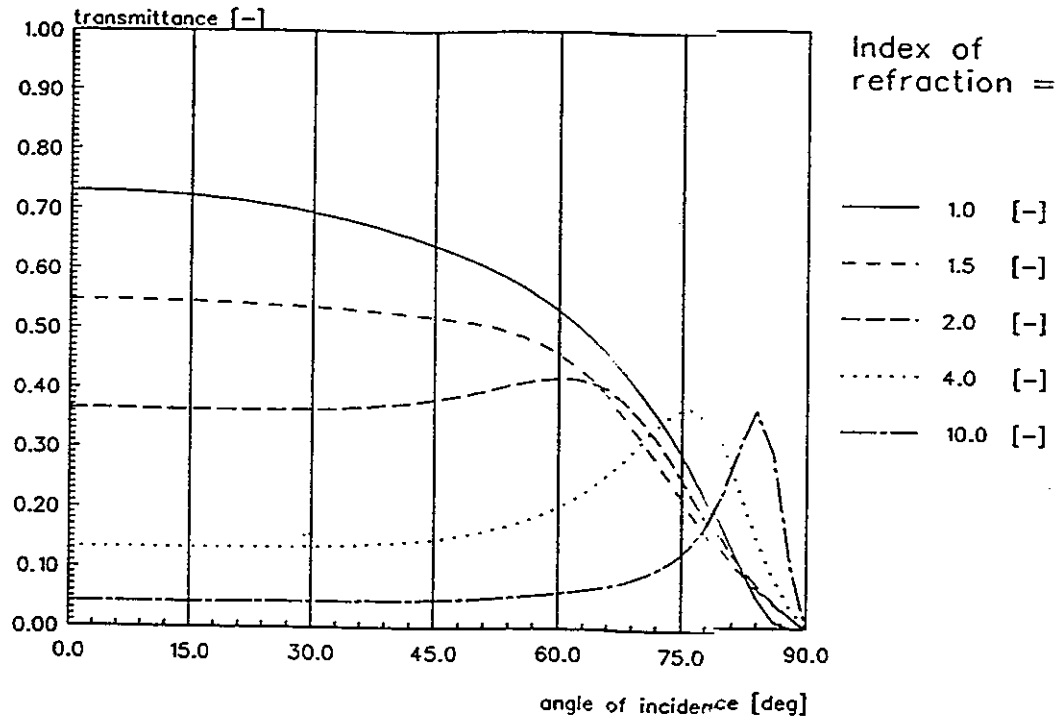

a. Transmittance

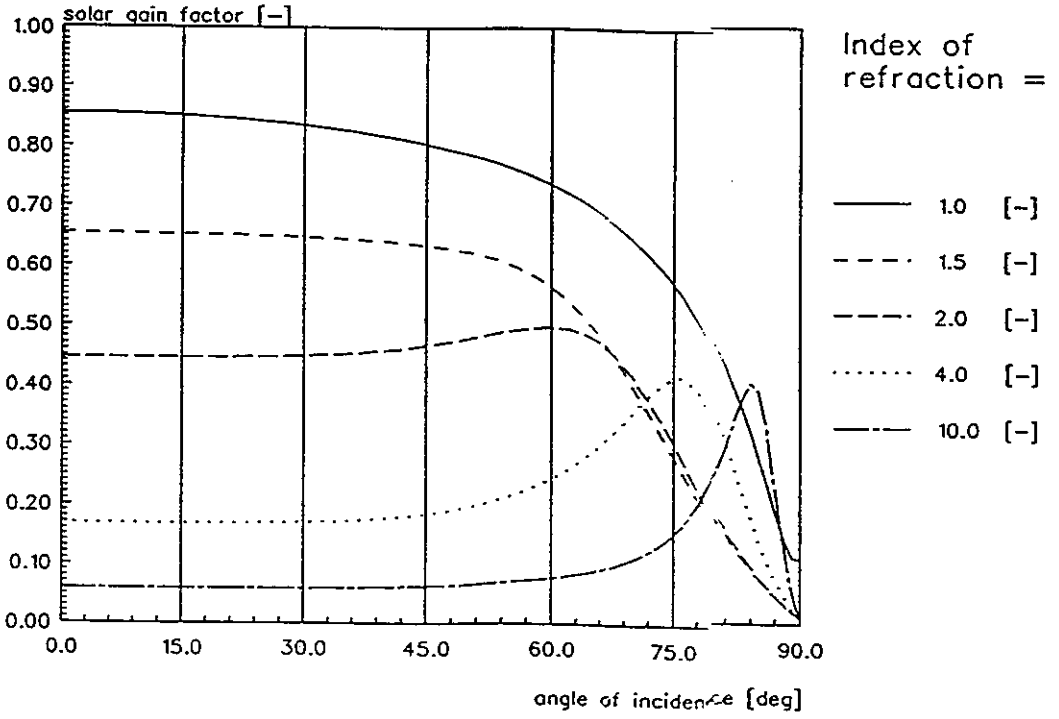

b. Solar gain factor

Figure 10: Four-layer-glazing with variable index of refraction (t = 4 mm, K = 0.0197 1/mm)

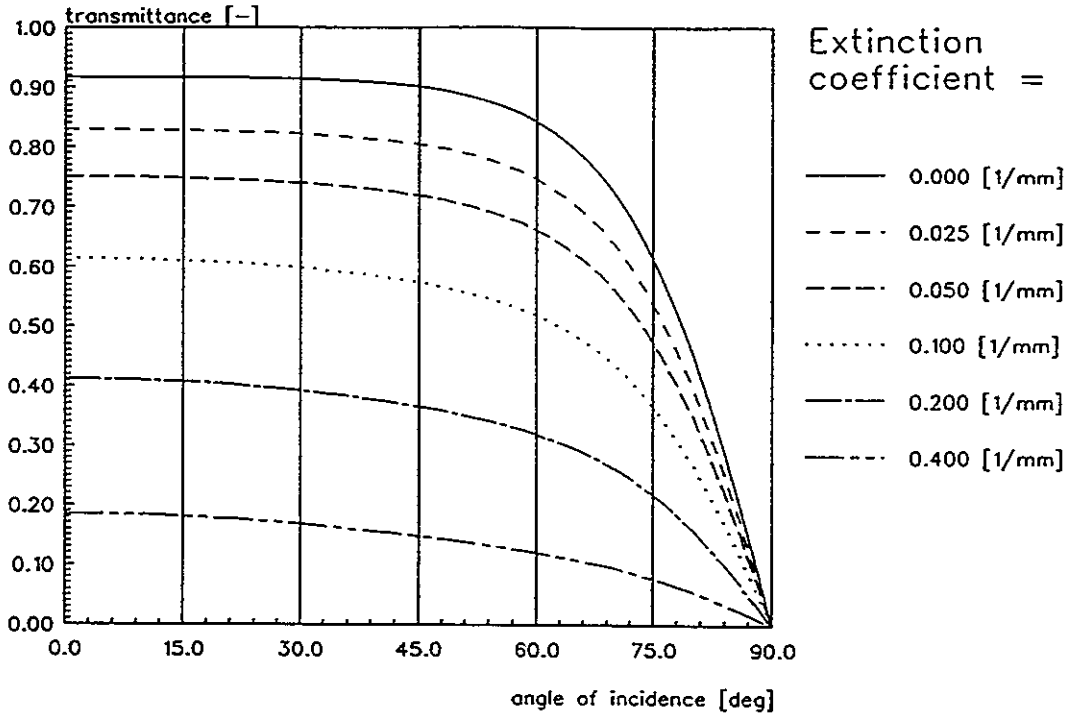

a. Transmittance

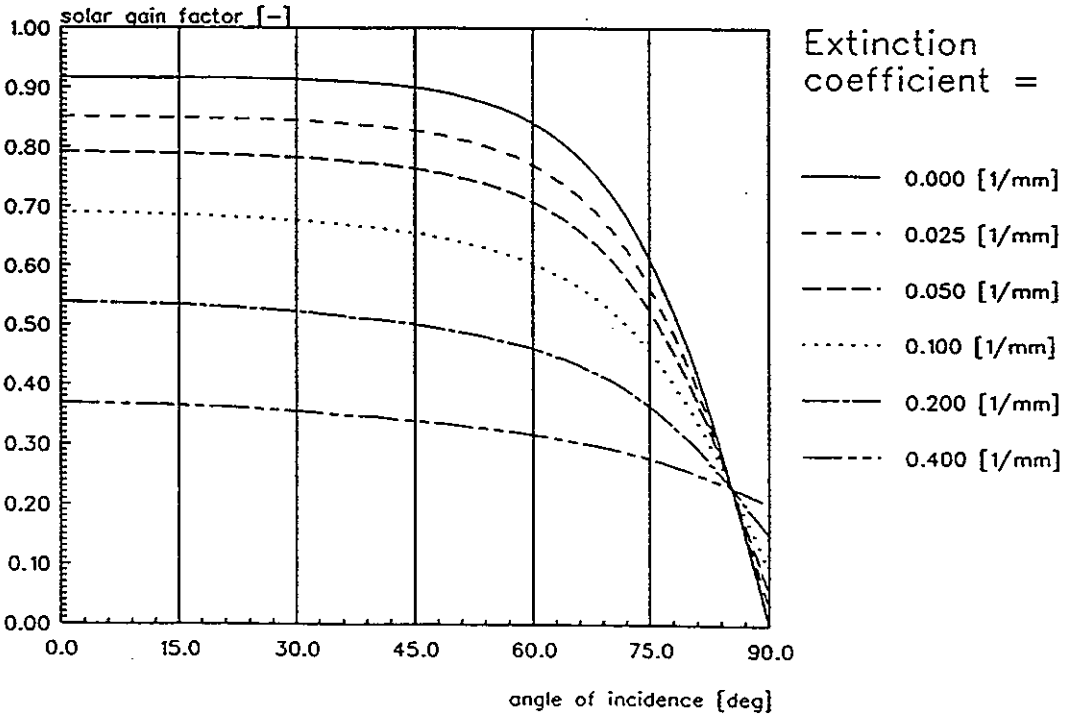

b. Solar gain factor

Figure 11: One-layer-glazing with variable extinction coefficient (t = 4 mm, n = 1.526)

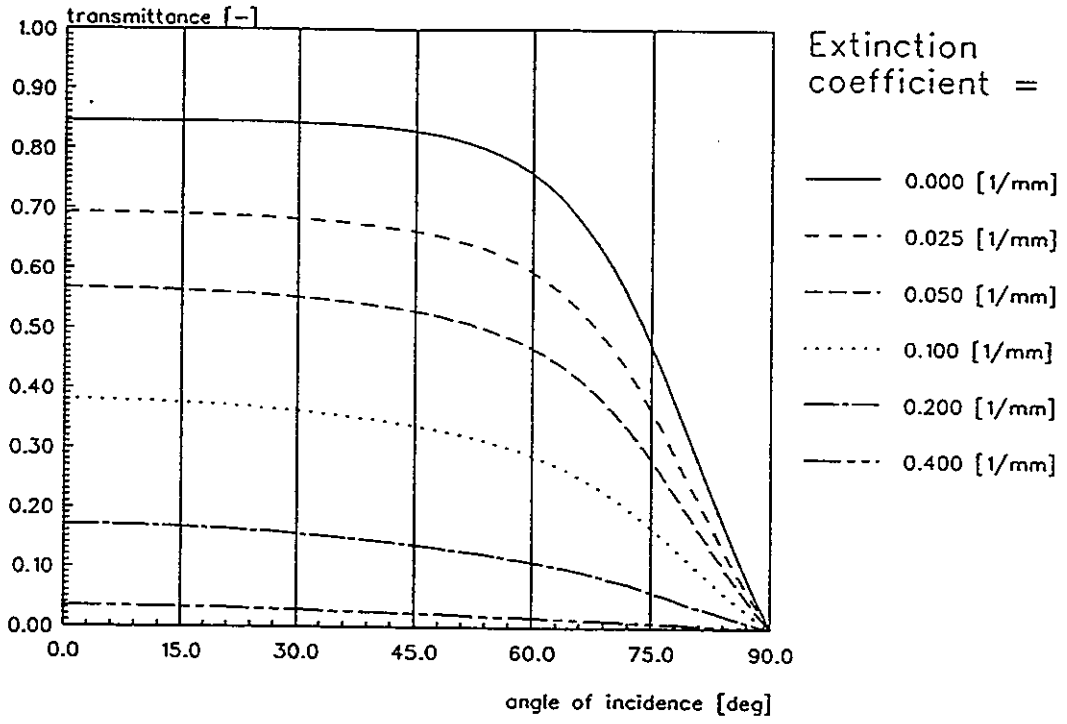

a. Transmittance

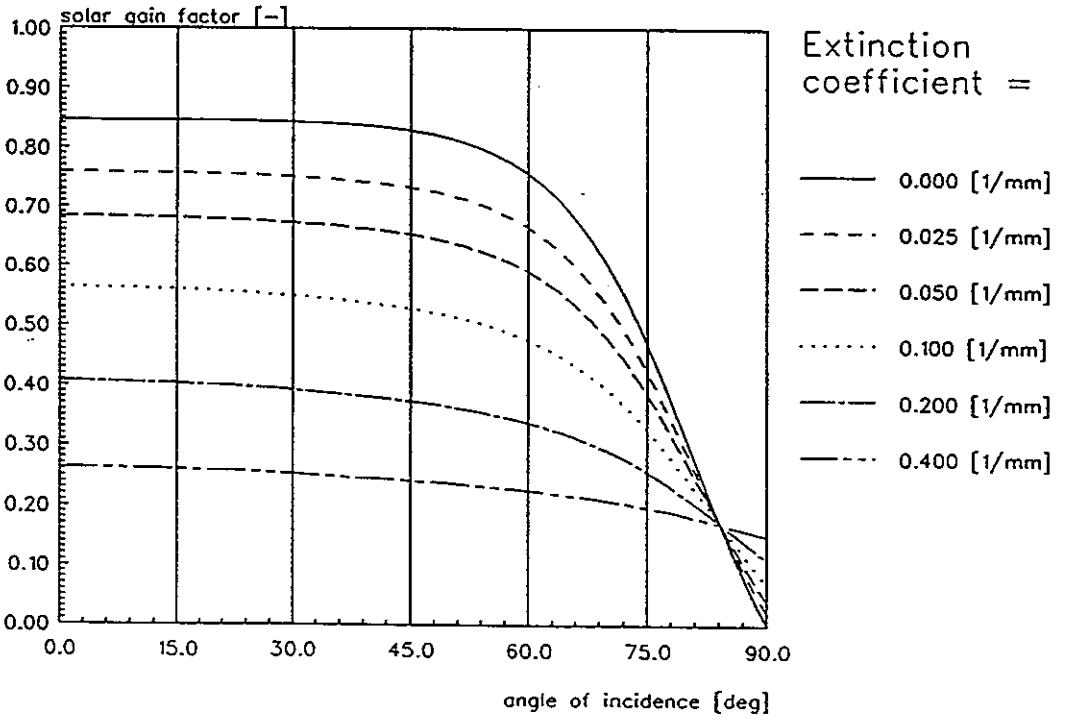

b. Solar gain factor

Figure 12: Two-layer-glazing with variable extinction coefficient (t = 4 mm, n = 1.526)

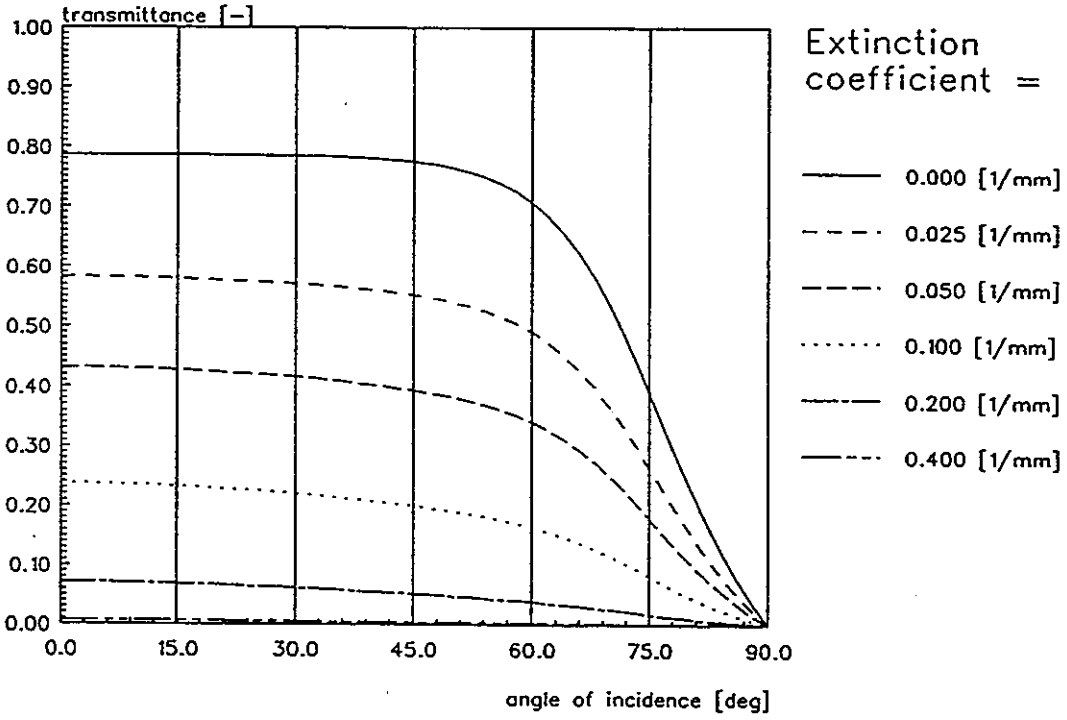

a. Transmittance

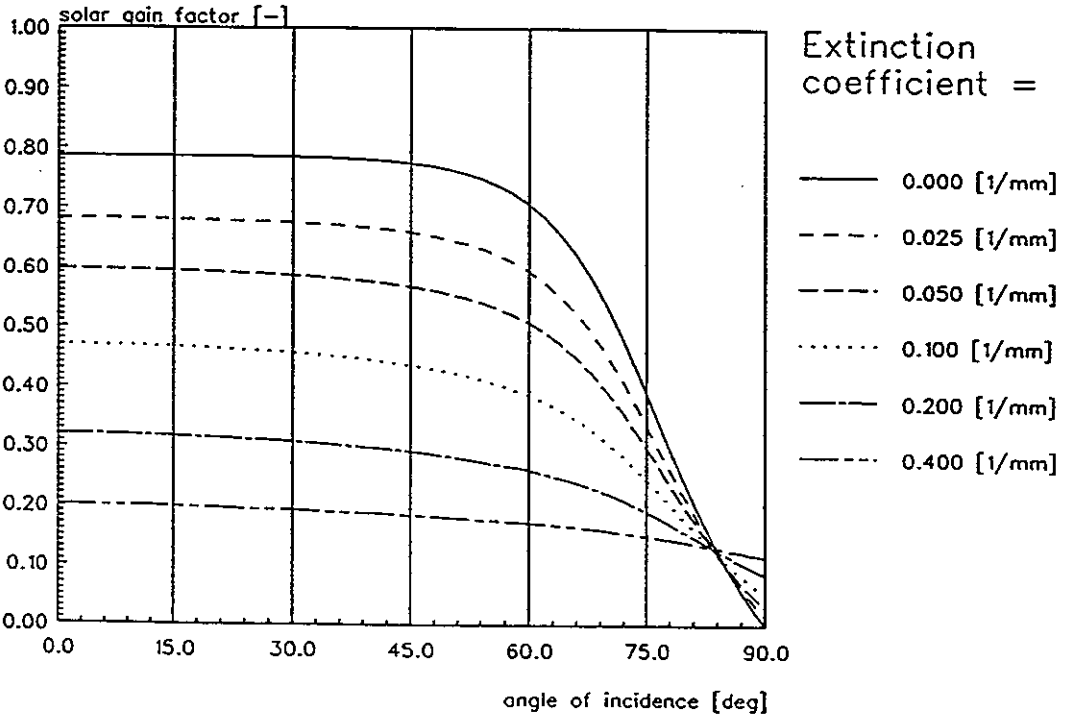

b. Solar gain factor

Figure 13: Three-layer-glazing with variable extinction coefficient (t = 4 mm, n = 1.526)

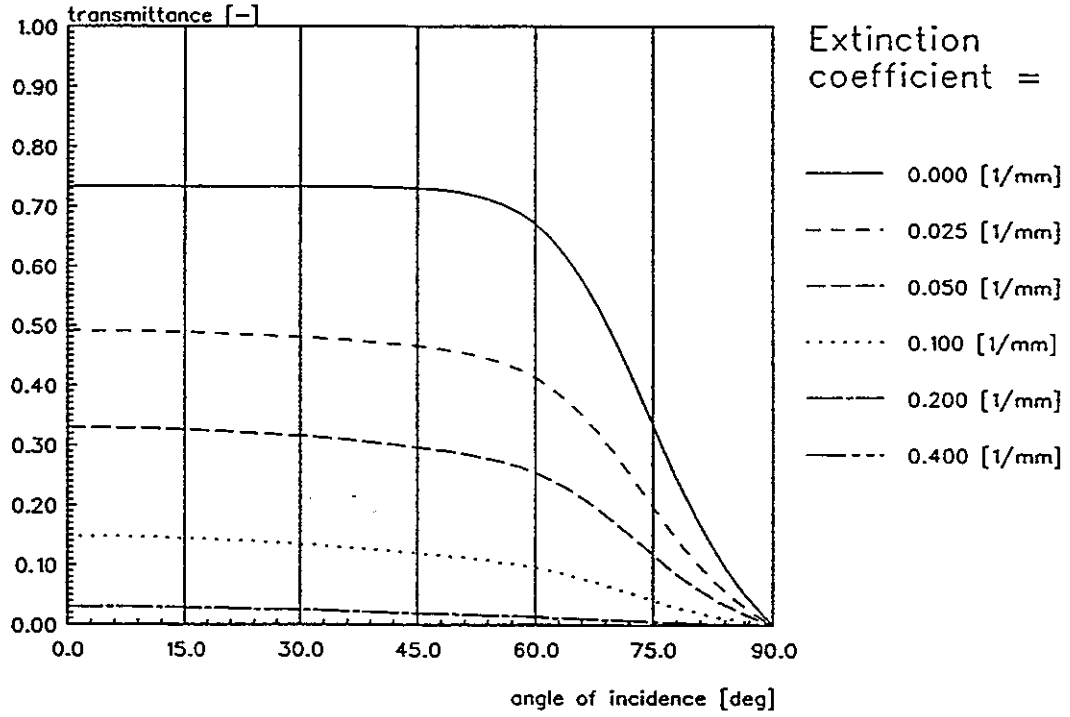

a. Transmittance

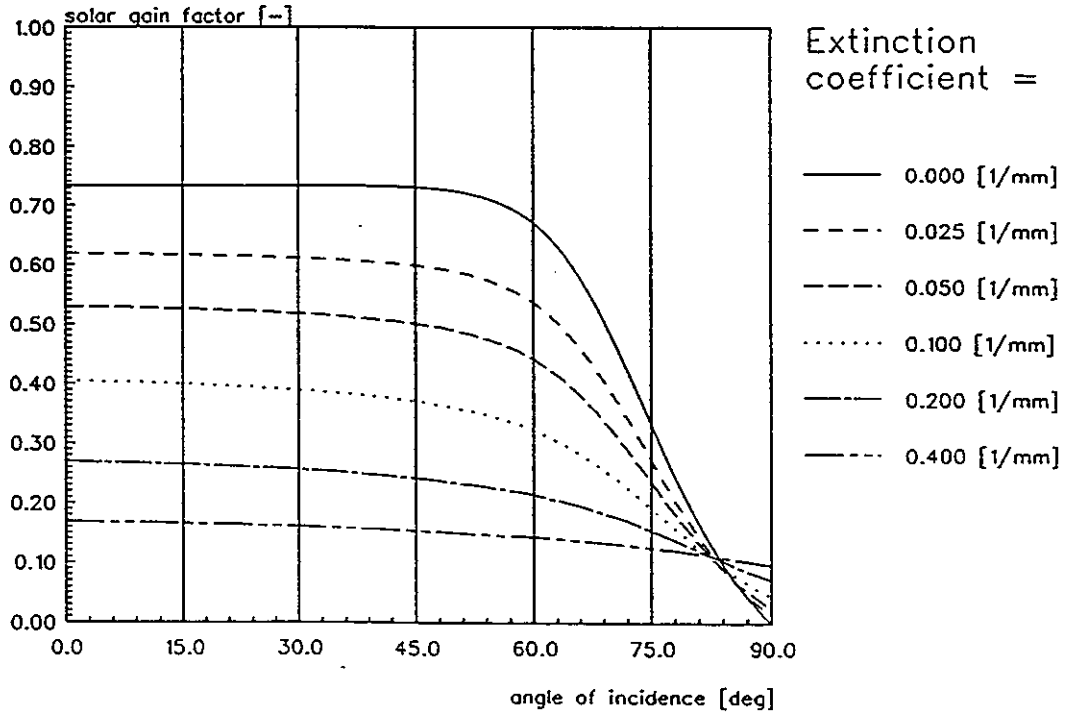

b. Solar gain factor

Figure 14: Four-layer-glazing with variable extinction coefficient (t = 4 mm, n = 1.526)

APPENDIX C

Wellinger, K.; Schneiter, P. und Schläpfer B.; Schweizer AG, Hedingen:

Transparent Insulation.

Subroutine TWDSYS of Fraunhofer-Institut für Solare Energiesysteme, Freiburg

Anhang

```
C     ================================================================
C
C     S U B R O U T I N E     T W D S Y S
C
C     ================================================================
      SUBROUTINE TWDSYS(TABS,TAUSS,THETA,ITYP,GGER,GDIF,ALAM,IERROR)
      IMPLICIT REAL*8 (A-H,O-Z)
      IMPLICIT INTEGER (I-N)
      INTEGER MAXTYP,MAXWIN,IERR,ITYP,IERROR,ITHETO,NTYP(15)
      REAL*8 LAMO(11),LAM1(11),LAM2(11),G(19,11),GD(11),G0,G1,GGER,GDIF
      COMMON/88/NDAY,NMO,NYR,IHR,DAY,MO,HR,YR,IDAY,IMO,IYR,IKK,NTYP
    1 FORMAT(2X,4F12.5,I4)
    2 FORMAT(2X,I8)
    3 FORMAT(2X,F12.5)
C     BERECHNET DIE SOLARTHERMISCHEN KENNDATEN VON TRANSPARENTEN WAERMEDAEMMUNGE
N.
C
C  BETA          NEIGUNG DER TRANSPARENTEN WAERMEDAEMMUNG  BETA=75*PI/180
C  TABS          ABSORBERTEMPERATUR  [CELSIUS]
C  TAUSS         TEMPERATUR DER AEUSSEREN ABDECKUNG (NICHT DER UMGEBUNG) [CELSIUS
C  THETA         AZIMUTHWINKEL DER GERICHTETEN EINSTRAHLUNG, -90 <= THETA <= 90
C                SONST GGER=0.
C  PHI           POLWINKEL DER GER. EINSTRAHLUNG, BISHER NICHT VERWENDET
C  ITYP          TYPNUMMER DER TWD  :   0  = KEINE TWD VORHANDEN
C                                       1  = LUFTSPALT + EINFACHVERGLASUNG
C                                       2  = AREL - MATERIAL   5 CM
C                                       3  = AREL - MATERIAL   8 CM
C                                       4  = AREL - MATERIAL  10 CM
C                                       5  = AREL - MATERIAL  15 CM
C                                       6  = AREL - MATERIAL  20 CM
C                                       7  = OKALUX-MATERIAL   5 CM
C                                       8  = OKALUX-MATERIAL   8 CM
C                                       9  = OKALUX-MATERIAL  10 CM
C                                      10  = OKALUX-MATERIAL  15 CM
C                                      11  = OKALUX-MATERIAL  20 CM
C
C  GGER          G-WERT FUER GERICHTETE EINSTRAHLUNG ALS FUNKTION VON THETA
C                UND PHI
C  GDIF          G-WERT FUER DIFFUSE EINSTRAHLUNG
C  ALAM          WAERMEDURCHLASSKOEFFIZIENT [WM-2K-1] VON ABSORBER BIS AEUSSERE
C                ABDECKUNG (NICHT UMGEBUNG)
C  IERROR        FEHLERNUMMER, 0: KEIN FEHLER
C                1: ITYP AUSSER BEREICH, ITYP=1,....MAXTYP
C
C*****************************************************************
C  ANTONIO PFLUEGER, FRAUNHOFER-INSTITUT FUER SOLARE ENERGIESYSTEME
C                    OLTMANNSSTR.22, D-7800 FREIBURG
C                    TEL. 0049 761 40 93 38
C                    VERSION VOM 14.JAN.1988, NR. 2
C*****************************************************************
C     IMPLICIT NONE
      MAXTYP=11
      MAXWIN=19
      DATA AL/0.02/
      DATA (LAMO(I), I=2,11)/
     &          1.67221,1.16783,0.97258,0.68583,0.529604,
     &          1.24601,0.84182,0.69176,0.47842,0.36561/
      DATA (LAM1(I), I=2,11)/
     &  1.53702E-2,1.0835E-2,9.03607E-3,6.38458E-3,4.93397E-3,
     &  1.078921E-2,7.251663E-3,5.955288E-3,4.112379E-3,3.137574E-3/
      DATA (LAM2(I), I=2,11)/
     &  5.716094E-5,3.995582E-5,3.344638E-5,2.364281E-5,1.838381E-5,
     &  3.769177E-5,2.552229E-5,2.089281E-5,1.441513E-5,1.107140E-5/
      DATA (GD(I), I=1,11)/0.8027,0.868,0.830,0.809,0.764,0.730,
     &       0.668,0.629,0.606,0.558,0.519/
```

```
      DATA (G(I,1), I=1,19)/
     &.8779,.8778,.8776,.8771,.8763,.8751,
     &.8730,.8698,.8648,.8570,.8448,.8259,
     &.7965,.7508,.6804,.5739,.4202,.2157,.0000/
      DATA ((G(I,J), I=1,19), J=2,6)/
     &.9500000,.9439942,.9379234,.9323837,.9268796,.9211577,
     &.9153519,.9090264,.9021402,.8943344,.8848873,.8731399,
     &.8576957,.8358021,.8025574,.7470653,.6423539,.4028947,.0,
     &.9500000,.9403906,.9308374,.9221739,.9135674,.9048323,
     &.8959230,.8864422,.8760843,.8643150,.8505598,.8333838,
     &.8110932,.7800834,.7336919,.6584246,.5239862,.2593315,.0,
     &.9500000,.9404826,.9311702,.9234511,.9159389,.9082731,
     &.9004557,.8920791,.8829206,.8724031,.8596621,.8436197,
     &.8218872,.7904063,.7412723,.6587960,.5097617,.2316841,.0,
     &.950000,.932182,.914670,.899151,.884139,.869273,
     &.854256,.838679,.822121,.803703,.782562,.756920,
     &.724587,.681006,.618372,.522896,.370362,.142084,.0,
     &.9500000,.9263766,.9035936,.8835348,.8646186,.8460308,
     &.8275076,.8088054,.7890608,.7676374,.7433494,.7147596,
     &.6791830,.6325084,.5672298,.4711614,.3271156,.1346788,.0/
      DATA ((G(I,J), I=1,19), J=7,11)/
     &.7500000,.7435800,.7371751,.7310569,.7249541,.7187437,
     &.7123401,.7055715,.6982630,.6899327,.6802144,.6684259,
     &.6532686,.6326333,.6026594,.5547989,.4684918,.2801784,.0,
     &.7500000,.7398280,.7296802,.7200311,.7105066,.7009699,
     &.6910442,.6807743,.6696008,.6572523,.6428830,.6255214,
     &.6035698,.5743533,.5327550,.4688382,.3610670,.1639254,.0,
     &.7500000,.7372600,.7247503,.7128139,.7011083,.6893874,
     &.6773803,.6649429,.6515260,.6366654,.6196288,.5992518,
     &.5736373,.5398666,.4926187,.4217977,.3075837,.1199568,.0,
     &.7500000,.7310400,.7125254,.6952708,.6784624,.6617311,
     &.6450204,.6278144,.6095890,.5896981,.5672432,.5407777,
     &.5086060,.4672999,.4117781,.3331966,.2189756,.0705352,.0,
     &.7500000,.7248200,.7007006,.6783278,.6568166,.6357748,
     &.6149606,.5938858,.5718520,.5482308,.5219576,.4918036,
     &.4558746,.4112332,.3534374,.2761954,.1736674,.0605136,.0/

      BETA=0.017453*75.0
      IERR=0
C     WRITE(8,1) TABS,TAUSS,THETA,PHI,ITYP
      IF(ITYP.EQ.0) GOTO 112
      IF(ITYP.NE.1) GOTO 100
C KONVEKTION
C AL    BREITE DES LUFTSPALTES (METER)
C (QUELLE FRICKE/BORST SEITE 263 FF.)
C DATEN VON 200K BIS 800K AUS FRICKE S.241
C QUELLE K.G.T. HOLLANDS ET AL., J. HEAT TRANSFER, MAY 1976, P. 189-193
      DT=ABS(TABS-TAUSS)
      TCEL=(TABS+TAUSS)/2.
      TK=TCEL+273.15
C     WRITE(8,3) TK
      ANU=1.
C       NUSSELTZAHL

      ANY=-5.5517960+(4.488035E-2+8.180780E-5*TK)*TK
C           KINEMATISCHE VISKOSITAET, FRICKE S.241
      ANY=ANY*1.E-6
      PR=0.85441333+(-7.744713E-4+(1.09397E-6-4.800384E-10*TK)*TK)*TK
C     WRITE(8,3) PR
C           PRANDTLZAHL
      GR=9.81*DT*AL**3/(TK*ANY**2)
C     WRITE(8,3) GR
C           GRASHOFZAHL
      RA=PR*GR
C     WRITE(8,3) RA
```

```
C           RAYLEIGHZAHL
C           RA*COS(75GRAD), SIEHE DUFFIE/BECKMAN
      RAC=RA*0.2588
C     WRITE(8,3) RAC
      AKL2=(RAC/5830.)**(0.3333333) - 1.
C     WRITE(8,3) AKL2
      IF(RAC.GT.1708.) ANU=ANU+1.44*(1.-1708./RAC)
     &                        *(1.-(SIN(1.8*BETA))**1.6*1708./RAC)
      IF(AKL2.GT.0.) ANU=ANU+AKL2
C     WRITE(8,3) ANU
      ALAMLU=7.019962E-4+(9.30962E-5-2.739067E-8*TK)*TK
      ALAM=ANU*ALAMLU/AL+2.268E-7*TK**3/(1./0.15+1./0.9-1.)
C     WRITE(8,3) ALAM
      ATHETA=ABS(THETA)
C     WRITE(8,3) ATHETA
      ITHET0=INT(ATHETA/5.)+1
C     WRITE(8,2) ITHET0
      IF(ITHET0.GE.19) GOTO 90
      G0=G(ITHET0,1)
C     WRITE(8,3) G0
      G1=G(ITHET0+1,1)
C     WRITE(8,3) G1
      ATHETA=(ATHETA-FLOAT((ITHET0-1)*5))/5.
C     WRITE(8,3) ATHETA
      GGER=G0+(G1-G0)*ATHETA
C     WRITE(8,3) GGER
      GOTO 91
90    GGER=0.0
91    GDIF=GD(1)
C     WRITE(8,3) GDIF
      GOTO 120
100   CONTINUE
      TM=(TABS+TAUSS)/2.
      ALAM=LAM0(ITYP)+(LAM1(ITYP)+TM*LAM2(ITYP))*TM
      ATHETA=ABS(THETA)
      ITHET0=INT(ATHETA/5.)+1
      IF(ITHET0.GE.19) GOTO 110
      G0=G(ITHET0,ITYP)*G(ITHET0,1)
      G1=G(ITHET0+1,ITYP)*G(ITHET0+1,1)
      ATHETA=(ATHETA-FLOAT((ITHET0-1)*5))/5.
      GGER=G0+(G1-G0)*ATHETA
      GOTO 111
110   GGER=0.0
111   GDIF=GD(ITYP)*GD(1)
      GOTO 120
112   ALAM=99999.9
      GGER=1.0
      GDIF=1.0
120   CONTINUE
      IERROR=IERR
      RETURN
      END
```

APPENDIX D

Schreiber, E.; Boy, E.; und Bertsch, K.; IBP–Stuttgart:

Energy Saving by Walls covered with TI–Materials

(PC–Program for calculating the total solar transmittance of TI–Material by Fraunhofer–Institut für Bauphysik, Stuttgart)

```
C   SUBROUTINE FOR CALCULATING EXTINCTION AND SHADING COEFFICIENTS
C   WITHIN SUNCODE, PERMITTING TO SELECT A PRESET TRANSMISSION/
C   ABSORPTION RATIO OF A GLAZED TROMBE WALL


C   VERSION 1.0
C   BY :                        UWE HEIM
C   DATE :                      1985-10-17
C   LAST MODIFICATION :         1989-12-14  M.LUTZ


C   VARIABLE QUANTITIES

C   THICKNESS OF LAYERS :               SD
C   NUMBER OF LAYERS :                  SA
C   INDEX OF REFRACTION :               BRE
C   EXTINCTION COEFF.:                  EX
C   NOMINAL TRANSMISSION :              TAU
C   NOMINAL ABSORPTION :                ALPHA
C   SHADING COEFFICIENT :               SC
C   ACTUAL FRAME/GLAZING RATIO :        RA
C
C
    DATA BRE/1.5393/
C
    PRINT*,'INDEX OF REFRACTION = (NO CHANGES) 0 <CR>)',BRE
    READ(5,*)X
    IF(X.GT.0.0) BRE=X
    PRINT*,'ACTUAL FRAME/GLAZING RATIO (0 <= RA < 1) '
    PRINT*,'      (NO FRAME : 0)'
    READ(5,*)RA
 1  PRINT*,'NOMINAL TRANSMISSION (0 < TAU < 1)'
    READ(5,*)TAU
    PRINT*,'NOMINAL ABSORPTION (0 < ALPHA < 1)'
    READ(5,*)ALPHA
    Z=ALPHA+TAU
    IF(Z.GT.1.0) THEN
        PRINT*,'SUM TAU+ALPHA > 1 !!!!!'
        GOTO 1
    ENDIF
    PRINT*,'NUMBER OF LAYERS '
    READ(5,*)SA
    PRINT*,'THICKNESS OF LAYERS [mm]'
    READ(5,*)SD
C
    PATH=SD*SA
    EX=1/PATH*LOG(ALPHA/TAU+1)
C
    X=(BRE-1)*(BRE-1)/((BRE+1)*(BRE+1))
    Y=(1-X)/(1+(2*SA-1)*X)
    T=Y*EXP(-EX*PATH)
    V=TAU/T
C
    SC=(1-RA)*V
C
C
    WRITE(5,2)TAU,ALPHA,RA,BRE,SD,SA,EX,SC
```

```
  2  FORMAT('0PRESET PARAMETERS :',//1X'NOMINAL TRANSMISSION   :',F10.5,
     */1X'NOMINAL ABSORPTION    :',F10.5,/1X'ACTUAL FRAME/GLAZING RATIO    :',F10.5
     *,/1X'INDEX OF REFRACTION     :',F10.5,/1X'THICKNESS OF GLAZING       :',F10.5
     *,/1X'NUMBER OF GLAZINGS     :',F10.5,///1X'SETTING PARAMETERS :',//
     *1X'EXTINCTION COEFFICIENT  >>    ext = ',F8.5,' 1/mm',//1X
     *'SHADING-COEFFICIENT   >>    SC = ',F8.5)
C
C
      END
```

APPENDIX E

Heim, U. :

Calculation of Required Switchable Set Point Temperature of Thermochromic Glazings Applied to Transparent Insulated Exterior Walls.

Subroutine TRANSPARENZ for calculating solar transmission of different transparent material structures (acrylfoam, aerogel, cell and cappillar structures) in combination with thermochrome switchable shading (TALD).

Fraunhofer–Institut für Bauphysik
Stuttgart, Germany.

```
CCCCCCCCCCCCCCCCCCCCCCCCCCCCCCCCCCCCCCCCCCCCCCCCCCCCCCCCCCCCCCCCCCCCCCC
      SUBROUTINE TRANSPARENZ(IOPAK,IW,PHI,NMAT,DMAT,EMAT,SYS,DIF,ABSW
     &                       ,TAUGS,ROGES,ABSGS,ABS4)
C
C     computes TALD system transmissions in angular dependency,
C     determining light transmission in both directions
C     (outside/inside and inside/outside)
C
C     Input :
C     -------
C
C     IOPAK    =  TALD switching control (1=opaque,0=transparent)
C     IW       =  number of wall
C     PHI      =  angle of incidence
C     NMAT     =  refractive indexes to air
C     DMAT     =  layer thickness
C     EMAT     =  layer extinction coefficients
C     SYS      =  system characteristics
C     DIF      =  control parameter for diffuse (0) or direct (1) radiation
C     ABSW     =  short-wave absorption coefficient of absorbing surface
C
C     Output :
C     --------
C
C     TAUGS    =  total transmission
C     ROGES    =  total reflection
C     ABSGS    =  layer absorption
C     ABSW     =  short-wave absorption coefficient of absorbing surface (corrected)
C     ABS4     =  additional absorption due to multiple reflection
C                 (assumed to be a heat source located at the interior surface
C                 of the second exterior glazing, as a detailed consideration appears
C                 negligible regarding the small quantity)
C
C
      PARAMETER(NW=4)
      CHARACTER*1 LDD
      REAL    PHI,NMAT(4),DMAT(4),EMAT(4),TAUGS(2),ROGES(2),ABSGS(2,4)
      REAL    RS(6),RP(6),TS(6),TP(6),N(4),ROS(2,4),TAS(2,4),ABSR(2,4)
      REAL    ROP(2,4),TAP(2,4),ABP(2,4),A(6),WI(6),RG(2),TG(2)
      REAL    AWI,PI,AG(2,3),RGS,TGS,AGS,KAPPA
      REAL    TA0(NW),XKP(NW),RODIFA(NW),TADIFA(NW)
      INTEGER SYS,DIF,ABS0,IT(3)
      COMMON /const1/ pi,pid1800,pid2,pid3,pid180,d3p6,d3600p
      COMMON  /LEGIS/LDD,tltdif(nw),tltdir(nw)
      COMMON  /OPAKTR/TLOTD(NW),TLORD(NW)
      COMMON /pmma/ pmmaa(4),pmmab(4),pmmac(4),pmmad(4)
      COMMON /aero/ aeroa(4),aerob(4),aeroc(4),aerod(4)
      COMMON /pchc/ pchcm(nw,3),pchcb(nw,3)
      COMMON /kapi/ akapm(nw,3),akapb(nw,3)
      COMMON /opak/ tg,ta0,td
C
C
      ROWA=1-ABSW
      IF(DIF.EQ.1) THEN
      WI(1)= pid3
      ELSE
        WI(1)=PHI
      END IF
C
```

```
C
C     Determining relative refractive indexes at boundary layers
C     ----------------------------------------------------------
C
      N(1)=NMAT(1)
C
C     Transparency properties in the opaque TALD range
C     ------------------------------------------------
C
      IF(IOPAK.EQ.1.AND.DIF.EQ.1) THEN
        AG(1,2)=1-TLOTD(IW)-TLORD(IW)
        AG(2,2)=AG(1,2)
        N(2)=1/N(1)
        DO 295 I=1,3
  295   IT(I)=1
C
C     Transparency of exterior glazing at PHI=0.0 dgr
C     ...............................................
C
        DO 300 J=1,2
        RS(J)=((1-N(J))/(1+N(J)))**2
  300   TS(J)=4*N(J)/(1+N(J))**2
        A(1)=EXP(-EMAT(1)*DMAT(1)*1000)
        CALL EINZELTRANS(IT,RS,TS,A,ROP,TAP,ABP)
        TA0(IW)=TAP(1,1)
C
C     Transparency of exterior glazing at PHI=60.0 dgr
C     ................................................
C
        DO 305 J=2,3
        AWI=SIN(WI(J-1))/N(J-1)
        IF(AWI.GT.1.0) AWI=1.0
  305   WI(J)=ASIN(AWI)
C
C     Vertical E-vector
C     .................
C
        DO 310 J=1,2
        RS(J)=(SIN(WI(J)-WI(J+1))/SIN(WI(J)+WI(J+1)))**2
  310   TS(J)=N(J)*COS(WI(J+1))/COS(WI(J))*
     &        (2*COS(WI(J))*SIN(WI(J+1))/SIN(WI(J)+WI(J+1)))**2
C
C     Parallel E-vector
C     .................
C
        DO 315 J=1,2
        RP(J)=(TAN(WI(J)-WI(J+1))/TAN(WI(J)+WI(J+1)))**2
  315   TP(J)=N(J)*COS(WI(J+1))/COS(WI(J))*
     &        (2*COS(WI(J))*SIN(WI(J+1))/SIN(WI(J)+WI(J+1))/
     &        COS(WI(J)-WI(J+1)))**2
C
C     Internal transmission
C     .....................
C
        A(1)=EXP(-EMAT(1)*DMAT(1)*1000/COS(WI(2)))
C
C     Computation of transmission, reflection and absorption components
C     of single glazings (for separate E-vectors)
C     ...........................................................
```

```
C
        CALL EINZELTRANS(IT,RS,TS,A,ROS,TAS,ABSR)
        CALL EINZELTRANS(IT,RP,TP,A,ROP,TAP,ABP)
        T60=0.5*(TAS(1,1)+TAP(1,1))
        R60=0.5*(ROS(1,1)+ROP(1,1))
C
C     Kappa value of exterior glazing
C     ...............................
C
      XKP(IW)=LOG(1-T60/TA0(IW))/LOG(1-COS(pid3))
C
C     Diffuse transmission and reflection of the exterior system in the opaque state
C     ..............................................................................
C
        TD=TA0(IW)*XKP(IW)*(XKP(IW)+3)/(XKP(IW)+2)/(XKP(IW)+1)
      TG(1)=TLOTD(IW)*TD/TA0(IW)
        TG(2)=TG(1)
      AG(1,2)=AG(1,2)*TD/TA0(IW)
        AG(2,2)=AG(1,2)
        RG(1)=1-AG(1,2)-TG(1)
      RG(2)=RG(1)
        GOTO 66
C
C     Direct radiation in the opaque state
C     ....................................
C
      ELSE IF(IOPAK.EQ.1.AND.DIF.NE.1) THEN
        AG(1,2)=1-TLOTD(IW)-TLORD(IW)
        AG(2,2)=AG(1,2)
        TPH=TA0(IW)*(1-(1-COS(WI(1)))**XKP(IW))
        TG(1)=TLOTD(IW)*TPH/TA0(IW)
        TG(2)=TG(1)
        AG(1,2)=AG(1,2)*TPH/TA0(IW)
        AG(2,2)=AG(1,2)
        RG(1)=1-AG(1,2)-TG(1)
        RG(2)=RG(1)
        DIF=1
        GOTO 66
      END IF
C
C
C     Determining transparency parameters for the base-case system
C     ------------------------------------------------------------
C                    Glazing-TALD-Glazing in the transparent state
C                    ---------------------------------------------
C
      N(2)=NMAT(2)/NMAT(1)
      N(3)=NMAT(3)/NMAT(2)
      N(4)=1/NMAT(3)
C
      DO 5 I=1,3
    5 IT(I)=I
C
C     Normal (vertical) incidence
C     ...........................
C
      IF(WI(1).EQ.0.0) THEN
        DO 10 J=1,4
        WI(J+1)=0.0
```

```
        RS(J)=((1-N(J))/(1+N(J)))**2
  10    TS(J)=4*N(J)/(1+N(J))**2
        DO 15 J=1,3,2
  15    A(J)=EXP(-EMAT(J)*DMAT(J)*1000)
        CALL EINZELTRANS(IT,RS,TS,A,ROP,TAP,ABP)
        DO 20 L=1,2
        DO 20 J=1,4
        ROS(L,J)=ROP(L,J)
        TAS(L,J)=TAP(L,J)
  20    ABSR(L,J)=ABP(L,J)
      ELSE
C
C     Non-Vertical incidence
C     ......................
C
        DO 25 J=2,5
        AWI=SIN(WI(J-1))/N(J-1)
        IF(AWI.GT.1.0) AWI=1.0
  25    WI(J)=ASIN(AWI)
C
C     Vertical E-vector
C     .................
C
        DO 30 J=1,4
        RS(J)=(SIN(WI(J)-WI(J+1))/SIN(WI(J)+WI(J+1)))**2
  30    TS(J)=N(J)*COS(WI(J+1))/COS(WI(J))*
     &        (2*COS(WI(J))*SIN(WI(J+1))/SIN(WI(J)+WI(J+1)))**2
C
C     Parallel E-vector
C     .................
C
        DO 35 J=1,4
        RP(J)=(TAN(WI(J)-WI(J+1))/TAN(WI(J)+WI(J+1)))**2
  35    TP(J)=N(J)*COS(WI(J+1))/COS(WI(J))*
     &        (2*COS(WI(J))*SIN(WI(J+1))/SIN(WI(J)+WI(J+1))/
     &        COS(WI(J)-WI(J+1)))**2
C
C     Internal transmission
C     .....................
C
        DO 40 J=1,3,2
  40    A(J)=EXP(-EMAT(J)*DMAT(J)*1000/COS(WI(J+1)))
C
C     Computation of transmission, reflection and absorption components
C     of single glazings (for separate E-vectors)
C     ...........................................................
C
        CALL EINZELTRANS(IT,RS,TS,A,ROS,TAS,ABSR)
        CALL EINZELTRANS(IT,RP,TP,A,ROP,TAP,ABP)
      END IF
C
C     Transmission inside TALD layer
C     ..............................
C
      TATAL=EXP(-EMAT(2)*DMAT(2)*1000/COS(WI(3)))
C
C     Determining the system parameters transmission, reflection and
C     absorption
C
```

```
C     INDEX=1   :   light transmission from outside to inside
C     INDEX=2   :                "          "  inside to outside
C     ..................................................
C
      INDEX=1
      CALL KOMBITRANS(INDEX,TATAL,ROP,ROS,TAP,TAS,ABP,ABSR
     &                ,RG,TG,AG)
      INDEX=2
      CALL KOMBITRANS(INDEX,TATAL,ROP,ROS,TAP,TAS,ABP,ABSR
     &                ,RG,TG,AG)
C
666   CONTINUE
C
C     System adaptation
C     -----------------
C
C     Systems without air gap and without LDD
C     ---------------------------------------
C
  66  IF (SYS.EQ.10 .OR. SYS.EQ.-10 .OR. SYS.EQ.0) THEN
        DO 45 J=1,2
        TAUGS(J)=TG(J)
        ROGES(J)=RG(J)
        DO 45 L=1,3
  45    ABSGS(J,L)=AG(J,L)
        GOTO 55
C
C     Systems with air gap but without LDD
C     ------------------------------------
C
      ELSE IF (SYS.EQ.20 .OR. SYS.EQ.-20) THEN
               IT(1)=4
               IT(2)=1
               IT(3)=4
           IF(DIF.EQ.1)  WI(4)= pid3
             IF(PHI.EQ.0.0) THEN
C
C     Normal (vertical) incidence
C     ...........................
C
               RS(4)=((1-NMAT(4))/(1+NMAT(4)))**2
               RS(5)=RS(4)
               TS(4)=4*NMAT(4)/(1+NMAT(4))**2
               TS(5)=TS(4)
               A(4)=EXP(-EMAT(4)*DMAT(4)*1000)
               CALL EINZELTRANS(IT,RS,TS,A,ROP,TAP,ABP)
               RGS=ROP(1,4)
               TGS=TAP(1,4)
               AGS=ABP(1,4)
C
             ELSE
C
C     Non-Vertical incidence
C     ......................
C
            IF(WI(4).NE.pid3) THEN
                WI(4)=WI(5)
              END IF
              WI(5)=ASIN(SIN(WI(4))/NMAT(4))
```

```
C
C     Vertical E-vector
C     .................
C
              RS(4)=(SIN(WI(4)-WI(5))/SIN(WI(4)+WI(5)))**2
              RS(5)=RS(4)
              TS(4)=NMAT(4)*COS(WI(5))/COS(WI(4))*
     &             (2*COS(WI(4))*SIN(WI(5))/SIN(WI(4)+WI(5)))**2
              TS(5)=TS(4)
C
C     Parallel E-vector
C     .................
C
              RP(4)=(TAN(WI(4)-WI(5))/TAN(WI(4)+WI(5)))**2
              RP(5)=RP(4)
              TP(4)=NMAT(4)*COS(WI(5))/COS(WI(4))*
     &              (2*COS(WI(4))*SIN(WI(5))/SIN(WI(4)+WI(5))/
     &              COS(WI(4)-WI(5)))**2
              TP(5)=TP(4)
C
C     Internal transmission
C     .....................
C
              A(4)=EXP(-EMAT(4)*DMAT(4)*1000/COS(WI(5)))
C
C     Computation of transmission, reflection and absorption components
C     of single glazing (for separate E-vectors)
C     ..........................................................
C
              CALL EINZELTRANS(IT,RS,TS,A,ROS,TAS,ABSR)
              CALL EINZELTRANS(IT,RP,TP,A,ROP,TAP,ABP)
C
C     Parameters of third glazing (both transmitting directions identical)
C     ....................................................................
C
              RGS=0.5*(ROS(1,4)+ROP(1,4))
              TGS=0.5*(TAS(1,4)+TAP(1,4))
              AGS=0.5*(ABSR(1,4)+ABP(1,4))
            END IF
C
      ELSE IF (SYS.GE.30 .OR. SYS.LE.-30) THEN
C
C     Systems with LDD
C     ----------------
C
            DM=DMAT(4)*1000
          IF(LDD.EQ.'P') THEN
C
C     Acrylic foam insulation (empirical approximation of transparency behaviour)
C     ...........................................................................
C
              IF(DIF.EQ.1) THEN
            TGS=tltdif(iw)
              ELSE
            TO= tltdir(iw)
            IF(ABS(PI/2-WI(5)).LT.0.0001) WI(5)= pid2-PI/360
                IF(WI(5).EQ.0.0) THEN
                  TGS=TO
                ELSE
```

```
            IF(WI(5).LT.pid3) THEN
              KAPPA=TAN(pmmaa(1)*WI(5)**3+pmmab(1)*WI(5)**2
     &                        +pmmac(1)*WI(5)   + pmmad(1))
                ELSE
              KAPPA=TAN(pmmaa(2)*WI(5)**3+pmmab(2)*WI(5)**2
     &                        +pmmac(2)*WI(5)   + pmmad(2))
                END IF
                TGS=T0*(1-(1-COS(WI(5)))**KAPPA)
              END IF
            END IF
            AGS=0.025
            RGS=1-TGS-AGS
C
C     Aerogel
C     .......
C
          ELSE IF(LDD.EQ.'A') THEN
C
              IF(DIF.EQ.1) THEN
            TGS=tltdif(iw)
              ELSE
            T0= tltdir(iw)
            IF(ABS(PI/2-WI(5)).LT.0.0001) WI(5)= pid2-PI/360
                IF(WI(5).EQ.0.0) THEN
                  TGS=T0
                ELSE
              IF(WI(5).LT.pid3) THEN
                KAPPA=TAN(aeroa(1)*WI(5)**3+aerob(1)*WI(5)**2
     &                        +aeroc(1)*WI(5)   + aerod(1))
                  ELSE
                KAPPA=TAN(aeroa(2)*WI(5)**3+aerob(2)*WI(5)**2
     &                        +aeroc(2)*WI(5)   + aerod(2))
                  END IF
                  TGS=T0*(1-(1-COS(WI(5)))**KAPPA)
                END IF
              END IF
              AGS=0.025
              RGS=1-TGS-AGS
C
C
C
C     PC Honeycomb structure (PCHC)
C     .............................
C
          ELSE IF(LDD.EQ.'H') THEN
C
                IF(DIF.EQ.1) THEN
              TGS=tltdif(iw)
                ELSE
                  IF(WI(5).EQ.0.0) THEN
                TGS=0.98
              ELSE
                IF (ABS(WI(5)-pid2).LT.0.0001) THEN
                          TGS=0.0
                          AGS=0.0
                          RGS=1.0
                    GOTO 48
                ELSE
                    IF(WI(5).LT.pid3) THEN
```

```
                    tgs = pchcm(iw,2)*wi(5) + pchcb(iw,2)
                  ELSE
                    tgs = pchcm(iw,3)*wi(5) + pchcb(iw,3)
                  END IF
                END IF
                  END IF
                END IF
                AGS=1.0-TGS
                RGS=0.0
 48             CONTINUE
C
C
C     Cappillary structure
C     ....................
C
            ELSE IF(LDD.EQ.'K') THEN
C
                IF(DIF.EQ.1) THEN
              TGS=tltdif(iw)
                ELSE
                  IF(WI(5).EQ.0.0) THEN
                TGS=0.98
              ELSE
                IF (ABS(WI(5)-pid2).LT.0.0001) THEN
                          TGS=0.0
                          AGS=0.0
                          RGS=1.0
                    GOTO 488
                ELSE
                    IF(WI(5).LT.pid3) THEN
                      tgs = akapm(iw,2)*wi(5) + akapb(iw,2)
                    ELSE
                      tgs = akapm(iw,3)*wi(5) + akapb(iw,3)
                    END IF
                END IF
                  END IF
                END IF
                AGS=1.0-TGS
                RGS=0.0
 488          CONTINUE
           END IF
      END IF
C
C     Combined values of transparency, reflection and layer absorption
C     for a four-layer system
C     ---------------------------------------------------------------
C
      absgs(2,4) = 1./(1.-RG(2)*RGS)
      taugs(1) = TGS * absgs(2,4)
      taugs(2) = TG(2) * absgs(2,4)
      ROGES(1)=RG(1)+RGS*TG(1) * taugs(2)
      ROGES(2)=RGS+RG(2)*TGS * taugs(1)
      TAUGS(1)=TG(1) * taugs(1)
      TAUGS(2)=TGS * taugs(2)
        DO 50 J=1,3
      ABSGS(1,J)=AG(1,J)+TG(1)*RGS*AG(2,J) * absgs(2,4)
 50   ABSGS(2,J)=TGS*AG(2,J) * absgs(2,4)
      ABSGS(1,4)=AGS*TG(1) * absgs(2,4)
      ABSGS(2,4)=AGS+TGS*RG(2)*AGS * absgs(2,4)
```

```
C
C     Absorbed energy of short-wave radiation reflected from absorbing surface.
C     The percentage determined for the insulating system is assumed to be a
C     heat source and assigned to the internal surface of the TALD-system
C     interior pane. The amount being rather low, this is considered
C     approximately permissible.
C     Regarding multiple reflections at the absorbing wall, the TALD system's
C     inside/outside diffuse transmission and reflection properties are taken
C     as the basic condition. For the opaque state, multiple reflections and
C     associated effects are neglected on account of the low system
C     transparency.
C     ------------------------------------------------------------------------
C
   55 IF(IOPAK.EQ.1) THEN
        ABSGS(1,1)=0.0
        ABSGS(1,3)=0.0
      IF(SYS.EQ.0) ABSGS(1,4)=0.0
        ABS4=0.0
        ABSW=1-ROWA
        GOTO 75
      END IF
C
      IF(DIF.EQ.1) THEN
        RODIFA(IW)=ROGES(2)
        TADIFA(IW)=TAUGS(2)
      END IF
C
      absw = 1./(1.-ROWA*RODIFA(IW))
      ABS4 = ROWA*absw - TADIFA(IW)*ROWA*absw
     &           -ROWA*RODIFA(IW)*absw
      ABSW=(1-ROWA)*absw
C
   75 RETURN
C
      END
C


CCCCCCCCCCCCCCCCCCCCCCCCCCCCCCCCCCCCCCCCCCCCCCCCCCCCCCCCCCCCCCCCCCCCCCCCCCCCCCC


CCCCCCCCCCCCCCCCCCCCCCCCCCCCCCCCCCCCCCCCCCCCCCCCCCCCCCCCCCCCCCCCCCCCCCCCCCCCCCC
C
      SUBROUTINE EINZELTRANS(IT,R,T,A,RO,TA,AB)
C
C     computes transparency, reflection and absorption of single TALD
C     system cover panes for both light transmission directions.

C     Input :
C     -------
C
C     IT        =  control quantity
C     R         =  layer reflection factor
C     T         =  internal transmission
C     A         =  layer absorption
C
C     Output :
C     --------
C
```

```
C     RO        =  reflection factor of single glazing
C     TA        =  transmission factor of single glazing
C     AB        =  absorption coefficient of single glazing
C
C
      REAL    R(6),T(6),RO(2,4),TA(2,4),AB(2,4),A(6)
      INTEGER IT(3)
C
      IZ=3
C
C     INDEX = 1  :  light transmission from outside to inside
C     INDEX = 2  :  light transmission from inside to outside
C
C     Outside/Inside
C     --------------
C
      DO 10 J=IT(1),IT(3),IT(2)
      RO(1,J)=R(J)+T(J)*T(J+1)*R(J+1)*A(J)**2/(1-(R(J+1)*A(J))**2)
      TA(1,J)=T(J)*T(J+1)*A(J)/(1-(R(J+1)*A(J))**2)
      AB(1,J)=(1-A(J))*T(J)/(1-R(J+1)*A(J))
C
C     Inside/Outside
C     --------------
C
      RO(2,IZ)=R(J+1)+T(J+1)*T(J)*R(J)*A(J)**2/(1-(R(J)*A(J))**2)
      TA(2,IZ)=T(J+1)*T(J)*A(J)/(1-(R(J)*A(J))**2)
      AB(2,IZ)=(1-A(J))*T(J+1)/(1-R(J)*A(J))
   10 IZ=IZ-2
C
      RETURN
      END
C

CCCCCCCCCCCCCCCCCCCCCCCCCCCCCCCCCCCCCCCCCCCCCCCCCCCCCCCCCCCCCCCCCCCCCC


CCCCCCCCCCCCCCCCCCCCCCCCCCCCCCCCCCCCCCCCCCCCCCCCCCCCCCCCCCCCCCCCCCCCCC
C
      SUBROUTINE KOMBITRANS(I,TAT,PR,SR,PT,ST,PA,SA,GR,GT,GA)
C
C
C     computes transparency, reflection and absorption for TALD systems
C     with a glazing/TALD/glazing composition by way of averaging the
C     separately calculated system values for parallel and vertical
C     E-field vectors.
C
C     Input :
C     -------
C
C     I         =  transmitting direction index
C     TAT       =  internal transmission inside TALD layer
C     PR        =  boundary layer reflection, parallel E-vector  |
C     SR        =  boundary layer reflection, vertical E-vector  |
C     PT        =  transmission, parallel E-vector               | for
C     ST        =  transmission, vertical E-vector               | single panes
C     PA        =  layer absorption, parallel E-vector           | each
C     SA        =  layer absorption, vertical E-vector           |
C
```

```
C     Output :
C     --------
C
C     GR         =  total reflection (system)
C     GT         =  total transmission (system)
C     GA         =  layer absorption (system)
C
      REAL    PR(2,4),SR(2,4),PT(2,4),ST(2,4),PA(2,4),SA(2,4)
      REAL    GR(2),GT(2),GA(2,3)
C
C     Reflection
C     ----------
C
      GR(I)=0.5*(PR(I,1)+TAT**2*PR(I,3)*PT(I,1)**2/
     &      (1-TAT**2*PR(I,1)*PR(I,2))+SR(I,1)+TAT**2*SR(I,3)
     &      *ST(I,1)**2/(1-TAT**2*SR(I,1)*SR(I,3)))
C
C     Transmission
C     ------------
C
      GT(I)=0.5*(TAT*PT(I,1)*PT(I,3)/(1-TAT**2*PR(I,1)*PR(I,3))
     &      +TAT*ST(I,1)*ST(I,3)/(1-TAT**2*SR(I,1)*SR(I,3)))
C
C     Layer absorption
C     ----------------
C
C
C     1st glazing
C     ...........
C
      GA(I,1)=0.5*(PA(I,1)+PA(I,1)*TAT**2*PR(I,3)*PT(I,1)/
     &        (1-TAT**2*PR(I,1)*PR(I,3))+SA(I,1)+SA(I,1)*TAT**2
     &        *SR(I,3)*ST(I,1)/(1-TAT**2*SR(I,1)*SR(I,3)))
C
C     Intermediate layer
C     ..................
C
      GA(I,2)=0.5*((1-TAT)*PT(I,1)+(1-TAT)*PR(I,3)*TAT*PT(I,1)*
     &      ((1+PR(I,1)*TAT)/(1-PR(I,1)*PR(I,3)*TAT**2))+
     &      (1-TAT)*ST(I,1)+(1-TAT)*SR(I,3)*TAT*ST(I,1)*
     &      ((1+SR(I,1)*TAT)/(1-SR(I,1)*SR(I,3)*TAT**2)))
C
C     2nd glazing
C     ...........
C
      GA(I,3)=0.5*(PA(I,3)*TAT*PT(I,1)/(1-TAT**2*PR(I,1)
     &        *PR(I,3))+SA(I,3)*TAT*ST(I,1)/(1-TAT**2*SR(I,1)
     &        *SR(I,3)))
C
      RETURN
      END
C
CCCCCCCCCCCCCCCCCCCCCCCCCCCCCCCCCCCCCCCCCCCCCCCCCCCCCCCCCCCCCCCCCCCCCCC
```